1

Ku-BAND INTERFEROMETRY

GEORGE D. PAPADOPOULOS

LOAN COPY

TECHNICAL REPORT 481

DECEMBER 31, 1970

MASSACHUSETTS INSTITUTE OF TECHNOLOGY
RESEARCH LABORATORY OF ELECTRONICS
CAMBRIDGE, MASSACHUSETTS 02139

The Research Laboratory of Electronics is an interdepartmental laboratory in which faculty members and graduate students from numerous academic departments conduct research.

The research reported in this document was made possible in part by support extended the Massachusetts Institute of Technology, Research Laboratory of Electronics, by the JOINT SERVICES ELECTRONICS PROGRAMS (U.S. Army, U.S. Navy, and U.S. Air Force) under Contract No. DA 28-043-AMC-02536(E), the National Aeronautics and Space Administration (Grant NGL 22-009-016), and the National Science Foundation (Grants GP-7046, GP-8415, GP-14854).

Requestors having DOD contracts or grants should apply for copies of technical reports to the Defense Documentation Center, Cameron Station, Alexandria, Virginia 22314; all others should apply to the Clearinghouse for Federal Scientific and Technical Information, Sills Building, 5285 Port Royal Road, Springfield, Virginia 22151.

MASSACHUSETTS INSTITUTE OF TECHNOLOGY

RESEARCH LABORATORY OF ELECTRONICS

Technical Report 481 December 31, 1970

Ku-BAND INTERFEROMETRY

George D. Papadopoulos

Submitted to the Department of Electrical Engineering at the Massachusetts Institute of Technology, February 23, 1970, in partial fulfillment of the requirements for the degree of Doctor of Philosophy.

(Manuscript received September 30, 1970)

Abstract

The construction of a Ku-band radio interferometer and some preliminary observations are reported. The interferometer was built for the purpose of mapping some discrete ratio sources: the Crab Nebula, Cas A, and Cyg A. The system contains two 8 ft parabolic antennas and receives radiation at 17.128 GHz (1.75 cm). The maximum baseline length of 100 m corresponds to a resolution of 35 seconds of arc. A PDP-8 computer is incorporated in the system and used for pointing, tracking, delay compensation, and real-time data analysis. The phase stability of the system was found to be better than 10° over a period of 2 hours. Consistent fringe components were obtained from the Crab Nebula with the baseline set at 8 m.

TABLE OF CONTENTS

CONTENTS

I. INTRODUCTION

The need for better angular resolution at wavelengths shorter than 3 cm in radio astronomical observations has been apparent for quite some time. For instance, our knowledge of the physical processes that give rise to the radiation from the Crab Nebula[1,2] and the planet Venus[3,4] could be greatly enhanced by observations at 2 cm with angular resolution better than 30 seconds of arc. With this problem in mind, the present work was undertaken. The objective was to show that a coherent interferometer can be built at 1.75 cm and used for aperture synthesis. We have built a phase-stable interferometer, thereby accomplishing the first part of our objective. Although consistent fringes have been obtained from the Crab Nebula, no aperture synthesis has been done. As well as the phase stability, we have also demonstrated the use of a small computer (4 k memory) in the control of such functions as antenna pointing and tracking, delay compensation, and real-time data processing.

In Section II, the theory of the earth-rotation synthesis, otherwise called "tracking interferometer," is presented. This technique was first used with the 178-MHz interferometer of Cambridge University[5,6] and has been treated by Zisk[7] and by Swenson and Mathur.[8] A review of other existing and proposed instruments designed for earth-rotation aperture synthesis has been given by Swenson.[9]

In Section III the data-processing technique is explained. The technique that was used is the least-square fit. A derivation is given of the interferometric signal-to-noise ratio; in this derivation we have included the effects of the processing technique.

Section IV gives a concise but complete description of the system. We felt it was necessary to give a thorough account of the equipment, since none of it existed at the beginning of this project. Some parts of it, such as the analog multiplier and the overall interface concept, are novel. The phase-lock system idea was first used by Alan E. E. Rogers in the OH interferometer between Haystack and Millstone at Lincoln Laboratory, M.I.T.[10] The A-D conversion method, as well as some of the designs, were suggested by Donald E. Troxel of the Cognitive Information Processing Group of the Research Laboratory of Electronics. In general, this has been written with the future users of the interferometer in mind, as well as any other reader who is interested in problems of interferometric design.

In section V we explain the software. We decided that a clear presentation of the program is necessary because it is an important part of the system, and also because such a presentation would facilitate the addition of improvements by future users.

In Section VI we tabulate and interpret some of the data that were obtained from Cygnus A, Cassiopeia A and the Crab Nebula (N.G.C. 1952, 1 M).

Finally, in Section VII modifications are suggested that will enable us to make a complete aperture synthesis.

II. INTERFEROMETER THEORY

We shall now develop the theory of an interferometric system. The basic assumptions germane to the system and to the nature of the source to be studied are the following.

1. The sources are discrete ratio sources; that is, $\Omega_S \ll \Omega_B$, where Ω_S is the width of the source and Ω_B is the beamwidth of the antennas.
2. The radiations from different points on the source are completely incoherent.
3. The antennas are continuously tracking the source.

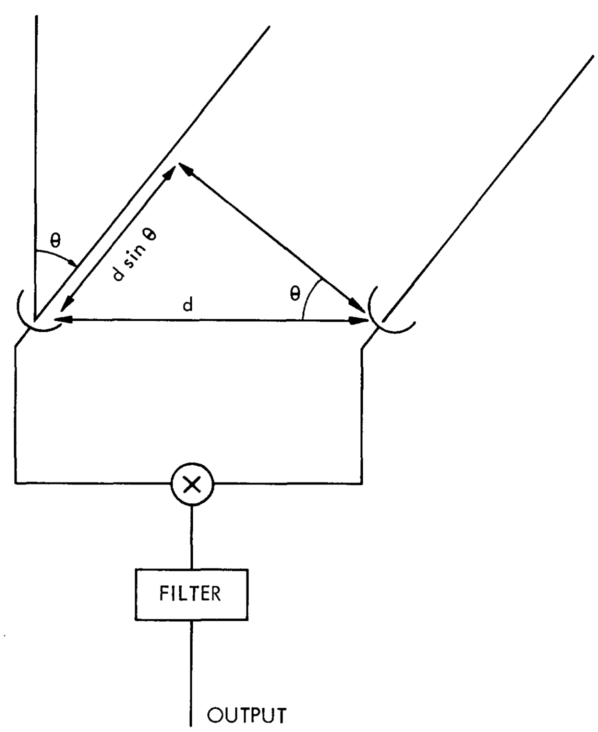

Fig. 1. Simple interferometer.

A simple interferometer is shown in Fig. 1. The response of this interferometer to a point monochromatic source is

$$v_o = A \cos \left[2\pi \frac{d}{\lambda} \sin\theta \right]. \tag{1}$$

The dependence of sin θ on the source and baseline coordinates, as well as the response of the interferometer to an extended polychromatic source, will be obtained.

2.1 SOURCE-BASELINE GEOMETRY

2.1.1 Spherical Triangle and Fringe Rate

Figure 2 shows the half of the celestial sphere that lies above the local horizon. P is the north celestial pole, R is the radio source that is being observed, and (L, L') are the points at which the baseline intersects the celestial sphere. For this interferometer the baseline lies on the horizon. In specifying the baseline we shall use the NW intersection point, L, for which $H_L = 9.75$ h and $D_L = 42.36°$.

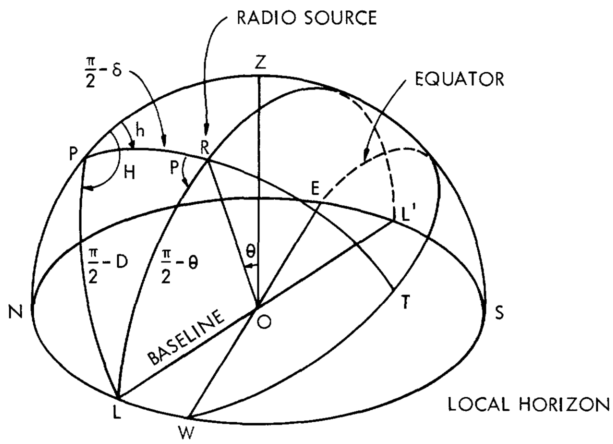

Fig. 2. Celestial sphere.

The angle formed by the line $\overline{0R}$ and the plane perpendicular to the baseline at 0 is called θ. Since, in this case, the baseline lies on the horizon, θ is the angle formed by $\overline{0R}$ and $\overline{0Z}$. The source, R, is specified by its hour angle, h, and declination δ.

The angle p is called the position angle. It is measured counterclockwise from the source hour circle PRT. The source-based orientation is such that North is toward the top, West toward the right and East toward the left. Figure 3 shows this orientation, as well as the sense of p. According to this orientation the angle p shown in

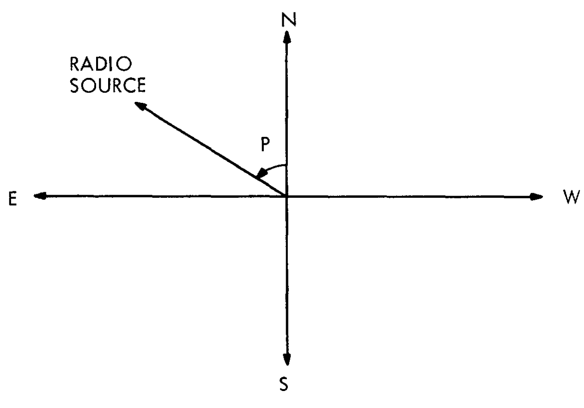

Fig. 3. Source-based orientation.

Fig. 2 is negative. As a matter of fact, it will be negative for a source in the western hemisphere and positive for a source in the eastern hemisphere.

For the spherical triangle LPR we obtain

$$\sin \theta = \sin \delta \sin D_L + \cos \delta \cos D_L \cos \frac{\pi}{12} (H_L - h). \tag{2}$$

Equation 2 can be expressed in terms of the sidereal time, t, by setting $h = t - a$. If the expression for $\sin \theta$ (2) is substituted in (1), the output of the interferometer becomes

$$v_o = A \cos \left[2\pi \frac{d}{\lambda} \left(\sin \delta \sin D_L + \cos \delta \cos D_L \cos \frac{\pi}{12} (H + a - t) \right) \right].$$

By expanding around t_o, where $t = t_o + t'$, we get

$$v_o = A \cos \left[2\pi \frac{d}{\lambda} \left[\sin \delta \sin D_L + \cos \delta \cos D_L \cos \frac{\pi}{12} (H + a - t_o) \right.\right.$$

$$\left.\left. + \frac{\pi}{12} t' \cos \delta \cos D_L \sin \frac{\pi}{12} (H + a - t) \right] \right]. \tag{3}$$

By studying (3), we can define the quantity fringe rate, $R(\delta, a, t_o)$:

$$R(\delta, a, t_o) = \frac{2\pi}{86400} \frac{d}{\lambda} \cos \delta \cos D_L \sin \frac{\pi}{12} (H + a - t_o) \frac{\text{fringes}}{\text{sid. sec.}}. \tag{4}$$

Therefore, over short intervals of time the output of the interferometer is a cosinusoidal function with a frequency given by Eq. 4. The fringe rate goes through zero when $H_L = h$.

2.1.2 Source Angular Coordinates and Projected Baseline Components

Let us consider an extended source as shown in Fig. 4. We can define the source-based angular coordinates x and y in terms of the source hour angle and declination (in radians):

$$x = (h - h_o) \cos \delta_o$$
$$y = \delta - \delta_o. \tag{5}$$

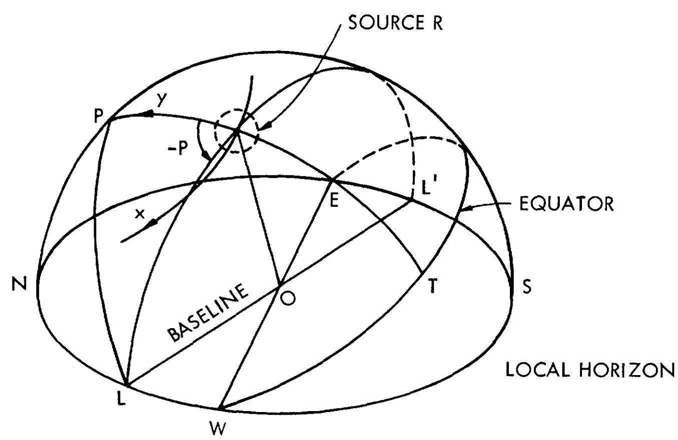

Fig. 4. Definition of angular source coordinates.

According to the source-based orientation defined here, positive x is toward the right (W), and positive y is toward the top (N).

Figure 5 shows the region of the sky around the source, R, the center (h_o, δ_o) of which coincides with the center of the antenna beam. We also show the projection of the baseline, $(d/\lambda) \cos \theta$, on the source plane (x, y). The solid projection is used when our

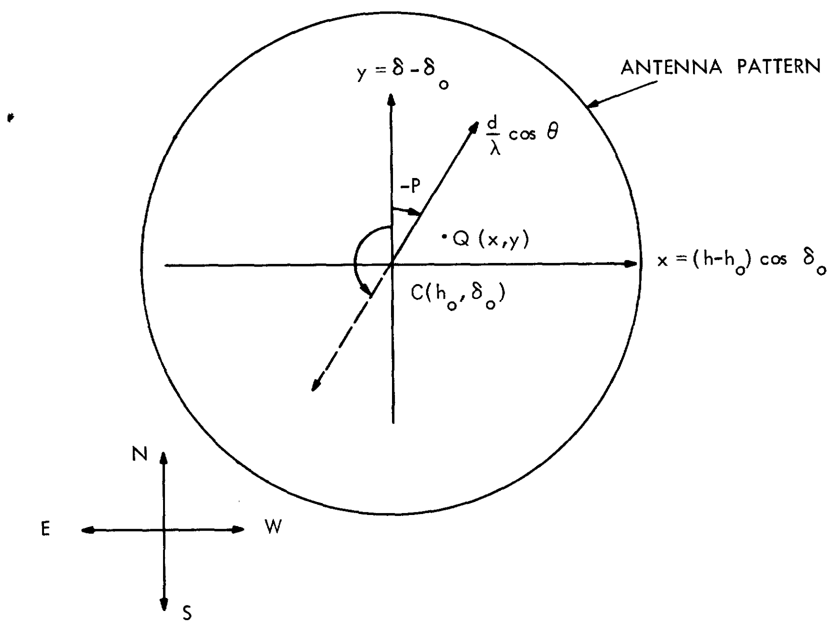

Fig. 5. Source-centered coordinates.

baseline is defined by the vector $0\bar{L}$ in Fig. 2, and the dotted projection is used when the baseline is defined by the vector $\bar{0}L'$. As mentioned previously, the vector $0\vec{L}$ will be used for our baseline. Then the components of the projected baseline in the western and northern directions are

$$\text{EW} \qquad u = -d/\lambda \cos \theta \sin p$$

$$\text{SN} \qquad v = d/\lambda \cos \theta \cos p. \tag{6}$$

By applying the laws of sine and cosine[12] in the spherical triangle LPR of Fig. 2, we obtain

$$u = d/\lambda \cos D_L \sin (H_L - h)$$

$$v = d/\lambda \left[\sin D_L \cos \delta - \cos D_L \sin \delta \cos (H_L - h)\right]. \tag{7}$$

These projected baseline components are the angular frequency coordinates to which the angular coordinates x, y transform. It can be demonstrated very simply by considering the point sources C and Q in Fig. 5. From Eq. 1 the interferometer response to C is $v_C = A \operatorname{Re} e^{j2\pi \frac{d}{\lambda} \sin \theta_o}$, and to Q it is $v_Q = A \operatorname{Re} e^{j2\pi \frac{d}{\lambda} \sin \theta}$. If we now expand $\sin \theta$

around (h_o, δ_o) and make use of (5) we obtain

$$\sin\theta = \sin\theta_o + \frac{1}{\cos\delta_o}\left(\frac{\partial \sin\theta}{\partial h}\right)_{(h_o,\,\delta_o)} x + \left(\frac{\partial \sin\theta}{\partial \delta}\right)_{(h_o,\,\delta_o)} y.$$

Recognizing that

$$u = \frac{1}{\cos\delta_o}\left(\frac{\partial \sin\theta}{\partial h}\right)_{(h_o,\,\delta_o)} \quad \text{and} \quad v = \left(\frac{\partial \sin\theta}{\partial \delta}\right)_{(h_o,\,\delta_o)},$$

we have

$$\frac{d}{\lambda}\sin\theta = \frac{d}{\lambda}\sin\theta_o + ux + vy. \tag{8}$$

Substituting (8) in the expression for v_Q, we obtain

$$v_Q = A \operatorname{Re} e^{j2\pi\frac{d}{\lambda}\sin\theta_o} e^{j2\pi(ux+vy)}.$$

We can now recognize the expressions for v_C and v_Q as Fourier transforms in the u,v plane of impulse functions in the x,y plane, one at the origin and the other at (x, y).

2.2 INCIDENT RADIATION

Let us consider the source-receiver configuration shown in Fig. 6 which is actually a different representation of the configuration on Fig. 4. The antenna is pointed in the direction z which connects the origin of the receiving aperture with the center of the source at (h_o, δ_o). The electric field, $\mathscr{E}$, on the plane of the aperture, because of radiation originating at a point Q on the source, will then be a function of the direction cosines[8, 11] $\cos\alpha_x$, $\cos\alpha_y$, $\cos\alpha_z$ and time t; that is,

$$\mathscr{E} = \mathscr{E}(\cos\alpha_x, \cos\alpha_y, \cos\alpha_z; t).$$

Since the dimension of the source is much smaller as compared with the distance R, we may say that

$$\cos\alpha_z = 1$$

$$\cos\alpha_x = x_Q$$

$$\cos\alpha_y = y_Q,$$

where x_Q and y_Q are in radians. With these approximations the electric field has the more convenient form $\mathscr{E}(x, y; t)$, where x and y are the angular coordinates on the source.

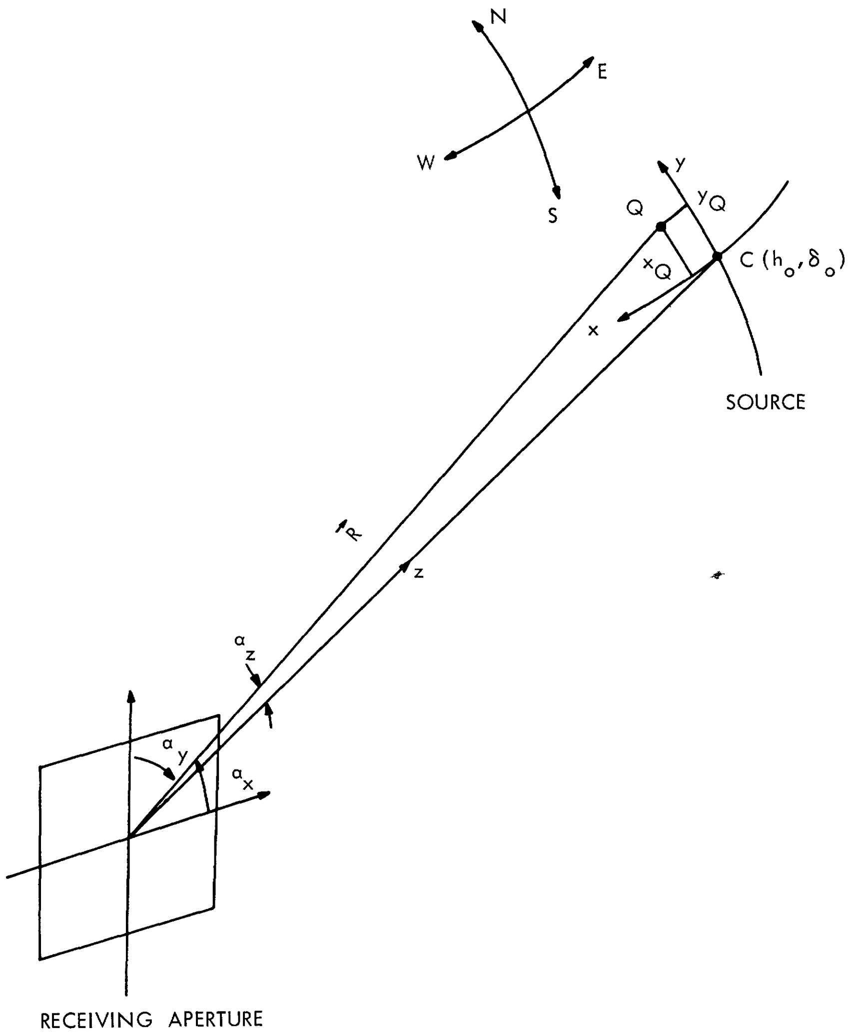

Fig. 6. Source receiver configuration.

If we now define the temporal Fourier transform of the electric field

$$\overline{E}(x, y; \nu) = \int_{-\infty}^{\infty} \mathscr{E}(x, y; t)\, e^{-j2\pi\nu t}\, dt, \tag{9}$$

then, as has been shown,[11] the intensity of radiation $(I(x, y; \nu)$ at the receiving site is

$$I(x, y; \nu) = \frac{1}{2}\sqrt{\frac{\epsilon}{\mu}}\, |\overline{E}(x, y; \nu)|^2. \tag{10}$$

The units of $I(x, y; \nu)$ are W/Hz-m^2-ster. The radiation intensity is related to the brightness temperature distribution of the source by

$$I(x, y; \nu) = \frac{2kT_B(x, y)}{\lambda^2}. \tag{11}$$

The output of the antenna expressed in units of power/Hz is[13, 14]

$$kT_A = \frac{1}{2} \iint I(x, y; \nu)\, A(x_o - x, y_o - y)\, dxdy, \tag{12}$$

where A is the effective area of the antenna and is related to the power of the antenna by

$$G_p = \frac{4\pi}{\lambda^2} A_o. \tag{13}$$

In writing (12) we have not included the effects of the atmosphere. Calculations[15] show that at our signal frequency of 17 GHz the atmospheric attenuation on an average day ($\rho_{H_2O} = 1\ g/cm^3$) is 0.06 dB and the emission temperature approximately 5°K. These numbers change drastically on cloudy or rainy days.[16] For observations taken on good days the atmospheric attenuation will be negligible. The atmospheric emission received by two spatially separated antennas is uncorrelated; therefore, it does not have to be included in the interferometer equations.

By making use of basic assumption 1, we can simplify (12) to

$$\begin{aligned} kT_A &= \frac{1}{2} A_o \iint I(x, y; \nu)\, dxdy \\ kT_A &= \frac{1}{2} A_o S(\nu), \end{aligned} \tag{14}$$

where $S(\nu)$ is the source flux defined by

$$S(\nu) = \iint I(x, y; \nu)\, dxdy. \tag{15}$$

Equation 14 gives us the output of a total-power radiometer. In interferometry, however, we are interested in the voltage output of the antenna. To get an expression for the voltage output, we made use of the electric field spectrum given in (9) and the antenna voltage gain given by

$$G_v = \sqrt{G_p} = \frac{2\sqrt{\pi}}{\lambda} \sqrt{A_o}. \tag{16}$$

Then, by making use of assumption 1, we can get an expression for the voltage output of the antenna

$$\overline{V}_a(\nu) = K\, G_v \iint \overline{E}(x, y; \nu)\, dxdy, \tag{17}$$

where

$$K = \left(\frac{\epsilon}{4\mu}\right)^{1/4} \frac{\lambda}{\sqrt{4\pi}}. \tag{18}$$

2.3 RESPONSE OF A WIDEBAND INTERFEROMETER TO AN EXTENDED SOURCE

In Fig. 7 the signals at the different points of the interferometer are defined.

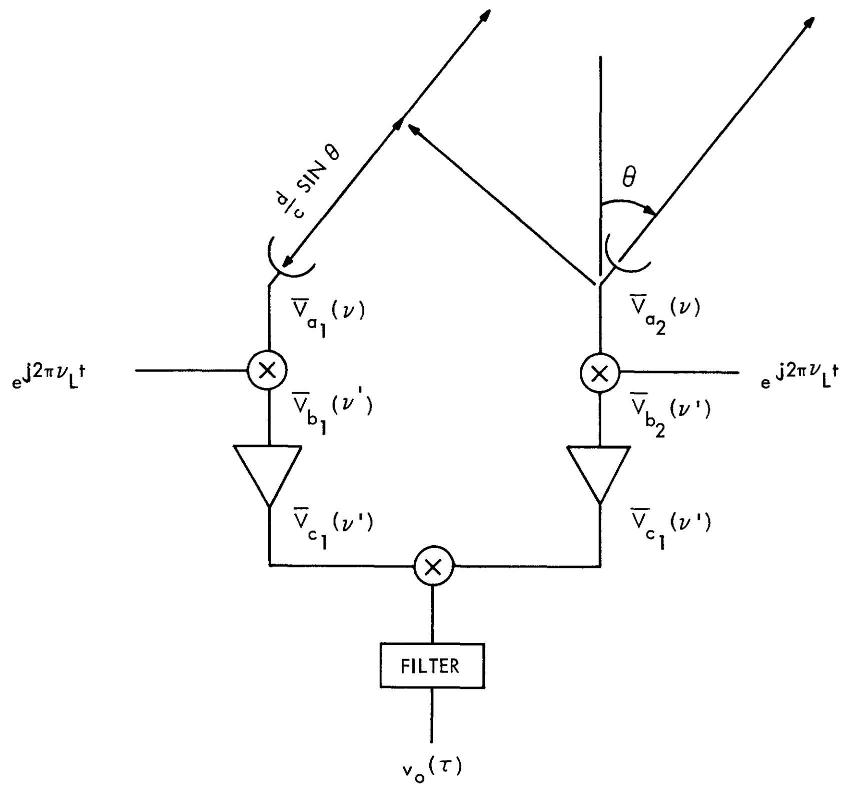

Fig. 7. Interferometer signals.

From Eq. 17 we can write expressions for the voltages $V_{a1}(\nu)$ and $V_{a2}(\nu)$:

$$\overline{V}_{a1}(\nu) = KG_v \iint \overline{E}_1(x, y; \nu)\, dxdy \tag{19a}$$

$$\overline{V}_{a2}(\nu) = KG_v \iint \overline{E}_2(x, y; \nu)\, dxdy. \tag{19b}$$

Since the incident field arrives at antenna 1 $\frac{d}{c}\sin\theta$ s later than it does at antenna 2, we can relate $\overline{E}_1(x, y; \nu)$ and $\overline{E}_2(x, y; \nu)$ by

$$\overline{E}_1(x, y; \nu) = \overline{E}_2(x, y; \nu)\, \exp\left(-j2\pi\nu \frac{d}{c} \sin\theta\right). \tag{20}$$

Use of (20) will be made later.

After mixing, the signals become

$$\overline{V}_{b_1}(\nu') = \overline{V}_{a_1}(\nu)\ e^{-j\pi\nu_L t} \tag{21a}$$

$$\overline{V}_{b_2}(\nu') = \overline{V}_{a_2}(\nu)\ e^{-j\pi\nu_L t}, \tag{21b}$$

where ν' is the IF frequency $\nu' = \nu - \nu_L$.

If the IF filter-amplifiers have identical frequency responses $H(\nu')$, then

$$\overline{V}_{c_1}(\nu') = \overline{V}_{b_1}(\nu')\ \overline{H}(\nu') \tag{22a}$$

$$\overline{V}_{c_2}(\nu') = \overline{V}_{b_2}(\nu')\ \overline{H}(\nu'). \tag{22b}$$

Finally the output of the crosscorrelator, $v_o(\tau)$, is

$$v_o(\tau) = \mathrm{Re}\left\{\lim_{T\to\infty} \frac{1}{2T} \int_{-T}^{T} v_{c_1}(t+\tau)\ v_{c_2}^*(t)\ dt\right\}, \tag{23}$$

where

$$v_{c_1}(t+\tau) = \int \overline{V}_{c_1}(\nu_1')\ \exp[j2\pi\nu_1'(t+\tau)]\ d\nu_1' \tag{24a}$$

$$v_{c_2}^*(t) = \int \overline{V}_{c_2}^*(\nu_2')\ \exp(-j2\pi\nu_2' t)\ d\nu_2'. \tag{24b}$$

If we now substitute Eqs. 24, 22, and 21 in Eq. 23, we obtain

$$\begin{aligned} v_o(\tau) = K^2G_v^2\ \mathrm{Re}\ &\left\{\lim_{T\to\infty} \frac{1}{2T} \int_{-T}^{T} dt \int d\nu_1' \int d\nu_2'\ \overline{V}_{a_1}(\nu_1)\ \overline{V}_{a_2}^*(\nu_2)\right. \\ &\left.\times\ \overline{H}(\nu_1')\ \overline{H}^*(\nu_2')\ \exp[-j2\pi t(\nu_2'-\nu_1')]\ \exp(j2\pi\nu_1'\tau)\right\}. \end{aligned} \tag{25a}$$

By using the fact that

$$\lim_{T\to\infty} \frac{1}{2T} \int_{-T}^{T} e^{-j2\pi t(\nu_2'-\nu_1')}\ dt = \delta(\nu_2'-\nu_1'),$$

(25a) becomes

$$v_o(\tau) = K^2G_p\ \mathrm{Re}\left\{\int \overline{V}_{a_1}(\nu)\ \overline{V}_{a_2}^*(\nu) \left|\overline{H}(\nu')\right|^2 e^{j2\pi\nu'\tau}\ d\nu'\right\}. \tag{25b}$$

If we now use Eqs. 19, 20, and assumption 2, we obtain

$$v_o(\tau) = K^2 G_p \,\mathrm{Re}\left\{\int d\nu' \iint dxdy\, |\overline{E}(x, y; \nu)|^2 \exp\left(-j2\pi\nu \frac{d}{c} \sin\theta\right) |\overline{H}(\nu')|^2\, e^{j2\pi\nu'\tau}\right\}. \tag{25c}$$

From Eqs. 10, 13, and 18 we have

$$K^2 G_p |\overline{E}(x, y; \nu)|^2 = \frac{1}{2} A_o I(x, y; \nu),$$

where the factor 1/2 accounts for the fact that we receive only one polarization. Then (25c) becomes

$$v_o(\tau) = \frac{1}{2} A_o \,\mathrm{Re}\left\{\int d\nu' \iint dxdy\, I(x, y; \nu) |\overline{H}(\nu')|^2 \exp\left(-j2\pi\nu \frac{d}{c} \sin\theta\right) e^{j2\pi\nu'\tau}\right\}. \tag{26}$$

The geometrical delay $\frac{d}{c}\sin\theta$ is next expanded around h_o, δ_o. The result of this expansion is given by Eq. 8. By substituting (8) in (26), we get

$$v_o(t) = \frac{1}{2} A_o \,\mathrm{Re}\left\{\int d\nu' \int dxdy\, I(x, y; \nu)\, e^{-j2\pi(ux+vy)} \right.$$
$$\left. \times \exp\left(-j2\pi\nu \frac{d}{c} \sin\theta_o\right) |\overline{H}(\nu')|^2\, e^{j2\pi\nu'\tau}\right\}. \tag{27}$$

Recognizing that $I(x, y; \nu)\, e^{-j2\pi(ux+vy)}$ is effectively constant over the passband, B, of $\overline{H}(\nu')$, (27) is simplified to

$$v_o(\tau) = \frac{1}{2} A_o \,\mathrm{Re}\left\{\int d\nu'\, |\overline{H}(\nu')|^2\, e^{j2\pi\nu'\tau} \exp\left(-j2\pi\nu \frac{d}{c} \sin\theta_o\right)\right.$$
$$\left. \times \iint I(x, y; \nu_o)\, e^{-j2\pi(ux+vy)}\, dxdy\right\}, \tag{28}$$

where ν_o is the mean frequency at which the radiation is received.

By means of Eq. 11, we can rewrite (28) as

$$v_o(\tau) = \frac{1}{2} A_o \frac{2k}{\lambda_o^2} \,\mathrm{Re}\left\{\int d\nu'\, |\overline{H}(\nu')|^2\, e^{j2\pi\nu'\tau} \exp\left(-j2\pi\nu \frac{d}{c} \sin\theta_o\right)\right.$$
$$\left. \times \iint T_B(x, y)\, e^{-j2\pi(ux+vy)}\, dxdy\right\}. \tag{29}$$

Equation 29 indicates that $v_o(\tau)$ is proportional to the Fourier transform of the source brightness temperature distribution $T_B(x, y)$.[17] The angular frequency coordinates of the transform plane are the parameters u and v defined in Eq. 7. The normalized Fourier transform of $T_B(x, y)$ is called <u>fringe visibility</u> and is defined by

$$\overline{V}(u,v) = \frac{\iint T_B(x,y)\, e^{-j2\pi(ux+vy)}\, dxdy}{\iint T_B(x,y)\, dxdy} \tag{30}$$

By substituting (11), (15), and (30) in (29), the correlator output, $v_o(\tau)$, becomes

$$v_o(\tau) = \frac{1}{2} A_o S \;\mathrm{Re}\left\{\overline{V}(u,v) \int |\overline{H}(\nu')|^2 e^{j2\pi\nu'\tau} \exp\left(-j2\pi\nu \frac{d}{c}\sin\theta_o\right) d\nu'\right\}. \tag{31}$$

We now proceed to solve the bandpass integral for the SSB and DSB cases.

(a) SSB Receiver

The bandpass characteristic for this case is illustrated by the following diagram.

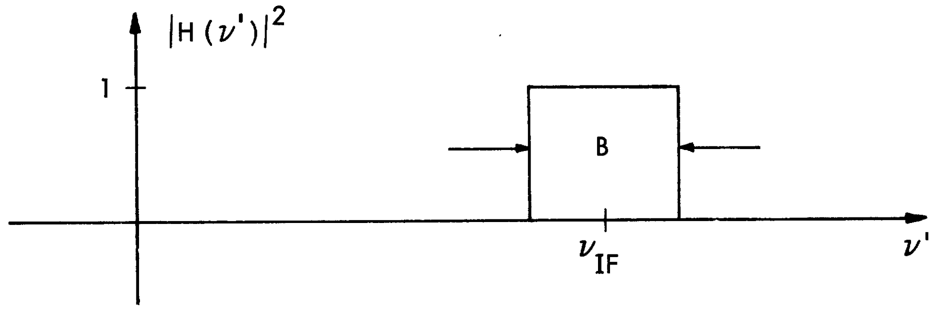

Here, ν_L is the local-oscillator frequency, and $\nu_{IF} = \nu_o - \nu_L$ is the center intermediate frequency.

After making the appropriate substitutions and carrying out the integration, the bandpass integral becomes

$$I_{SSB} = \exp\left(-j2\pi\nu_L \frac{d}{c}\sin\theta_o\right) \int_{\nu_{IF}-B/2}^{\nu_{IF}+B/2} \exp\left[j2\pi\nu'\left(\tau - \frac{d}{c}\sin\theta_o\right)\right] d\nu'$$

$$= B\,\frac{\sin \pi B\left(\tau - \frac{d}{c}\sin\theta_o\right)}{\pi B\left(\tau - \frac{d}{c}\sin\theta_o\right)} \exp\left[-j2\pi\nu_L \frac{d}{c}\sin\theta_o + j2\pi\nu_{IF}\left(\tau - \frac{d}{c}\sin\theta_o\right)\right].$$

Substituting I_{SSB} in Eq. 31, we obtain

$$v(\tau) = \frac{1}{2} A_o SB\,\frac{\sin \pi B\left(\tau - \frac{d}{c}\sin\theta_o\right)}{\pi B\left(\tau - \frac{d}{c}\sin\theta_o\right)} \left|\overline{V}(u,v)\right| \cos 2\pi\left[\nu_o \frac{d}{c}\sin\theta_o - \nu_{IF}\tau + \phi(u,v)\right], \tag{32}$$

where we have written $\overline{V}(u,v)$ in terms of its amplitude and phase:

$$\overline{V}(u, v) = \left|\overline{V}(u, v)\right| e^{-j\phi(u, v)}. \tag{33}$$

(b) DSB Receiver

The bandpass characteristic for this case is illustrated by the following diagram.

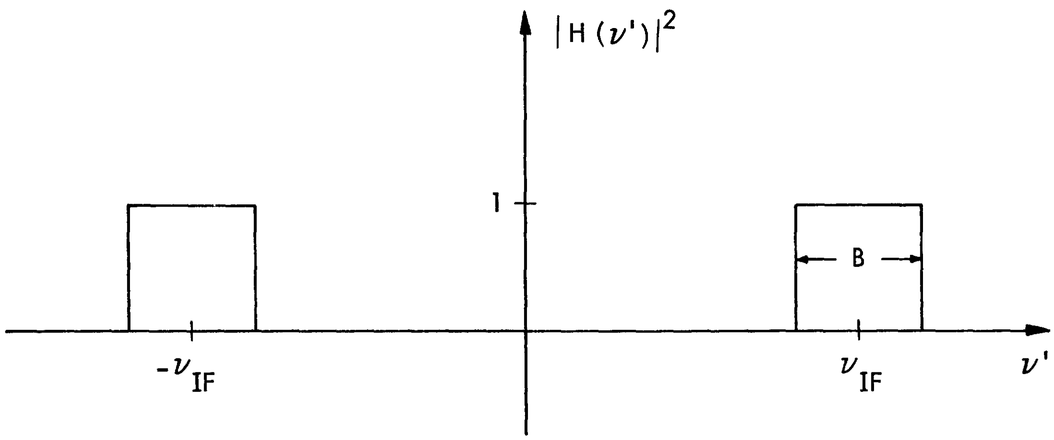

Here, as before, $\nu' = \nu - \nu_L$, and $\nu_{IF} = \nu_o - \nu_L$, with ν_o the mean frequency in the upper sideband. For this configuration the bandpass integral, I_{DSB}, from Eq. 31, can be written

$$I_{DSB} = \exp\left(-j2\pi\nu_L \frac{d}{c} \sin\theta_o\right) \left[\exp\left[-j2\pi\nu_{IF}\left(\tau - \frac{d}{c}\sin\theta_o\right)\right] B \frac{\sin \pi B\left(\tau - \frac{d}{c}\sin\theta_o\right)}{\pi B\left(\tau - \frac{d}{c}\sin\theta_o\right)}\right.$$

$$\left. + \exp\left[j2\pi\nu_{IF}\left(\tau - \frac{d}{c}\sin\theta_o\right)\right] B \frac{\sin \pi B\left(\tau - \frac{d}{c}\sin\theta_o\right)}{\pi B\left(\tau - \frac{d}{c}\sin\theta_o\right)}\right].$$

Simplifying further, we obtain

$$I_{DSB} = 2B \frac{\sin \pi B\left(\tau - \frac{d}{c}\sin\theta_o\right)}{\pi B\left(\tau - \frac{d}{c}\sin\theta_o\right)} \cos 2\pi\nu_{IF}\left(\tau - \frac{d}{c}\sin\theta_o\right) \exp\left(-j2\pi\nu_L \frac{d}{c}\sin\theta_o\right).$$

Substituting I_{DSB} in (31), we obtain

$$v_o(\tau) = A_oSB \frac{\sin \pi B\left(\tau - \frac{d}{c}\sin\theta_o\right)}{\pi B\left(\tau - \frac{d}{c}\sin\theta_o\right)} \cos 2\pi\nu_{IF}\left(\tau - \frac{d}{c}\sin\theta_o\right)$$

$$\times \left|\overline{V}(u, v)\right| \cos 2\pi\left[\nu_L \frac{d}{c}\sin\theta_o + \phi(u, v)\right]. \tag{34}$$

Equations 32 and 34 will be discussed in more detail in section 3.2.

2.4 FRINGE VISIBILITY PLANE AND APERTURE SYNTHESIS

2.4.1 Locus of Fringe Visibility Points for a Tracking Interferometer

We have established that the output of the interferometer is proportional to the fringe visibility $\overline{V}(u, v)$ which is the normalized Fourier transform of $T_B(x, y)$. Therefore, by measuring $\overline{V}(u, v)$ at a sufficient number of points, the brightness temperature distribution $T_B(x, y)$ can be reconstructed. For a tracking interferometer the samples of $\overline{V}(u,v)$ taken with a fixed baseline length lie on an ellipse in the u-v plane. This can be shown by eliminating the variable parameter H-h in Eq. 7. Then the equation of the locus is

$$\frac{u^2}{a^2} + \frac{(v-v_o)^2}{b^2} = 1.$$

This is indeed the equation of an ellipse, with

$$\begin{aligned} &u \quad \text{semiaxis} \quad a = d/\lambda \cos D_L \\ &v \quad \text{semiaxis} \quad b = d/\lambda \cos D_L \sin \delta \end{aligned} \qquad (35)$$

and center $(0, v_o) = (0, d/\lambda \sin D_L \cos \delta)$.

By changing the spacing of the antennas, we obtain several ellipses and thereby fill up the u-v plane. According to the sampling theorem the samples of $\overline{V}(u, v)$ need not be taken any closer than

$$\Delta u, \Delta v < \frac{1}{2X_c}, \frac{1}{2Y_c},$$

where X_c and Y_c are the maximum dimensions of the source.

A rough estimate of the number of points that are needed to reconstruct $T_B(x, y)$ is given by $N = \frac{U_{max}}{\Delta u} \times \frac{V_{max}}{\Delta v}$. Since $U_{max} = V_{max} = d/\lambda$, we have

$$N = 4(d/\lambda)^2 X_c Y_c. \qquad (36)$$

Actually, half of these points are redundant because $\overline{V}(u, v) = \overline{V}(-u, -v)$; this is a property of the Fourier transforms of real functions like $T_B(x, y)$.

2.4.2 Accessible Part of the Locus

The section of the u-v plane ellipse that can be mapped is called "accessible." There is a limitation because the source is above the horizon only part of the day. A good discussion of this problem has been given by Zisk.[7] Our approach will be to determine the accessible part of the locus by finding the (u, v) coordinates for three positions of the source that are above the horizon. These positions are the rise, the set, and the 0^h positions. Figure 8 shows the source at the rise, R, and set, R', positions. To

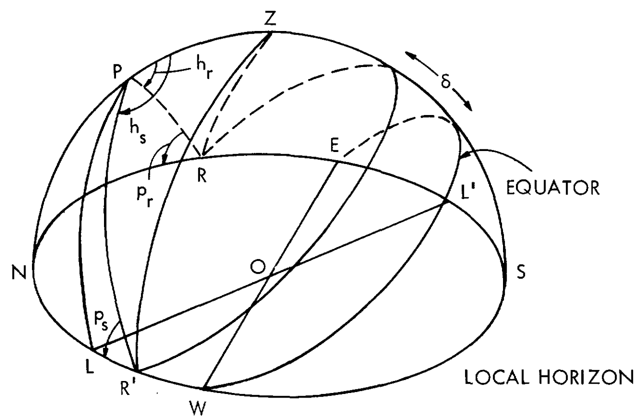

Fig. 8. Spherical triangles for the rise and set positions of the source.

compute (u, v) at these positions we have to find h_s and h_r. These angles can be found by solving spherical triangles[12] ZPR and ZPR':

$$\cos h_{s,r} = -\frac{\sin \phi \sin \delta}{\cos \phi \cos \delta}. \tag{37}$$

If $\delta > 0$, then $90 < h_s < 180°$ and $180 < h_r < 270°$. If $\delta < 0$, then $0 < h_s < 90°$ and $270 < h_r < 360°$.

We shall now find the accessible locus for two declinations: $\delta = 22°$, which is the declination of the Crab Nebula, and $\delta = -10°$, which is close to the declination of some interesting Southern Sky sources that are like the Orion Nebula.

To find the accessible locus we shall use Eqs. 7, 35, and 37. The values of the baseline parameters are $H_L = 146°$, $D_L = 42°$, $d = 2000\ \lambda$. The latitude, ϕ, is 42°.

1. $\delta = 22°$

   $h_r = 250°$, $h_s = 110°$

   $a = 1500$, $b = 500$, $v_o = 1240$

   $(u, v)/0^h = (835, 1700)$

   $(u, v)/h_r = (-1435, 1390)$

   $(u, v)/h_s = (875, 788)$.

This locus is shown in Fig. 9a.

2. $\delta = -10$

$h_r = 279°$, $h_s = 81°$

$a = 1500$, $b = 256$, $v_o = 1320$

$(u, v)/0^h = (835,\ 1107)$

$(u, v)/h_r = (-1180,\ 1145)$

$(u, v)/h_s = (1345,\ 1427)$.

This locus is shown in Fig. 9b.

In Fig. 9 we have drawn the lines joining the origin with the rise and set points. The position angles p_s and p_r are equal and negative to each other. To show this, we

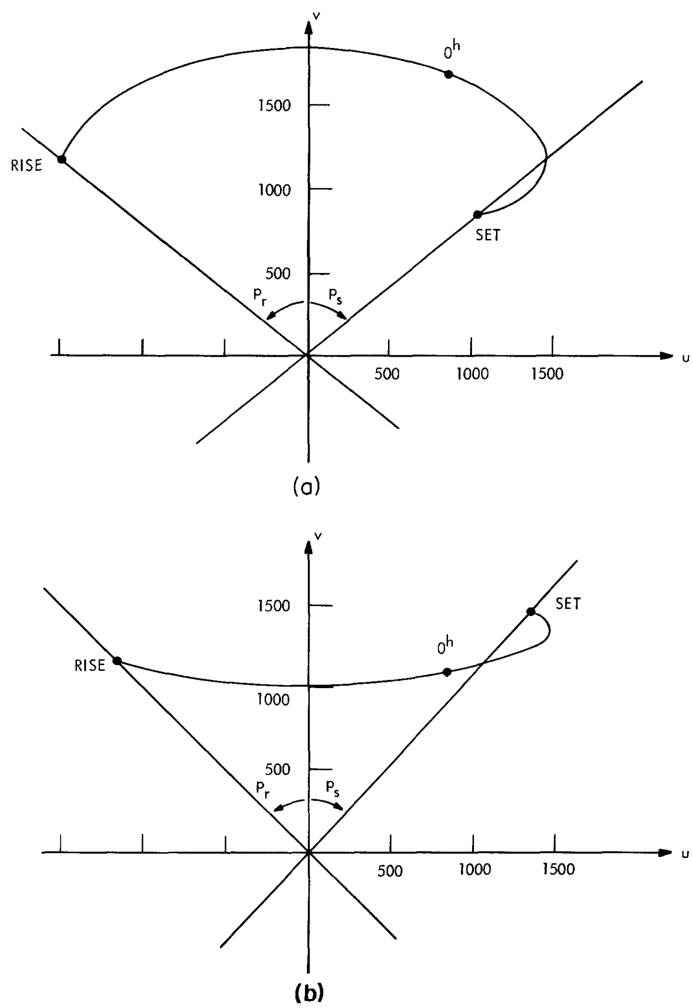

Fig. 9. u-v plane loci. **(a)** $\delta = 22°$. (b) $\delta = -10$.

solve triangles ZPR and ZPR' of Fig. 8. Then we obtain

$$\sin p_r = \frac{\sin \phi}{\cos \delta}$$

$$\sin p_s = - \frac{\sin \phi}{\cos \delta}. \qquad (38)$$

III. INTERFEROMETER OUTPUT AND DATA ANALYSIS

The interferometer equations obtained in Section II will now be applied to the Ku-band interferometer. The interferometer is composed of two 8-ft dishes with a possible separation range of 10-100 m. The local-oscillator frequency is 17.128 GHz, corresponding to a wavelength of 1.75 cm. The radiation is mixed down to a 60-MHz intermediate frequency, by means of a double-sideband heterodyne receiver. The IF bandwidth is 20 MHz.

3.1 SIGNAL AND NOISE LEVELS

The antenna temperature can be obtained from Eq. 14.

$$T_A = \frac{1}{2} \frac{A_o S}{k},$$

where A_o is the effective dish area corresponding to a dish efficiency of 35%; therefore, $A_o = 1.9 \text{ m}^2$. The efficiency is lower than expected. This can be attributed mainly to two factors: (a) there is some uncertainty about the focusing; and (b) the primary pattern is such that there is an excessive amount of spillover.

The noise temperature, T_R, of the receiver is approximately 1600°K. The rms noise at the output of the second detector is given by

$$\Delta T_{rms} = \frac{T_R}{\sqrt{B\tau}}, \tag{39}$$

where B is the IF bandwidth, and τ is the integration time of the second detector. For an integration time of 3 minutes, the rms noise is:

$$\Delta T_{rms} = 0.025°\text{K}.$$

Table 1. Antenna temperatures, signal-to-noise ratios. (A_o=1.9 m^2, T_R=1600°K, B=20 MHz, $\tau=3^m$, ΔT_{rms}=0.025°K.)

Source	Flux Units at 17 GHz	T_A °K	S/N
Crab Nebula	420	0.29	11.5
CAS A	320	0.22	8.5
CYG A	80	0.055	2
3C273	40	0.028	1

Table 1 lists the antenna temperatures and signal-to-noise ratios for four interesting radio sources: Crab Nebula, Cas A, Cyg A, and 3C273.

3.2 DELAY COMPENSATION

3.2.1 SSB Receiver

Equation 32 gives us the output of the interferometer for an SSB system:

$$v_o(\tau) = \frac{1}{2} A_o BS \underbrace{\frac{\sin \pi B\left(\tau - \frac{d}{c}\sin\theta_o\right)}{\pi B\left(\tau - \frac{d}{c}\sin\theta_o\right)}}_{\text{Bandpass Envelope}}$$

$$|V(u, v)| \underbrace{\cos 2\pi\left[\nu_o \frac{d}{c}\sin\theta_o\right.}_{\text{Fringes}} \left. - \nu_{IF}\tau + \phi(u, v)\right].$$

By studying Eq. 32, we can draw the following conclusions:

1. The bandpass envelope will wipe out the fringes unless we compensate in the IF strip so that

$$\pi B\left(\tau - \frac{d}{c}\sin\theta\right) \ll 1. \tag{40a}$$

2. Any phase changes in the IF will appear as a phase error in the fringes.

From (40a) we can compute the maximum change in the geometric delay, τ, that can be tolerated:

$$\Delta\tau = \frac{d}{c}\cos\theta\Delta\theta \ll \frac{1}{\pi B}. \tag{40b}$$

For a bandwidth of 20 MHz, $\Delta\tau$ is 6 ns.

As long as condition (40a) is satisfied, the fringes are always under the peak of the envelope. These fringes are called "white fringes."

The time intervals at which one should compensate can be found from the inequality (40b).

$$\pi B \frac{2\pi}{24}\frac{\Delta t}{3600}\cos\theta \ll 1,$$

where Δt is the time interval at which we should compensate.

For our baseline orientation we may assume that the maximum value of $\cos\theta$ is equal to 1/2. Then

$$\Delta t \ll \frac{c}{d}\frac{86400}{\pi^2 B}. \tag{41}$$

3.2.2 DSB System

The interferometer output for a DSB system is given by Eq. 34.

$$v_o(\tau) = A_o SB \frac{\sin \pi B\left(\tau - \frac{d}{c} \sin \theta_o\right)}{\pi B\left(\tau - \frac{d}{c} \sin \theta_o\right)}$$

$$\times \cos \underbrace{2\pi\nu_{IF}\left(\tau - \frac{d}{c}\sin\theta_o\right)}_{\text{Envelope}} |V(u,v)| \underbrace{\cos 2\pi\left[\nu_L \frac{d}{c}\sin\theta_o}_{\text{Fringes}} + \phi(u,v)\right].$$

The conclusions that we draw from Eq. 34 are the following.

1. The amount of compensation and the rate at which we must compensate depends on the center IF frequency, ν_{IF}, and not on the IF bandwidth as in the SSB case.

2. Phase changes in the IF strip cancel out and do not appear as phase errors in the fringes.

In a way similar to that of the SSB system we can compute the maximum change in the geometrical delay that can be tolerated and the time intervals at which we should compensate. These are

$$\Delta\tau \ll \frac{1}{2\pi\nu_{IF}}$$

and

$$\Delta t \ll \frac{c}{d} \frac{86400}{2\pi^2\nu_{IF}}. \tag{42}$$

In Table 2 we give the compensation intervals for the case of the longest baseline which is 100 m. The inequalities are converted to equalities by multiplying the right-hand side of inequalities (41) and (42) by 1/5.

Table 2. Compensation intervals.
(λ=1.75 cm, d=100 m, B=20 MHz, ν_{IF}=60 MHz.)

Case	Basic Compensation Delay, $\Delta\tau$(ns)	Minimum Compensation Intervals (min)
SSB	6	4
DSB	1	0.7

Although the compensation rates are smaller in an SSB system, we decided in favor of a DSB for the following reasons: (i) simpler front end; (ii) signal-to-noise ratio better by 3 dB for the broadband mixer that we are using; (iii) IF phase changes do not produce an error in the phase of fringes; and (iv) the use of a small computer to control the system makes it possible to compensate at high rates.

A basic amount of compensation delay of 1.25 ns and a fixed compensation interval of 1 min were chosen. The maximum compensation delay needed is equal to the separation distance of the two antennas. For the maximum spacing of 100 m the required compensation delay is 330 ns. This delay is generated digitally by using the 1.25 ns delay as the basic unit. Then the other delays are 2.5, 5, 10, 20, 40, 80, and 160 ns.

We shall now describe the way in which the digital delay is computed and inserted. At the end of each 1-min compensation interval, the program computes $\frac{d}{c} \sin \theta$ and then divides it by the basic delay of 1.25 ns. The result is an 8-bit binary number; the high-order bit controls the 160-ns delay, and so on. If $\sin \theta$ is positive, the delay is inserted in the IF signal path of the northern antenna and vice versa. The reason for this is the convention that was adopted (see Section II) according to which the baseline is specified by its northwest intersection, L, with the celestial sphere.

The implementation of the delay compensation will be explained further in sections 4.4 and 5.26.

3.3 DATA PROCESSING

As we have mentioned, the interferometer output, over short intervals of time, is a sinusoid the frequency of which is given by Eq. 4. This sinusoid is buried in the system noise; its amplitude and phase are detected by a real-time least-squares fit processing.

The output of the correlator is sampled every 0.2 s which is sufficiently smaller than the minimum fringe period of 2 s; this period occurs at the longest baseline spacing. The sample is then converted into a 10-bit digital number which is transferred into the computer. The program knows the exact time at which the sample was accepted and proceeds to the real-time processing. Let us call the sample taken at time t_i, y_i. Then the least-squares fit detection demands that

$$\epsilon = \sum_{i=1}^{N} (y_i - a_1 \cos \gamma_i - a_2 \sin \gamma_i)^2 \tag{43}$$

be a minimum, where N is the number of samples taken in the integration interval

$$\gamma_i = 2\pi \frac{d}{\lambda} \sin \theta_i, \tag{44}$$

and a_1, a_2 are the in-phase and quadrature components related to the fringe amplitude and phase by

$$a_1 \cos \gamma_i + a_2 \sin \gamma_i = A(u, v) \cos \left[2\pi \frac{d}{\lambda} \sin \theta_i + \phi(u, v)\right]. \tag{45}$$

Then

$$A(u, v) = a_1^2 + a_2^2 \tag{46}$$

and

$$\phi(u, v) = -\tan^{-1} \frac{a_2}{a_1} \tag{47}$$

We can now solve for a_1 and a_2 from Eq. 43 by setting

$$\frac{\partial \epsilon}{\partial a_1} = 0, \qquad \frac{\partial \epsilon}{\partial a_2} = 0.$$

Solving these two equations, we obtain

$$a_1 = \frac{\sum_{i=1}^{N} y_i \cos \gamma_i - \sum_{i=1}^{N} y_i \sin \gamma_i \sum_{i=1}^{N} \cos \gamma_i \sin \gamma_i \Big/ \sum_{i=1}^{N} \sin^2 \gamma_i}{\sum_{i=1}^{N} \cos^2 \gamma_i} \tag{48}$$

$$a_2 = \frac{\sum_{i=1}^{N} y_i \sin \gamma_i - \sum_{i=1}^{N} y_i \cos \gamma_i \sum_{i=1}^{N} \cos \gamma_i \sin \gamma_i \Big/ \sum_{i=1}^{N} \cos^2 \gamma_i}{\sum_{i=1}^{N} \sin^2 \gamma_i}. \tag{49}$$

Therefore, after each integration cycle we have obtained a point in the u, v plane. The spacing between successive points in the (u, v) plane need not be any closer than

$$\Delta u \leqslant \frac{1}{2X_c} \quad \text{and} \quad \Delta v \leqslant \frac{1}{2Y_c}. \tag{50}$$

By means of inequality (50) we can calculate the maximum time interval over which we are allowed to integrate without violating the sampling theorem. From Eq. 7, after expanding in time, we have

$$(\Delta u)_{max} = \frac{d}{\lambda} \frac{2\pi}{86400} \Delta t, \tag{51}$$

where Δt is in sidereal seconds. Combining Eqs. 51 and 50, we obtain

$$(\Delta t)_{max} \leqslant \frac{1}{2X_c} \frac{\lambda}{d} \frac{86400}{2\pi}. \tag{52}$$

In Table 3 we list the maximum integration times for different baseline lengths and for X_c = 5 minutes of arc, which is typical of the width of the Crab Nebula and Cas A.

3.4 SIGNAL-TO-NOISE RATIO ANALYSIS

We shall obtain an expression of the signal-to-noise ratio for the fringe components (a_1, a_2) and for the brightness temperature distribution $T_B(x, y)$. The

Table 3. Maximum integration times for different baseline lengths. (λ=1.75 cm, X_c=5 minutes of arc.)

Baseline Length, d (m)	d/λ	Maximum Integration Time (min)
10	570	90
20	1140	45
30	1710	30
40	2280	25
50	2850	16
100	5700	8

steps involved are shown in Fig. 10. We have assumed that the multiplier is ideal; the output of the filter can be expressed as

$$v_o(k\Delta t) = \frac{1}{\Delta t}\int_{(k-1)\Delta t}^{k\Delta t} x(t)\, y(t)\, dt, \tag{53}$$

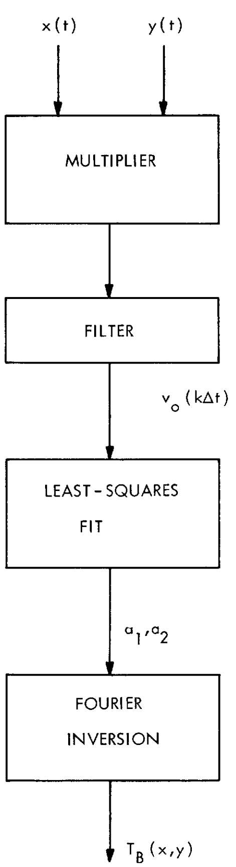

Fig. 10. Processing sequence.

where Δt is the sampling interval, and the index k varies from 0 to N. N is the ratio of $T/\Delta t$ when T is the total integration time. The fringe components a_1, a_2 are given by Eqs. 48 and 49. These equations can be simplified if we neglect the second-order terms. Then a_1, a_2 have the form

$$a_1 = \frac{\sum_{k=1}^{N} v_o(t_k)\cos\gamma_k}{\sum_{k=1}^{N}\cos^2\gamma_k} \tag{54}$$

$$a_2 = \frac{\sum_{k=1}^{N} v_o(t_k)\sin\gamma_k}{\sum_{k=1}^{N}\sin^2\gamma_k}. \tag{55}$$

The inputs x(t) and y(t) can be written as the sum of the coherent signal and the noise signal:

$$x(t) = s_1(t) + n_1(t)$$
$$y(t) = s_2(t) + n_2(t). \tag{56}$$

Both s(t) and n(t) are narrow-band Gaussian processes; any narrow-band Gaussian process can be expressed in the form[18]

$$f(t) = F(t) \cos [\omega_c t + \phi(t)], \tag{57}$$

where F(t) has a Rayleigh probability density, and $\phi(t)$ is uniformly distributed. With these definitions in mind we can now write the general expressions for $s_1(t)$ and $s_2(t)$:

$$\begin{aligned} s_1(t) &= A_1(t) \cos [\omega_c t + \alpha(t)] \\ s_2(t) &= A_2(t) \cos [\omega_c t + \alpha(t) + \phi], \end{aligned} \tag{58}$$

where ϕ is the phase resulting from the RF delay.

Let us now consider the case in which the output of the filter is sampled every Δt second and the total integration time is T.

If we now substitute in Eq. 53 the expressions for x(t) and y(t) as given in (56), we obtain

$$v_o(k\Delta t) = S_k + N_{1k} + N_{2k} + N_{3k}, \tag{59}$$

where

$$S_k = \frac{1}{\Delta t} \int_{(k-1)\Delta t}^{k\Delta t} s_1(t)\, s_2(t)\, dt \tag{60a}$$

$$N_{1k} = \frac{1}{\Delta t} \int_{(k-1)\Delta t}^{k\Delta t} s_1(t)\, n_2(t)\, dt \tag{60b}$$

$$N_{2k} = \frac{1}{\Delta t} \int_{(k-1)\Delta t}^{k\Delta t} s_2(t)\, n_1(t)\, dt \tag{60c}$$

$$N_{3k} = \frac{1}{\Delta t} \int_{(k-1)\Delta t}^{k\Delta t} n_1(t)\, n_2(t)\, dt. \tag{60d}$$

Our objective is to compute the rms noise components σ_{a_1} and σ_{a_2}. These noise terms are equal. Therefore it suffices to evaluate one of them only. By means of Eqs. 59 and 60 we can write a_1 from (54) as

$$a_1 = \frac{\sum_{k=1}^{N} (S_k + N_{1k} + N_{2k} + N_{3k}) \cos \gamma_k}{\sum_{k=1}^{N} \cos^2 \gamma_k},$$

where $N = T/\Delta t$. Since $\sum_{k=1}^{N} \cos^2 \gamma_k = \frac{1}{2} \frac{T}{\Delta t}$, we have

$$a_1 = \frac{\sum_{k=1}^{N} (S_k+N_{1k}+N_{2k}+N_{3k}) \cos \gamma_k}{\frac{1}{2} \frac{T}{\Delta t}} \tag{61}$$

The exact expression for S_k, under the assumption of a DSB system, is given in Eq. 34. For the case of white fringes we can write

$$S_k = A_o SB|V(u, v)| \cos \left[2\pi \frac{d}{\lambda} \sin \theta_k + \phi\right]. \tag{62}$$

Then

$$\sum_{k=1}^{N} S_k \cos \gamma_k = \frac{1}{2} \frac{T}{\Delta t} A_o SB|V| \cos \phi. \tag{63}$$

Substituting (63) in (61), we have

$$a_1 = A_o SB|V| \cos \phi + N, \tag{64}$$

where N is the sum of the three noise terms:

$$N_1 = \frac{\sum_{k=1}^{N} N_{1k} \cos \gamma_k}{\frac{1}{2} \frac{T}{\Delta t}} \tag{65a}$$

$$N_2 = \frac{\sum_{k=1}^{N} N_{2k} \cos \gamma_k}{\frac{1}{2} \frac{T}{\Delta t}} \tag{65b}$$

$$N_3 = \frac{\sum_{k=1}^{N} N_{3k} \cos \gamma_k}{\frac{1}{2} \frac{T}{\Delta t}}. \tag{65c}$$

Then the variance of a_1 is

$$\sigma_{a_1}^2 = \sigma_{N_1}^2 + \sigma_{N_2}^2 + \sigma_{N_3}^2.$$

Since N_1 and N_2 have the same form $\sigma_{N_1}^2 = \sigma_{N_2}^2$,

$$\sigma_{a_1}^2 = 2\sigma_{N_1}^2 + \sigma_{N_3}^2. \tag{66}$$

By using (65a), we can write the expression for the variance of N_1

$$\sigma^2_{N_1} = \frac{\sum\limits_{k,j}^{N} E(N_{1k}N_{1j}) \cos \gamma_k \cos \gamma_j}{\left(\frac{1}{2}\frac{T}{\Delta t}\right)^2}$$

$$= \frac{\sum\limits_{k=1}^{N} E\left(N^2_{1k}\right) \cos^2 \gamma_k}{\left(\frac{1}{2}\frac{T}{\Delta t}\right)^2}$$

$$= \frac{\sigma^2_{N_{1k}}}{\frac{1}{2}\frac{T}{\Delta t}}. \tag{67}$$

N_{1k} is a zero-mean random variable and is given by Eq. 60b; it is the averaged product of two Gaussian processes each with a rectangular spectrum of bandwidth B. By means of the sampling theorem we can write

$$s_1(t) = \sum_{i=1}^{2\Delta tB} \frac{1}{\sqrt{2B}} s_i\psi_i(t)$$
$$n(t) = \sum_{i=1}^{2\Delta tB} \frac{1}{\sqrt{2B}} n_i\psi_i(t). \tag{68}$$

Then (60b) becomes

$$N_{1k} = \frac{1}{2B\Delta t} \sum_{i=1}^{2\Delta tB} s_i n_i$$

and the variance of N_{1k} can be written

$$\sigma^2_{N_{1k}} = \frac{1}{(2B\Delta t)^2} \sum_{i,\ell}^{2\Delta tB} s_i s_\ell \, E(n_i n_\ell)$$

$$= \frac{\sigma^2_n}{(2B\Delta t)^2} \sum_{i=1}^{2\Delta tB} s_i^2$$

$$= \frac{\sigma^2_n}{2B(\Delta t)^2} \int_0^{\Delta t} s^2(t)\, dt.$$

The variance, σ^2_n, of the noise at the input of the multiplier is given by

$$\sigma^2_n = k\, T_R\, B, \tag{69}$$

where k is Boltzmann's constant.

The signal power is given by

$$\frac{1}{\Delta t}\int_0^{\Delta t} s^2(t)\,dt = \frac{1}{2} A_o SB. \tag{70}$$

If we substitute (69) and (70) in the expression for $\sigma^2_{N_{1k}}$, we obtain

$$\sigma^2_{N_{1k}} = \frac{kT_R BA_o S}{4\Delta t}. \tag{71}$$

Substituting (71) in (67), we obtain

$$\sigma^2_{N_1} = \frac{kT_R BA_o S}{2T}.$$

Since $A_o S = 2kT_A$, $\sigma^2_{N_1}$ becomes

$$\sigma^2_{N_1} = \frac{k^2 T_R T_A B}{T}. \tag{72}$$

In a manner similar to that for the evaluation of $\sigma^2_{N_1}$ we can compute the variance of N_3:

$$\sigma^2_{N_3} = \frac{\sigma^2_{N_{3k}}}{\frac{1}{2}\frac{T}{\Delta t}}$$

$$= \frac{E\left\{\frac{1}{\Delta t}\int_{(k-1)}^{k\Delta t} n_1(t)\, n_2(t)\, dt\right\}^2}{\frac{1}{2}\frac{T}{\Delta t}}$$

$$= \frac{\left(\frac{1}{\Delta t}\right)^2 E\left[\sum_{i}^{2B\Delta t} \frac{1}{2B} n_{1i} n_{2i}\right]^2}{\frac{1}{2}\frac{T}{\Delta t}}$$

$$= \frac{\frac{1}{(2B\Delta t)^2}\sum_{i,j}^{2B\Delta t} E(n_{1i}n_{1j}n_{2i}n_{2j})}{\frac{1}{2}\frac{T}{\Delta t}}$$

$$= \frac{\frac{1}{(2B\Delta t)^2}\sum_{i=1}^{2B\Delta t} E\left(n^2_{1i}\right) E\left(n^2_{2i}\right)}{\frac{1}{2}\frac{T}{\Delta t}}$$

$$\sigma^2_{N_3} = \frac{\frac{1}{2B\Delta t}(kT_RB)^2}{\frac{1}{2}\frac{T}{\Delta t}}$$

$$= \frac{(kT_R)^2 B}{T}. \tag{73}$$

Combining (66), (72), and (73), we obtain

$$\sigma^2_{a_1} = \frac{k^2B}{T}\left(2T_RT_A+T_R^2\right). \tag{74}$$

Usually we speak in terms of the fringe amplitude and phase that are defined by Eqs. 46 and 47,

$$A^2 = a_1^2 + a_2^2$$

$$\phi = -\tan^{-1}\frac{a_2}{a_1}.$$

The variance of A can be calculated easily if we make two reasonable assumptions: (i) that the noise components of a_1 and a_2 are Gaussian by the strength of the Central Limit theorem[18], and (ii) that $\overline{a_1}/\sigma_{a_1}$ is sufficiently greater than 1, which is true for the sources that we plan to observe. Using these two assumptions, we can show[18] that the probability density of A is approximately Gaussian with the same variance as a_1 and a_2. Then the expression for the rms deviations in A is given by

$$\sigma_A = k\sqrt{\frac{B}{T}\left(T_R^2+2T_RT_A\right)}. \tag{75}$$

The signal component of A is $A_oSB|V|$; therefore, by means of Eqs. 14 and 75, we can get the signal-to-noise ratio for the fringe amplitude:

$$\left(\frac{S}{N}\right)_A = 2T_A|V|\sqrt{\frac{B\,T}{2T_RT_A+T_R^2}}.$$

Since $T_R \gg T_A$, $\left(\frac{S}{N}\right)_A$ becomes

$$\left(\frac{S}{N}\right)_A = 2T_A|V|\frac{\sqrt{B\,T}}{T_R}. \tag{76}$$

The phase variations can be obtained by differentiating Eq. 47.

$$\Delta\phi = -\frac{a_1\Delta a_2 - a_2\Delta a_1}{a_1^2 + a_2^2}.$$

Then the phase variance is

$$\sigma^2_{\Delta\phi} = \frac{\sigma^2_{a_1}}{a_1^2 + a_2^2}$$

and

$$\sigma_{\Delta\phi} = \frac{1}{2\sqrt{B\,T}} \frac{T_R}{T_A|V|} . \tag{77}$$

In Table 4 we list the computed signal-to-noise ratios and rms phase, with the fringe visibility amplitude as a parameter, for 4 different sources. We have used the antenna temperatures calculated in Table 1.

Table 4. Fringe amplitude signal-to-noise ratios and rms phase. (T_R=1600°K, B=20 MHz, T=3 min.)

	Crab Nebula		CAS A		CYG A		3C273*	
$\lvert V\rvert$	$(S/N)_A$	$\sigma_{\Delta\phi}$ (rad)	$(S/N)_A$	$\sigma_{\Delta\phi}$	$(S/N)_A$	$\sigma_{\Delta\phi}$	$(S/N)_A$	$\sigma_{\Delta\phi}$
1	22	3°	17	4°	4.5	15°	1.5	30°
0.5	11	6°	8	8°	2.0	30°		
0.25	5.5	12°	4	16°	1.0	60°		

*3C273 is not resolved; therefore, $|V| = 1$ always.

The signal-to-noise ratio is improved when the fringe visibility is inverted to obtain the source brightness distribution $T_B(x, y)$. To show this, let us consider the simple case of a one-dimensional temperature distribution $T_B(x)$. Then

$$T_B(x) = b \int_{-d/\lambda}^{d/\lambda} [a_1(u)+ja_2(u)]\, e^{j2\pi ux}\, du, \tag{78}$$

where b is a normalization constant.

The variance of $T_B(x)$ is given by

$$\sigma^2_{T_B} = E[T_B(x)-\overline{T_B}(x)]^2 .$$

Making use of (78) and subtracting the mean, $\overline{T_B}(x)$, we obtain

$$\sigma^2_{T_B} = b^2 \iint du du'\; E[\Delta a_1(u)\Delta a_1(u')+\Delta a_2(u)\Delta a_2(u')]\, e^{j2\pi(u-u')x}$$

$$= b^2 \int_{-d/\lambda}^{d/\lambda} du\, \{E[\Delta a_1(u)^2 + E[\Delta a_2(u)]^2\}$$

$$= 2b^2\sigma_A^2 \frac{d}{\lambda}, \tag{79}$$

where σ_A^2 is given by Eq. 75.

We can now express the signal-to-noise ratio for $T_B(x)$ as

$$(S/N)_{T_B(x)} = \frac{\overline{T_B}(x)}{\sigma_{T_B}}$$

$$= \frac{1}{\sqrt{d/\lambda}} \int_{-d/\lambda}^{d/\lambda} \frac{[\overline{a_1}(u)+j\overline{a_2}(u)]\, e^{j2\pi ux}\, du}{\sigma_A}. \tag{80}$$

For a point source Eq. 80 becomes

$$(S/N)_{T_B} = \sqrt{d/\lambda}\ (S/N)_A,$$

where $(S/N)_A$ is the signal-to-noise ratio for the amplitude of each individual fringe vector.

In the discrete case d/λ corresponds to the number of points, N, in the u-v plane for which fringe vectors were measured. Thus, after inversion, the signal-to-noise ratio for a point source becomes

$$(S/N)_{T_B} = \sqrt{N}\ (S/N)_A. \tag{81}$$

IV. Ku-BAND INTERFEROMETER SYSTEM

4.1 ANTENNAS

The antennas are shown in Fig. 11. They are 8-ft dishes on equatorial mounts driven by stepping motors. At the present time, we have no indication whether the motor advances by a step each time a stepping pulse is sent by the computer. We know, however, that had the motor missed 10-20 pulses in the course of an observation the antennas would not return to their index position. The fact that they always do return indicates that no pulses are missed. At the operating frequency of 17.128 GHz the beamwidth is 30 minutes of arc. The pointing of the dishes was determined by computer-controlled sun scans; the pointing accuracy is within ±1 minute of arc. The efficiency of the dishes was estimated to be approximately 35%.

4.2 RADIOMETER

A picture of the radiometer is shown in Fig. 12 and its schematic in Fig. 13. A small amount of Dicke-switched noise, approximately 5°K, is injected in series with the signal. This noise signal is then detected by a synchronous detector and used as a continuous monitor of the gain stability of the system. More will be said about this concurrent calibration scheme.

The double-sideband noise figure, F, of the system was found to be 8 dB, and the noise temperature, T_R, is 1600°K.

The center intermediate frequency is 60 MHz and the IF bandwidth is 20 MHz. The two sidebands of each radiometer were studied by connecting a Ku-band sweeper at the input of the radiometer and observing the detected output of the IF amplifier. The results are shown in Fig. 14 for radiometers No. 1 and No. 2.

4.3 PHASE-LOCK SYSTEM

The local oscillators of the two radiometers must be phase-locked to a common stable frequency in order to preserve the coherence of the input RF signals. Figure 15 shows the complete phase-lock system for this interferometer. The two synchronizing frequencies are 28 MHz and 300 MHz; the 28-MHz frequency is generated from a 1-MHz Selzar oscillator and the 300-MHz frequency from a 100-MHz crystal oscillator. The schematic diagrams of the comb generators are shown in Appendix A.

The two synchronizing frequencies are then sent, as shown in Fig. 15, to the antenna sites where they are demultiplexed. The 57^{th} harmonic of the 300 MHz frequency is mixed with the 17.128 GHz local oscillator, thereby producing a difference frequency of 28 MHz. The difference is then compared with the reference 28 MHz frequency by means of the phase comparator; the output of the phase comparator is used to adjust the klystron reflector voltage, which completes the feedback loop.

The stability of the local oscillator is determined by the stability of the 300 MHz frequency which is one part in 5×10^7. The exact local oscillator frequency was

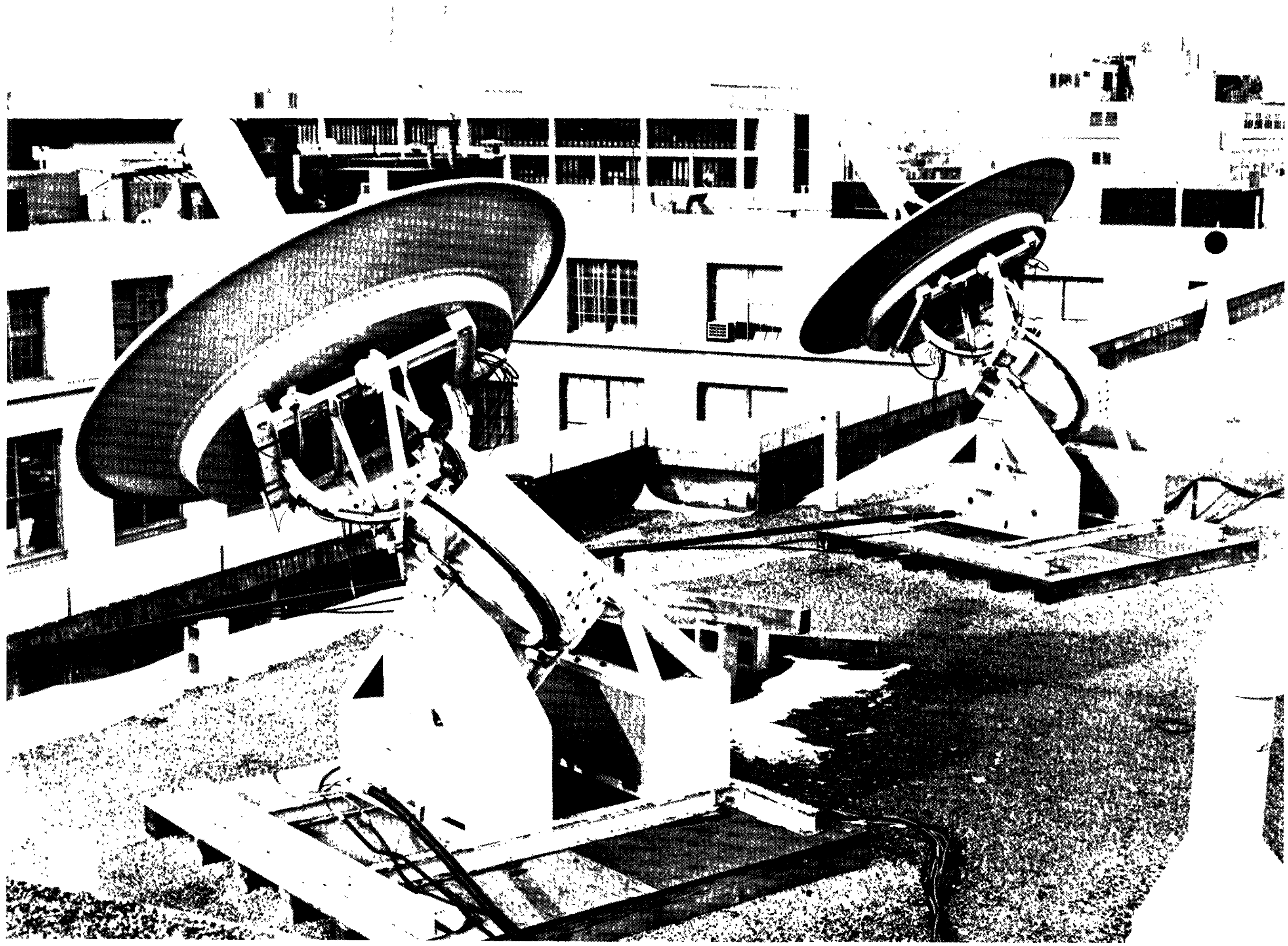

Fig. 11. Ku-band Interferometer.

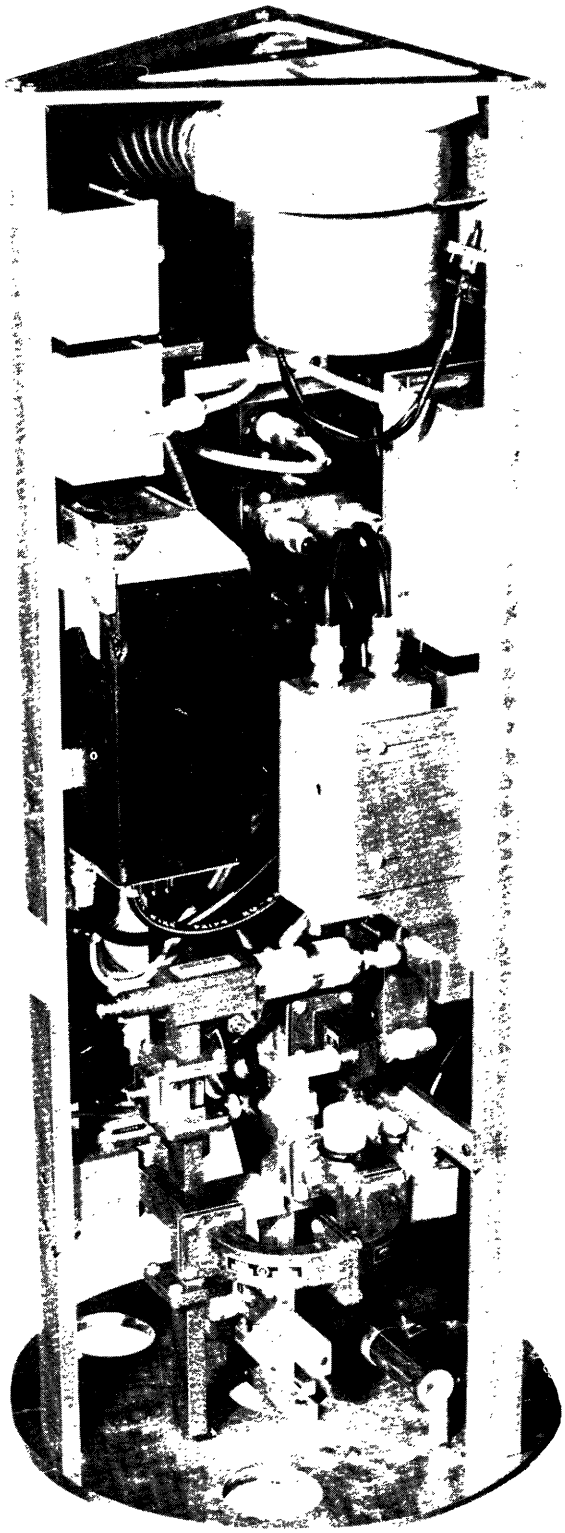

Fig. 12. Radiometer.

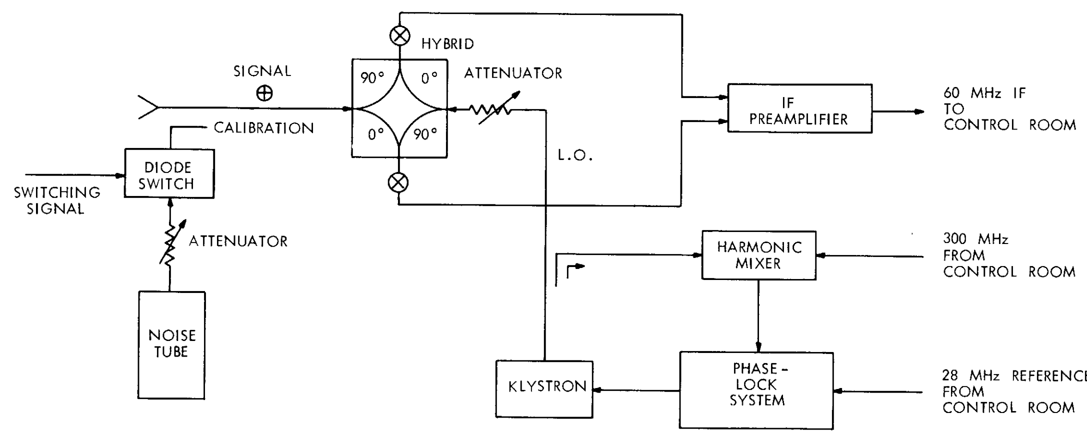

Fig. 13. Radiometer front end.

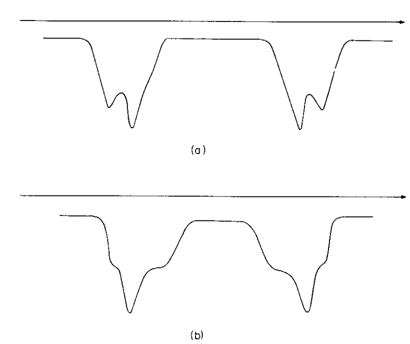

Fig. 14. Sidebands of radiometers 1 and 2.

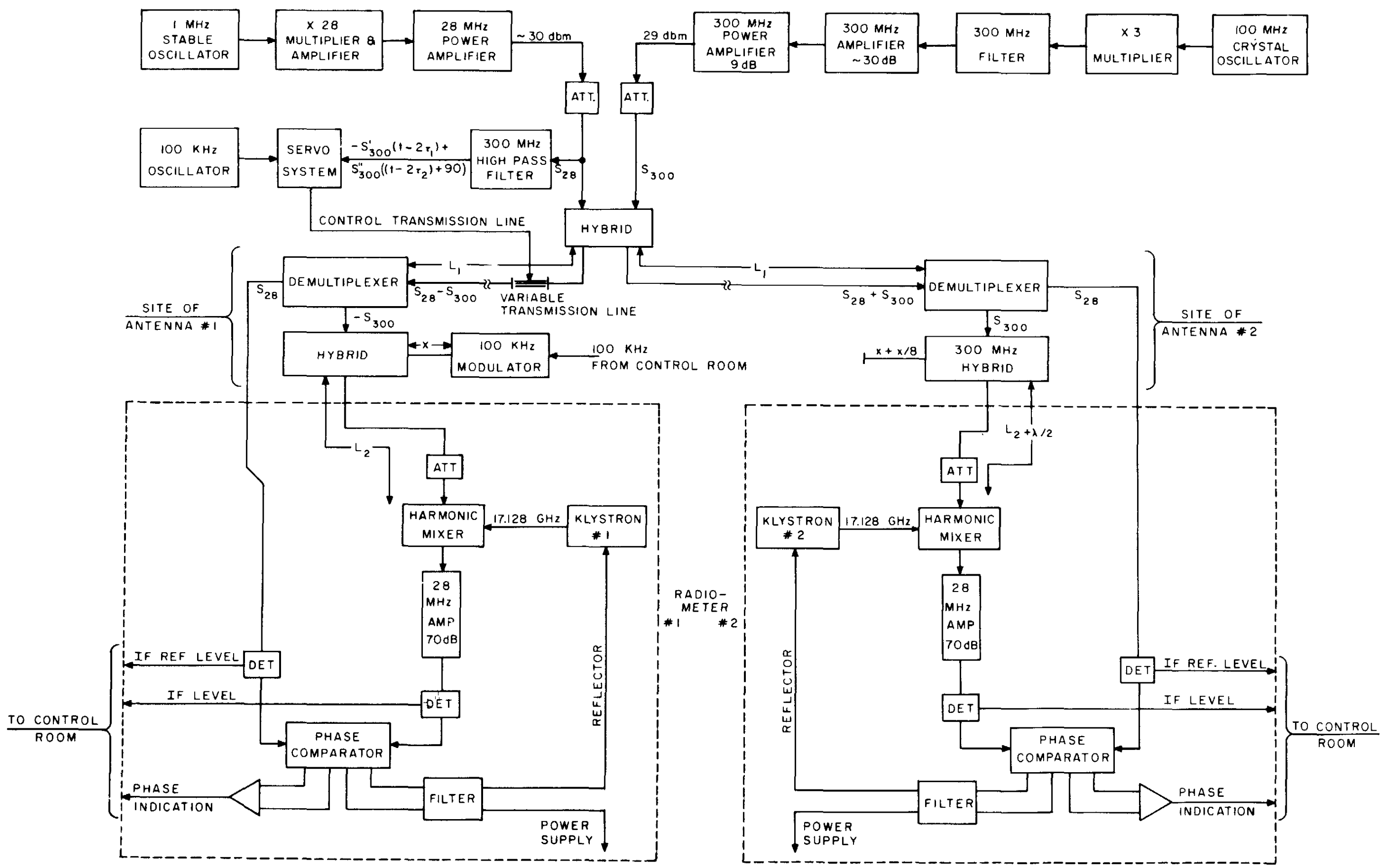

Fig. 15. Phase-lock system.

measured by a counter and found to be 17,127770; its stability was indeed between 10^{-7} and 10^{-8}.

The over-all phase stability of the system was determined by feeding a 17,188 MHz signal to the inputs of the two radiometers and monitoring the output of the correlator.

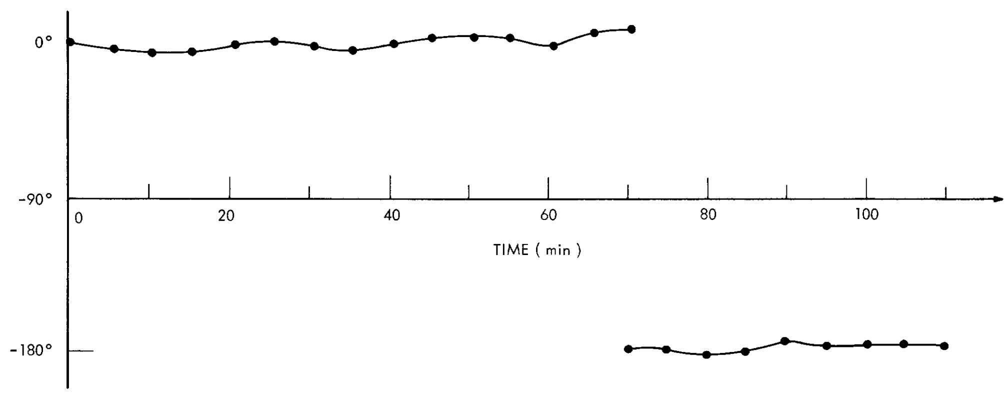

Fig. 16. Phase stability test for the Ku-band interferometer.

Figure 16 shows the output for a period of 2 hours; a 180° phase shift was introduced in one of the IF strips after 1 hour of monitoring. Over this time interval the phase stability of the system was better than 10°.

4.4 BACK END

The complete schematic of the back end is shown in Fig. 17. As can be seen from Fig. 13, the 60-MHz IF signals are transmitted from the two antenna sites to the control room where the appropriate compensation delay is inserted in the IF signal paths; the units that introduce and control the delays are called compensation boxes. The outputs of the compensation boxes are then amplified further in the postamplifiers. The IF outputs of the postamplifiers are applied to the analog multiplier, the averaged output of which is the interferometer output plus noise. The detected outputs of the amplifiers are brought to a synchronous detector where the gain calibration noise is detected.

The constituent blocks of the back end will now be explained individually.

4.4.1 Compensation Boxes

The basic function of the compensation boxes was explained in section 3.2. From Fig. 17 we see that each box has 8 delay sections varying from 1.25 ns to 160 ns. The delays were constructed by using the appropriate length of RG-9 cable; the schematic of the circuit that switches the delays in and out is shown in Fig. 18. When the delay is out the signal goes through an attenuation pad that has the same attenuation as the

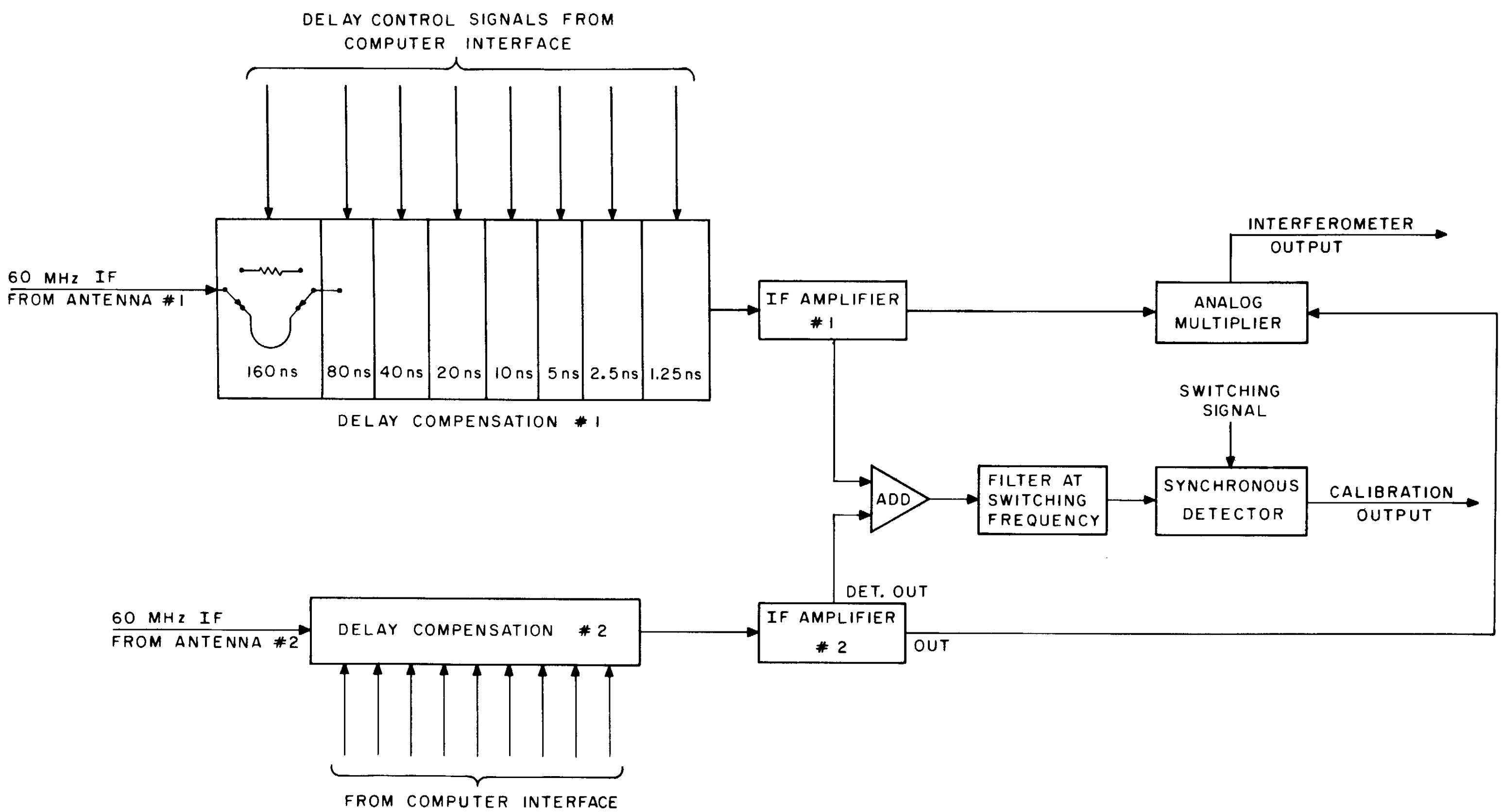

Fig. 17. Interferometer back end.

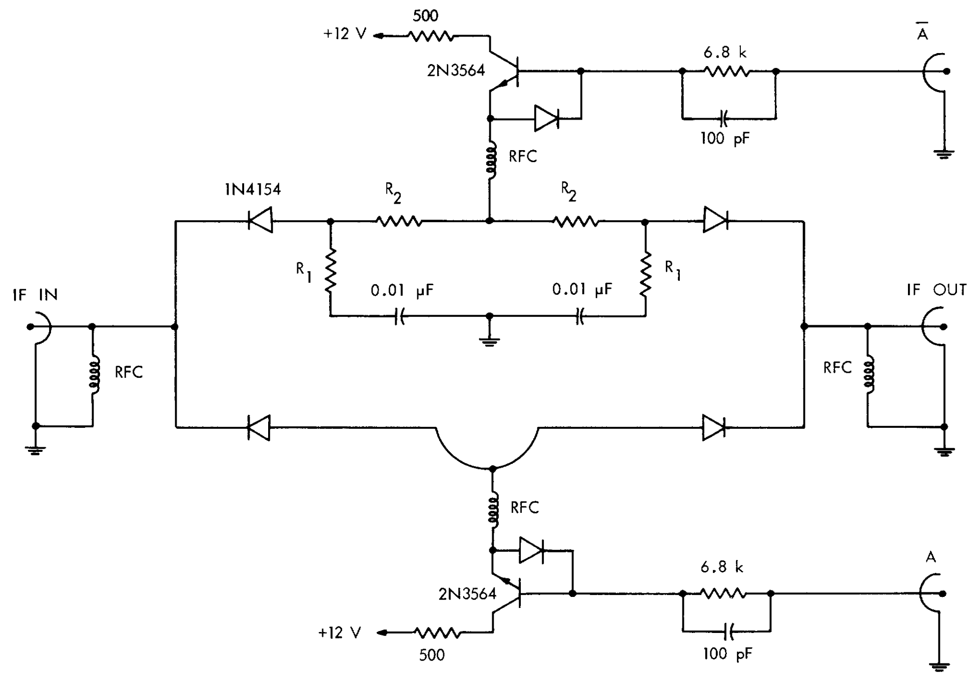

Fig. 18. Switching circuit for the compensation delays.

corresponding delay; thus, a constant total attenuation for the compensation box is maintained independent of the delays that are switched in or out. The switching signals are generated in the interface and are controlled by the program as is explained in section 4.6.2 and Section 5.26.

4.4.2 Gain Calibration

A schematic diagram of the gain calibration circuit is shown in Fig. 19. It is designed to handle the gain calibration of a four-polarization radiometer (the interferometer in its present form receives only the horizontal polarization). For instance, the four inputs to the adder-and-filter circuit are the detected outputs DET. R_1, DET. L_1, DET. R_2, and DET. L_2 of the IF amplifiers corresponding to the right circular polarization of antenna No. 1, left circular of antenna No. 1, right circular of antenna No. 2, and left circular of antenna No. 2, respectively. These four detected outputs are proportional to the temperatures of the injected calibration signals T_{CAL1}, T_{CAL2}, T_{CAL3}, and T_{CAL4}. Then the outputs OUT1, OUT2, OUT3, and OUT4 of the adder-and-filter circuit in Fig. 19 are proportional to

OUT1 ~ (DET. R_1) + (DET. R_2)

OUT2 ~ (DET. R_1) + (DET. L_2)

OUT3 ~ (DET. L_1) + (DET. R_2)

OUT4 ~ (DET. L_1) + (DET. L_2)

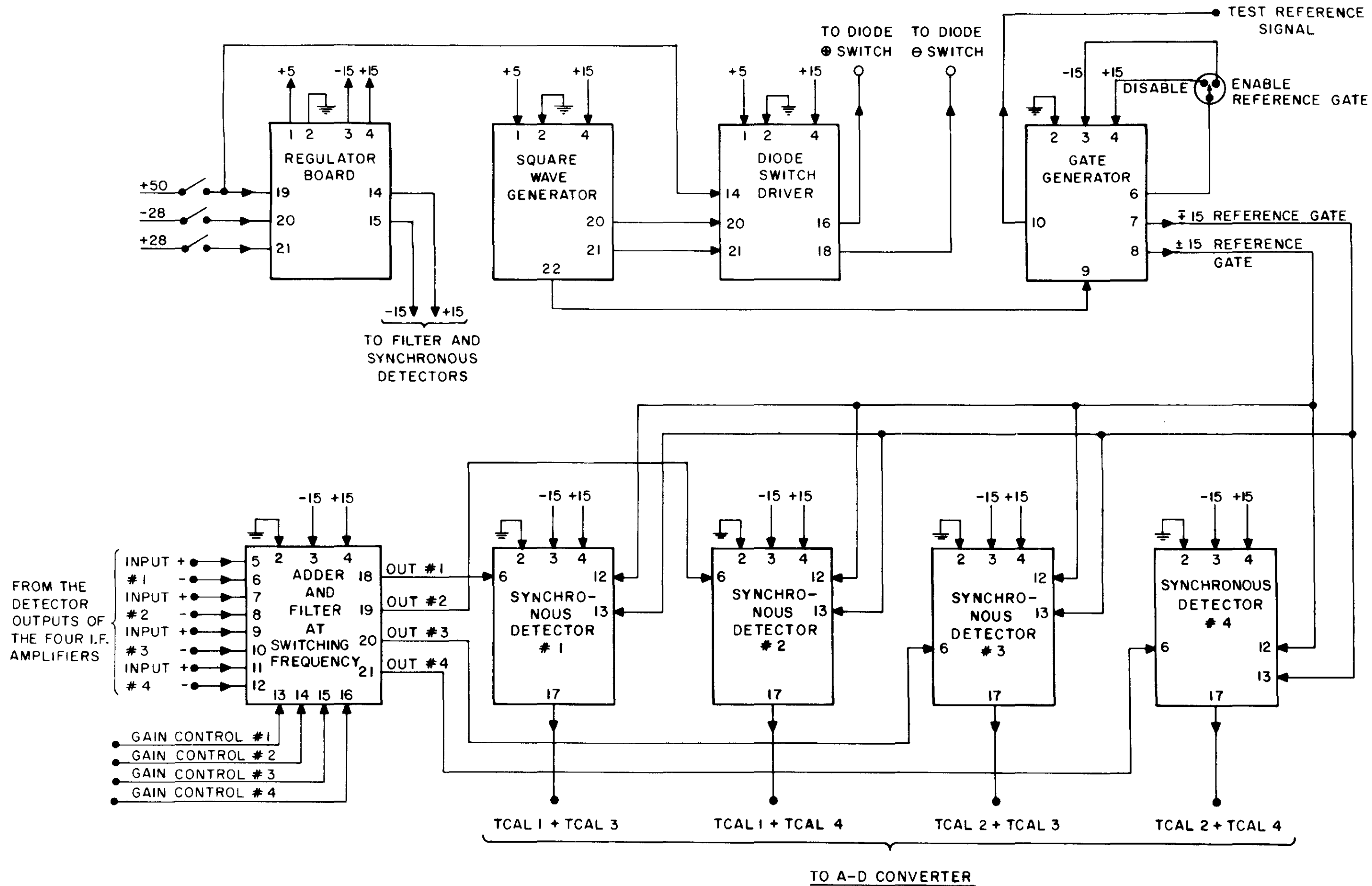

Fig. 19. Concurrent-gain calibration circuit.

These 4 outputs are next fed into 4 different synchronous detectors, the outputs of which are the calibration voltages associated with the following interferometric output signals: $\overline{R_1 \times R_2}$, $\overline{R_1 \times L_2}$, $\overline{L_1 \times R_2}$ and $\overline{L_1 \times L_2}$. The calibration voltages go to the A-D converter where they are sampled by the computer at the end of each integration cycle.

4.5 ANALOG MULTIPLIER

The analog multiplier shown in Fig. 17 gives the averaged product of the two IF signals. It has a dynamic range of 80 dB, and its frequency response is flat within 1 dB in the IF bandpass 50-70 MHz.

4.5.1 Theory and Circuit Description

The multiplication is accomplished by means of a balanced FET bridge. The field-effect transistors operate in their low-current region where their i-v characteristic is similar to that of a variable resistance. Figure 20a shows the bridge with the driving

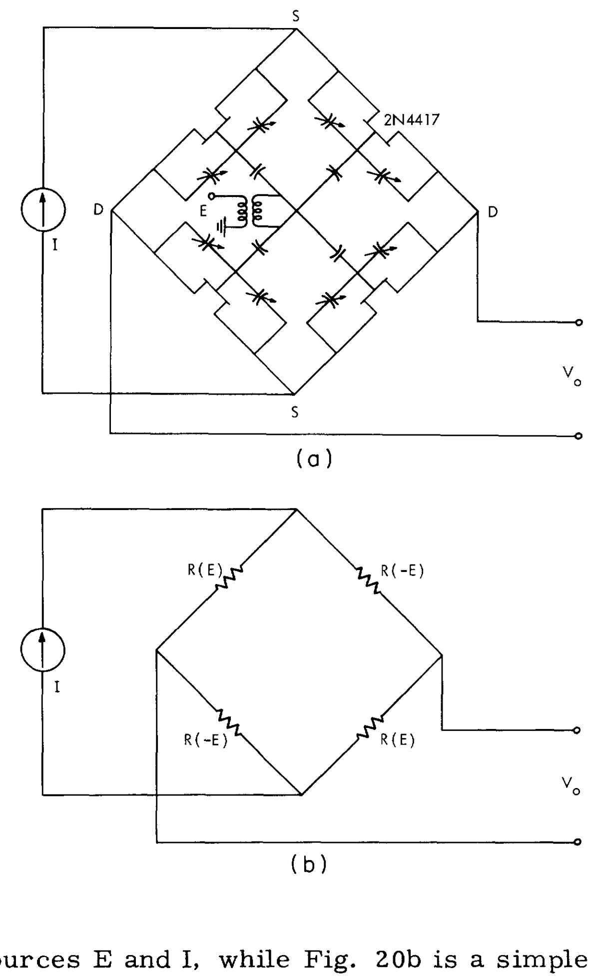

Fig. 20.
FET multiplier equivalent circuit.

sources E and I, while Fig. 20b is a simple resistive model of the bridge; this model is valid if the variable compensating capacitors shown in Fig. 20a are properly adjusted.

The 2N4417 field-effect transistors were chosen as a compromise between good high-frequency response and relatively small turn-on resistance (150 Ω). Actually, to reduce the turn-on resistance further two 2N4417's were put in parallel. Because of this low resistance, a current source is needed to drive the source terminals of the bridge. The gate terminals are driven by a balanced voltage source; this gate voltage determines the instantaneous resistance of each transistor as shown in Fig. 20b. If we now expand according to a Taylor series, we obtain

$$R(E) = R_o + R_1 E + R_2 E^2 + \ldots$$

$$R(-E) = R_o - R_1 E + R_2 E^2 + \ldots . \tag{82}$$

Then by making use of these expansions we can solve for the bridge output voltage

$$V_o \sim R_1 \; E \; I. \tag{83}$$

Equation 83 tells us that the output of the bridge is proportional to the product of the two input signals, provided that (a) the FET's have been biased properly so that they all have the same expansion (82); (b) the gate voltage drive, E, is small enough so that third-order terms can be neglected, and (c) the compensating capacitors are properly adjusted so that the output of the bridge attributable to the gate drive, E, is zero.

The complete schematic of the multiplier is shown in Fig. 21. Since geometric symmetry is very important at the frequency of operation, the source driver and the bridge were built on the same printed circuit board; the source driver uses a complementary pair of transistors (2N918 and 2N4958) to transform the voltage from input No. 1 into a current drive. The voltage inputs to the source, as well as to the gates, are brought to the printed circuit board by means of coaxial cables; these coaxial cables are also used to transmit the bias voltages for the source driver transistors and the FET's. The output of the bridge goes to a lowpass amplifier that has a gain of approximately 5×10^5; the output of this amplifier is the interferometer output.

The bridge is balanced by means of the gate bias network and the compensating capacitors. The gate bias network is adjusted so that the bridge output is zero, with input No. 2 terminated and input No. 1 driven hard. The compensating capacitors are adjusted for zero bridge output but with the input conditions reversed.

4.5.2 Tests and Evaluation

The test setup used for the measurement of the dynamic range and frequency response is shown in Fig. 22. Inputs No. 1 and No. 2 of the multiplier were obtained from the same oscillator. When the attenuators in series with the input signals are set at 45 dB the output of the multiplier is equal to the fluctuations caused by the flicker noise of the high-gain lowpass amplifier. So, 45 dB defines the lower limit of the dynamic range. The attenuation was then removed gradually by the same steps for both attenuators and in each step the output voltage was recorded.

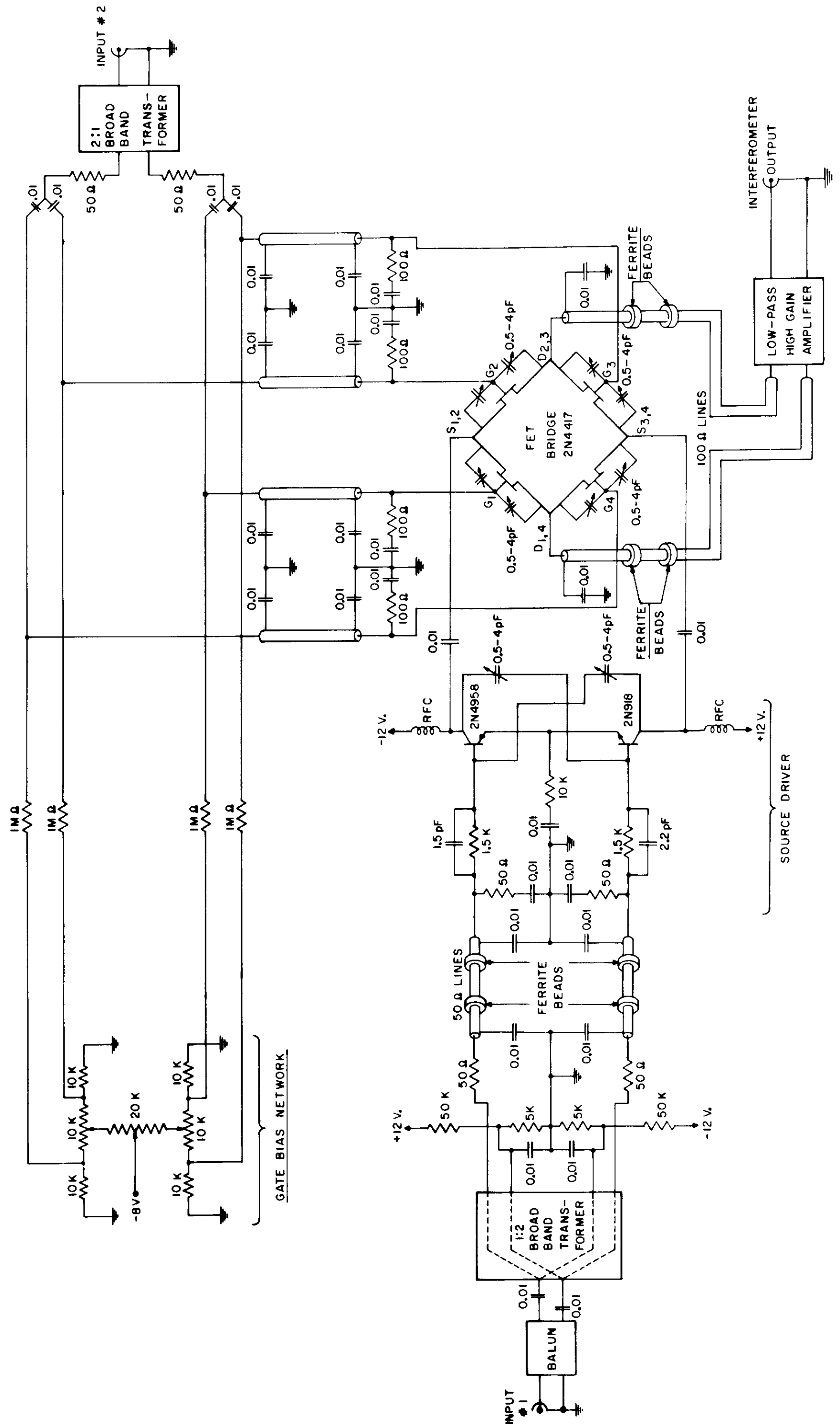

Fig. 21. Analog multiplier.

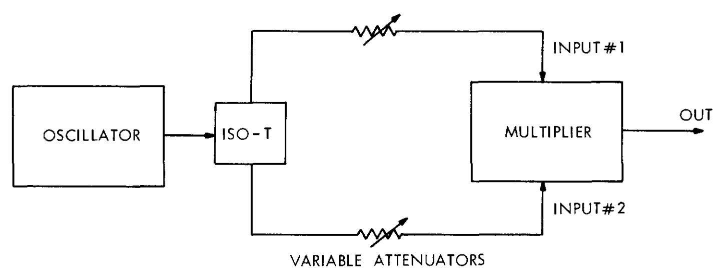

Fig. 22. Test arrangement for determining the dynamic range of the multiplier.

If the output voltage is V_i and V_{i+1} for steps i and i + 1, then the linearity condition is

$$\frac{V_{i+1}}{V_i} = 10^{\delta/10},$$

where δ is the dB amount that was taken out from each of the attenuators. The linearity condition was satisfied until both of the attenuators were down to 5 dB; thus, 5 dB sets the upper limit for the dynamic range. Then the total dynamic range is $2 \times (45-5) = 80$ dB.

Table 5. Linearity data for the analog multiplier at three frequencies.

Attenuator Settings (dB)	Output Voltage (V)		
	50 MHz	60 MHz	70 MHz
30	0.02	0.02	0.017
20	0.2	0.2	0.17
15	0.63	0.63	0.55
12	1.27	1.27	1.1
9	2.55	2.55	2.2
6	5.1	5.1	4.4
4.5	7.5	7.3	6.4

Table 5 shows the linearity data taken at 3 frequencies: 50, 60, and 70 MHz. The attenuator settings ranged from 30 dB to 5 dB. The voltage outputs at these three frequencies indicate a frequency response that is flat within 1 dB in the range 50-70 MHz.

4.6 COMPUTER-SYSTEM INTERFACE

The general functions performed by the interface are the following.

1. Sampling the interferometer output once every 0.2 s, converting the sample into

a 10-bit digital number and depositing it in the accumulator of the computer. This part of the interface is presented in Fig. 23.

2. Controlling the compensation delays by translating the computer command into the appropriate voltage levels and directing it to the appropriate delays. This part of the interface is presented in Fig. 24.

3. Generating the system clock of 0.2 s, as well as the other timing clocks of 1 s and 10 s by dividing down a 1 MHz signal. This part of the interface is shown in Fig. 25.

4. Generating the tracking pulses for the two antennas. It does this by using as a basic unit a 1-ms clock derived from the counter chain of Fig. 25. This part of the interface is shown in Fig. 26.

The communication links between the computer and interface that make possible the transfer of data and commands are the following.

1. The wires that transfer data numbers from the interface to the accumulator directly. These wires are designated in Fig. 23 as AC2-AC11.

2. The wires that transfer numbers from the accumulator buffer to the interface; these are designated as AC4-AC11 in Fig. 24.

3. The SKIP and INTERRUPT buses by means of which the interface can cause a skip or an interrupt in the program.

4. The memory buffer wires designated as MB3-MB8 in Fig. 24; these wires carry the device selection commands from the computer to the interface.

5. The buses for the input-output pulses IOP1, IOP2, and IOP4, designated as such in Fig. 24. The code numbers for these pulses are 6XY1, 6XY2, and 6XY4. The XY part of the code number is transmitted on the memory buffer wires MB3-MB8 and designates the device to which the input-output pulses are directed; for instance, if the device code is 64 then the memory buffer wires will transmit the binary number 110100.

We shall now proceed to explain briefly the four interface block diagrams.

4.6.1 A-D Converter (Fig. 23)

The analog-to-digital conversion process begins with IOT2(DS), which is the IOP2 pulse designated only for the sampling of the interferometer signals. This pulse reads into the selection device boards the code of the device that is to be sampled. This code is carried by inputs F1, F2, F3, F4; therefore, it is possible to sample 15 devices sequentially. In addition to reading in the code, IOT2(DS) performs two more functions.

1. It sets the bit-conversion flip-flop Q1 to 1 and resets the others. This brings the output of the D-A ladder right at the center of its range, 4 V. The output of the ladder is 8 V when all the flip-flops (Q1-Q10) are 1 and 0 V when they are all 0.

2. It triggers the timing circuit; this generates 10 successive pulses (TP) of 100 ns pulsewidth and separated by 0.5 μs. These pulses generate sequentially the conversion bits.

Let us say that five TP pulses have already been generated; these first five pulses will establish the final level of the first five flip-flops Q1-Q5. In addition, the fifth pulse will set Q6 to 1. The other flip-flops, Q7-Q10, will be 0. The voltage level at the output of the D-A ladder is determined by the new Q-levels. The comparator driver serves as a buffer between the D-A ladder and the comparators; its voltage output ranges between ±2 V. The output of the comparator is compared simultaneously with all of the inputs (RR, RL, etc.); this produces 8 comparison levels (C1, C2, . . . C7, C8). Only the comparison level that corresponds to the output that is currently being sampled, however, will affect the "SELECT" level coming out of the selection device board #2. This new "SELECT" level will now set a gating condition for the next TP pulse (#6). For instance, if the select level is 1, TP #6 will reset Q6 to 0; if it is 0, however, Q6 will remain 1. In addition, TP #6 automatically sets Q7 to 1.

This process continues until all 10 Q-levels have been established. The last TP(#10) generates a new pulse, STOPP, which reads the Q-levels into the level converters; the outputs of the level converters are deposited straight into the accumulator of the computer.

4.6.2 Level Converter, Gates, and Compensation (Figs. 24 and 26)

The level converter converts the memory buffer signals and the IOP pulses from the computer levels to interface levels. The converted memory buffer levels are then used in board #12 of Fig. 24 and boards #7 and #9 of Fig. 26 to produce gating conditions for IOP1, IOP2, and IOP4. The correspondence between device and code number is as follows.

1. 3, 4 are the code numbers of the teletype,

2. 31 is the code number of the "SKIP" device; this device is shown in Fig. 29 and explained in Section 5.10. The IOP pulses directed to this device are designated IOT1(31) and IOT2(31); in conjunction with the 0.2 s clock they activate the "SKIP" mechanism of the computer.

3. 35 is the code number that produces IOT1(35); this pulse controls the compensation delays that are in series with IF #1.

4. Gate #30 generates IOT1(30) which controls the compensation delays in series with IF #2.

5. Gate #36 is used in the circuit that acknowledges the interrupts from the pulses destined for the hour-angle axis of antenna No. 2; its output gated with IOP2 generates IOT2(36) which is the stepping pulse.

6. Gate #37 serves the same function as gate #36 but for antenna No. 1.

7. Gate #41 generates IOT1(41) and IOT2(41) which check whether the stepping pulses sent to the motors have been received.

8. Gate #43 generates IOT1(43) which is the stepping pulse for the declination motor of antenna No. 2.

9. Gate #45 generates IOT1(45) which is the stepping pulse for the declination motor of antenna No. 1.

As mentioned previously, IOT2(DS) starts the process of analog-to-digital conversion.

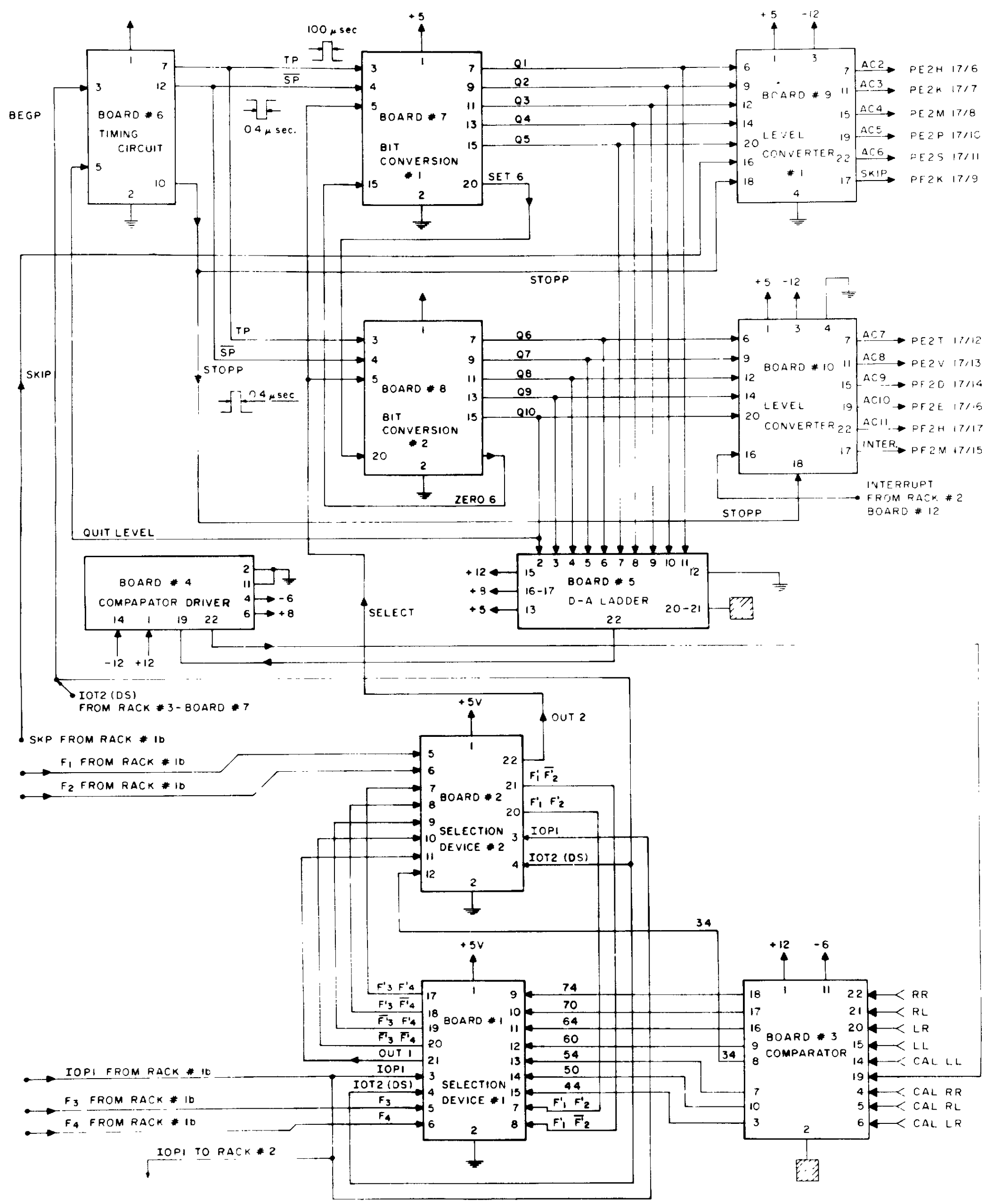

Fig. 23. A-D converter.

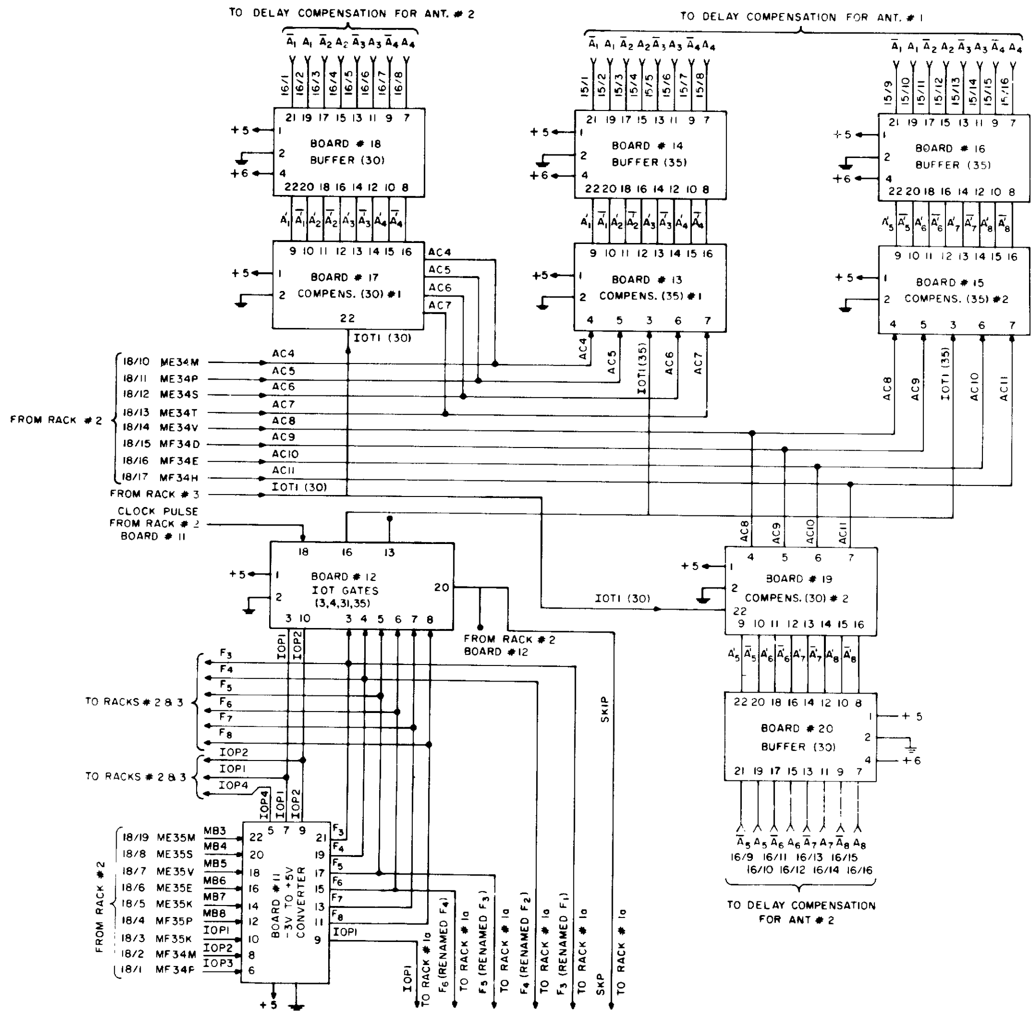

Fig. 24. Level converters and compensation-computer interface.

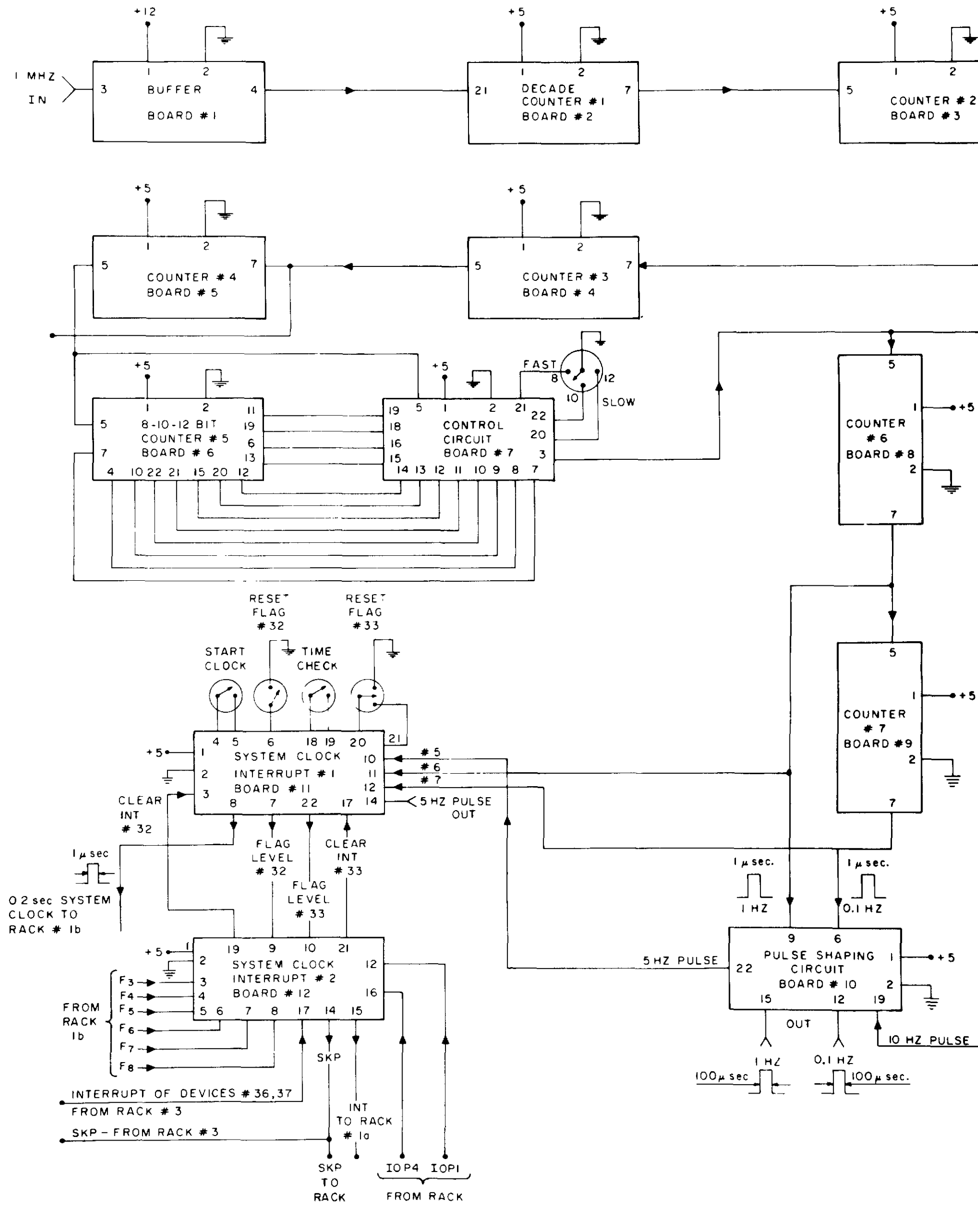

Fig. 25. Clock-computer interface.

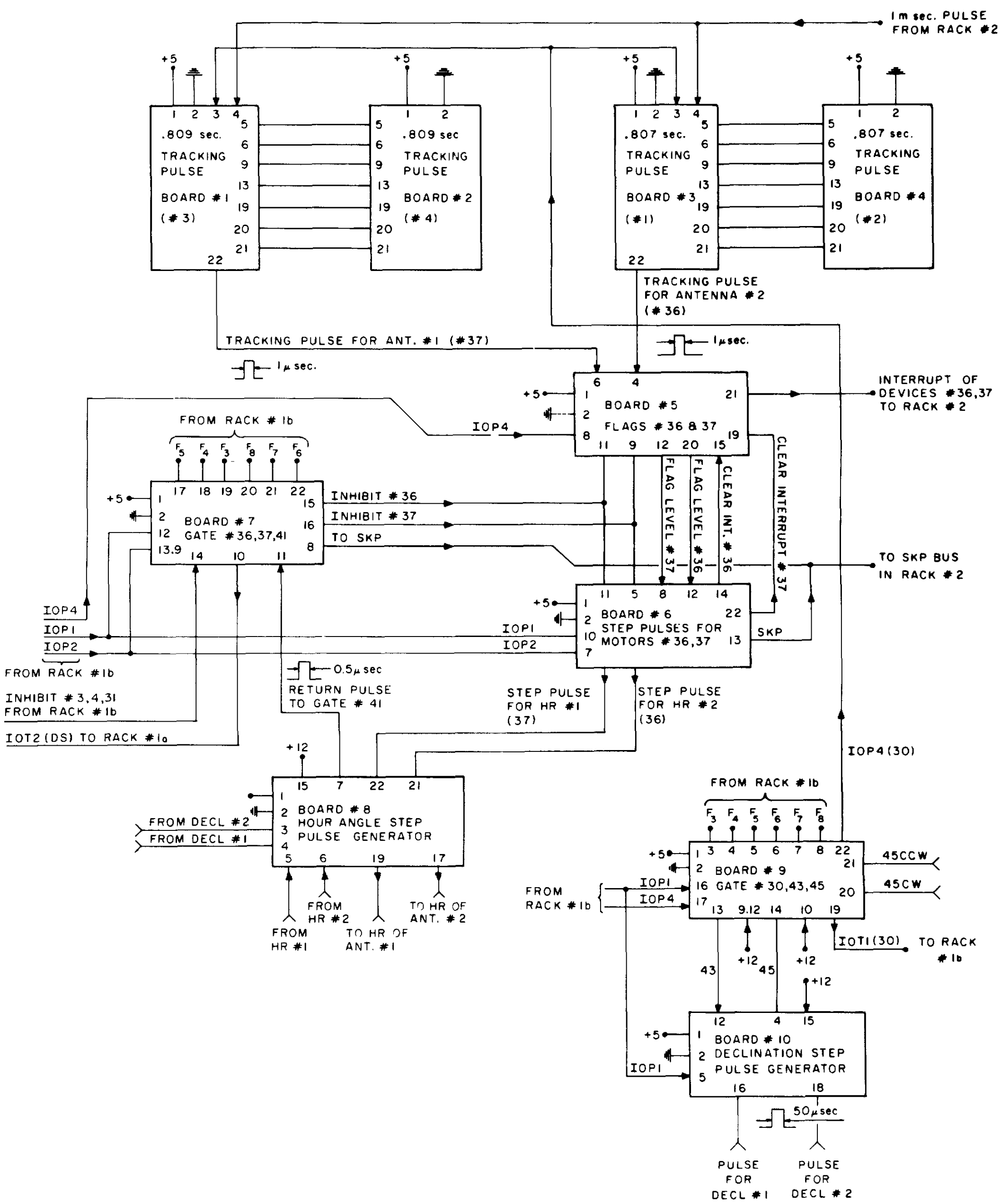

Fig. 26. Antenna-computer interface.

Therefore IOP2 is converted to IOT2(DS) only when the interferometer outputs are to be sampled. Since IOP2 is also used by the devices 3, 4, 31, 36, 37, 41, an INHIBIT gate is used to prevent IOP2 meant for these devices from getting to the A-D converter. The gate is implemented in board #12 of Fig. 24 and board #7 of Fig. 26. IOT2(DS) is generated in the latter board.

In Section 5.26, the part of the program that computes the compensation delays is explained. For instance if delay is to be added in series with IF #1, the computer will compute this delay in binary form and deposit it in the accumulator buffer from which it is transmitted to the interface on the wires labeled as AC4-AC11 (see Fig. 24). It then sends IOT1(35) which reads the information carried by the buffer wires into the compensation (35) boards. The buffer boards are used to drive the delay switching circuits (see Fig. 18). Since the delay in series with IF #2 is zero, the program will deposit zeros in the accumulator buffer; then, by means of IOT1(30), will read these zeros into the compensation (30) boards which control the delay in series with IF #2. The reverse will be true if delay is to be added in IF #2.

4.6.3 Clocks and Interrupts (Fig. 25)

The system clocks are produced by dividing down a 1-MHz signal generated from a stable oscillator. The fifth counter of the divider is coupled with a control circuit which can speed up or slow down the count. Out of the counter chain we get three clocks; 0.2 s, 1 s, and 10 s. By means of the speed-up or slow-down control circuit, the 10-s clock can be made to occur exactly on the minute within 1/2 s; then, the 1-s clock is aligned with the 1-s WWV timing signal within 5 ms. Once the clocks have been synchronized, the observation can begin; the starting procedure is explained in Section 5.10 along with the associated program. Every time a 0.2 s pulse is received by

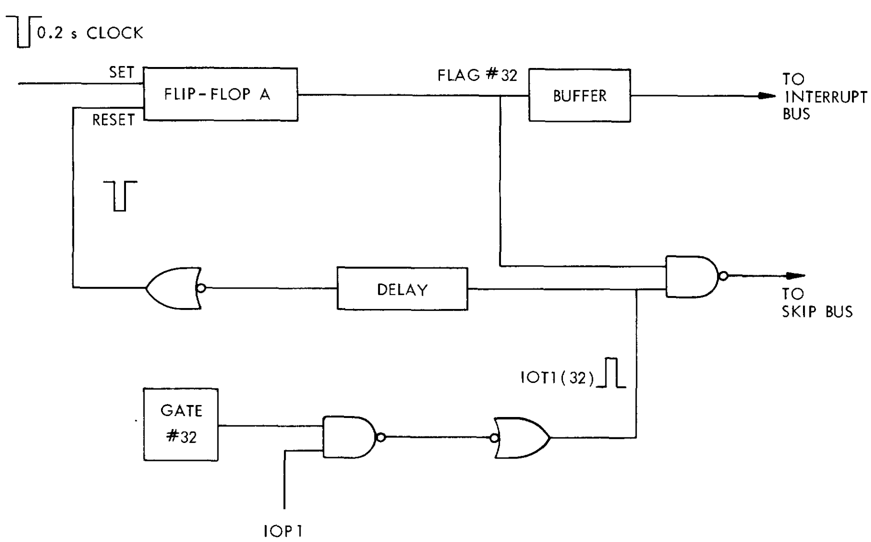

Fig. 27. Clock interrupt circuit.

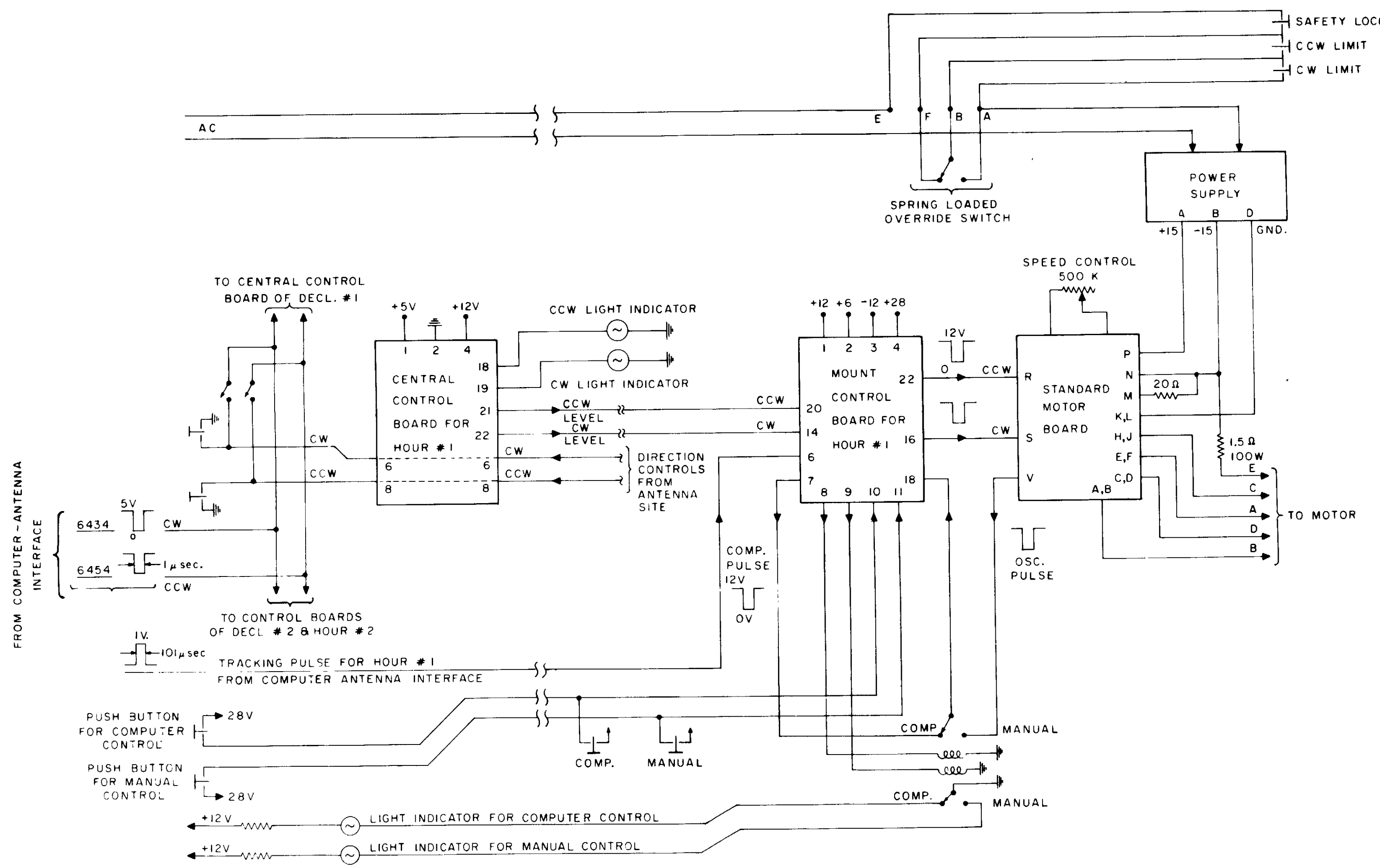

Fig. 28. Antenna and direction controls.

the computer the program increments the sidereal-time register by 0.2 (1+0.0027) s. The 0.2 s pulse is acknowledged either by the "SKIP" or the "INTERRUPT" computer mechanisms; the "SKIP" method is explained in Section 5.10.

The interrupt mechanism serves 4 devices: Device #32 associated with the clock interrupt; Device #33 associated with the time-check interrupt; and Devices #36 and #37 (explained in section 4.6.2).

When one of these devices causes an interrupt, the program will jump out of the current location and enter a routine which checks which device caused the interrupts. Figure 27 shows the implementation of the clock-interrupt method. When a 0.2 s pulse arrives, it will drive the interrupt bus to zero, thereby causing the program to enter the routine that checks which device caused the interrupt; the checking is done by gating the flag of each device with IOT1(36), IOT1(37), IOT1(32), and IOT1(33), respectively. For instance, in the case under consideration, the interrupt was caused by the clock; therefore; flag #32 in Fig. 27 is up. Thus, when IOT1(32) comes, it will drive the "SKIP" bus to zero, then the program exits the "check" routine and goes to serve the clock interrupt by adding 0.2 (1+0.0027) s to the sidereal-time register.

In addition to driving the "SKIP" bus to ground, IOT1(32) resets FLIP-FLOP A, thereby removing the cause of the interrupt.

4.7 ANTENNA CONTROL

In Fig. 28, the antenna control schematic is depicted. Two kinds of control mechanisms are included in this diagram: computer/manual control, and direction control. Both functions can be controlled either from the central room or from the antenna site.

V. PROGRAM

The program was written in machine language and all computations were done in fixed point. It was designed to perform the following general functions.

1. Accept the necessary input parameters through the teletype.
2. Point the antennas to the source and track the source.
3. Keep a record of the sidereal time by means of a stable external clock.
4. Take data.
5. Do a least-squares fit on the data.
6. Insert the appropriate compensation delay in the IF strip.
7. Decide whether to track the source or the calibration source.
8. Repeat the data-taking cycle.

The different sections of the program will now be explained. The computer organization is presented in Appendix B and the complete program listing in Appendix C.

The main program will be explained from beginning to end. To facilitate this explanation, the program is broken up into sections. These sections are identified by the numbers of the first and last registers which they contain. The numbers are in octal and vary from 0 to 7200.

5.1 — 0-117

These locations are used to store the symbols that are more commonly used and likely to be addressed from any page. The only exceptions are locations 0 and 1 which are reserved for the interrupt, and locations 10-17 which are the "self-indexing registers."

5.2 — 6510-6524

The program starts at location 6510. It clears and initiates the timing and antenna control devices in the interface and then transfers control to location 200.

5.3 — 200-226

In this section the program accepts the input parameters through the teletype by means of the SICONV subroutine supplied by DEC. These numbers are deposited sequentially by means of the self-indexing register "10" into storage locations 6610-6651. The format and function of the input parameters are given below in the order they are typed.

Number of days since January 0 of the current year

Number of integrations on the source

Number of integrations on the calibration source

Greenwich civil time (G. C. T.) in hours, minutes, seconds, and fractional seconds

Calibration source right ascension (R. A.) in hours, minutes, seconds, and fractional seconds

Source right ascension (R. A.) in hours, minutes, seconds, and fractional seconds
Baseline hour angle in hours, minutes, seconds, and fractional seconds
Calibration source declination (Dec.) in degrees, minutes, seconds, and fractional seconds
Source declination (Dec.) in degrees, minutes, seconds, and fractional seconds
Baseline declination in degrees, minutes, seconds, and fractional seconds
Baseline length in meters, centimeters, and millimeters.

5.4 — <u>227-273</u>

The input parameters corresponding to G. C. T., calibration source R. A., source R. A. and baseline hour angle have the same format and dimensions. Therefore, they are operated upon sequentially and converted into numbers of a single unit which is the unit "hours." After they have been converted they are deposited in triple precision registers and their fixed point format is

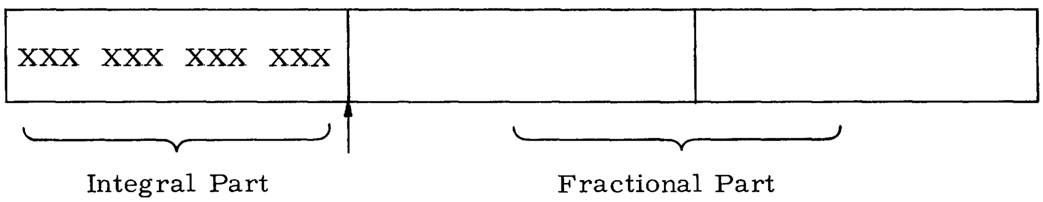

5.5 — <u>274-426</u>

The input parameters for the calibration source Dec., the source Dec. and the baseline Dec. are operated upon sequentially and converted into the units of both radians and degrees. The format for the degrees is

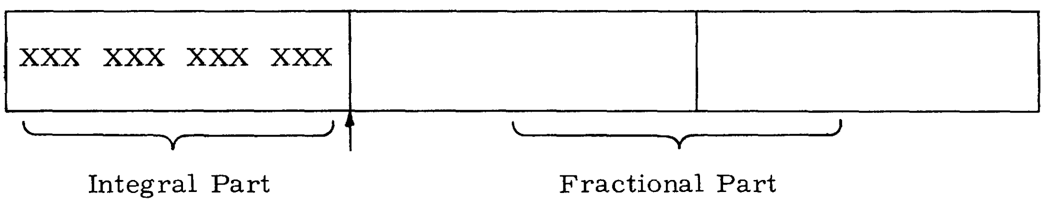

and for the radians

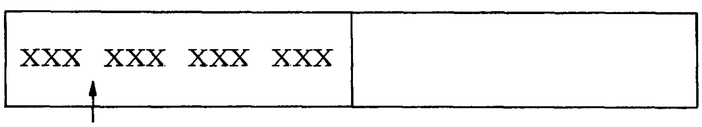

5.6 — <u>427-443</u>

The baseline length input parameters are converted into a double precision number in meter units.

5.7 — <u>444-640</u>

The G. C. T. at which the program is to start is converted into the local sidereal time (L. S. T.)

$$LST = GST - LONGITUDE$$

$$GST = GCT + SIDHRO + (UTHR) * C_1$$

$$UTHR = (NDAYS) * (24) + GCT,$$

where GST is Greenwich sidereal time, SIDHRO is Greenwich sidereal time at 0 hours of January 0 of the current year, NDAYS is the number of days that have elapsed since January 0, and $C_1 = 9.857/3600$ is the conversion factor from solar time to sidereal time.

5.8 — <u>641-667</u>

The index hour and declination of each antenna are converted into the appropriate system of units by means of the subroutine TRANSF located at address 1721. This subroutine takes a coordinate number given in (hours, minutes, seconds) or (degrees, minutes, seconds) and converts it into a triple precision number in units of hours or degrees, respectively.

5.9 — <u>670-1022</u>

As the antennas track the source a continuous record is kept of their current hour angles in registers HR1 and HR2. This is done by incrementing the contents of these registers by a fixed number each time a stepping pulse is sent to the motor drives. These numbers, which are different for the two antennas because of the different gear ratios, are computed in this section.

STEP NUMBER = (1.8 degrees/gear ratio) × (1/15) hours,

where 1.8° is the amount by which the stepping motor advances when it receives a pulse.

Next, the ratio, d/λ = baseline length/wavelength is computed and stored in register BSLAMD in the format

XXX XXX XXX XXX	XXX XXX XXX XXX
Integral Part	Fractional Part

5.10 — <u>1023-1034</u>

At this point the program halts and waits for the "START CLOCK" command. The waiting is accomplished by putting the program into a loop from which it exits when the first clock pulse arrives. The instant at which the first 0.2 s pulse arrives coincides exactly with the starting time specified in our input parameters. This is accomplished by synchronizing the 1-s and 10-s clocks derived from our stable oscillator with the WWV timing signals. Figure 29 is a diagram explaining how the starting of the clock is accomplished. The program section associated with Fig. 29 is

```
6311
6312
JMP.-1
```

Instruction 6311 generates the pulse IOTI(31) which clears the Flip-Flop B in Fig. 29. The next two instructions form a loop that is only broken when the computer "skip" bus is driven to zero; this will occur at the time when the first 0.2 s clock arrives and sets Flip-Flop B. This time is the observation starting time, and is

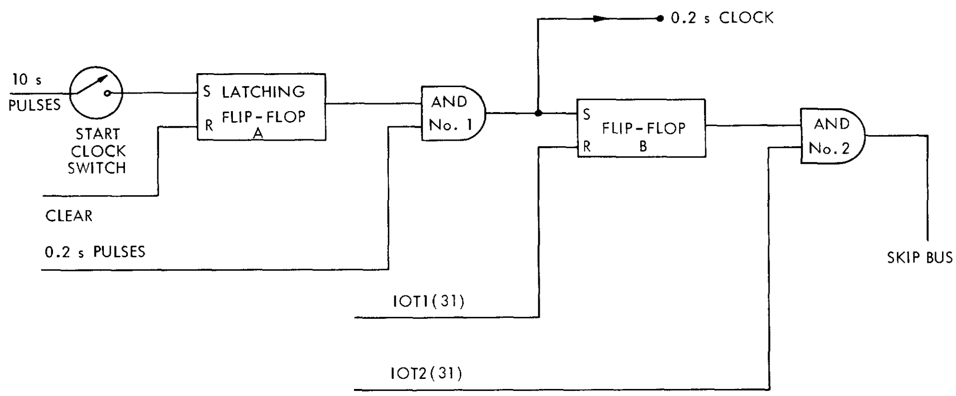

Fig. 29. Timing control diagram.

controlled by the "START CLOCK" switch which when closed allows the 10-s clock to set the Latching Flip-Flop A. Our timing signals are synchronized with those of WWV; thus the 10-s clock that sets Flip-Flop A arrives exactly on the minute specified by the observer.

5.11 – <u>1036-1052</u>

In this section the program decides whether it should point to the calibration source or to the source that has to be studied.

5.12 – <u>1053-1321</u>

Once the source to be tracked has been chosen the program addresses the registers where the declination and right ascension of the source are stored and computes the following functions:

CONST9 = h + α

$(d/\lambda)\sin D\cos\delta$, $(d/\lambda)\sin\delta\cos D$, $(d/\lambda)\cos D$, $(d/\lambda)\sin\delta\sin D$,

$(d/\lambda)\cos\delta\cos D$,

where H is the baseline hour angle, α the right ascension of the source, δ the declination of the source, and D the declination of the baseline.

5.13 — 1322-1353

The antennas are moved on the declination axis and pointed to the declination of the source. The parts of this section that are repeated many times in the course of the observation (for example, going from one source to the other or going back to the index position) are converted into subroutines. These subroutines and their locations are the following.

DEC12 (2000-2045) — common to both antennas

DEC45 (5410-5430) — for antenna No. 1 only

DEC43 (6464-6504) — for antenna No. 2 only

PULSEP (5431-5447) — common to both antennas.

5.14 — DEC12

The function of this subroutine is presented as a flow chart in Fig. 30.

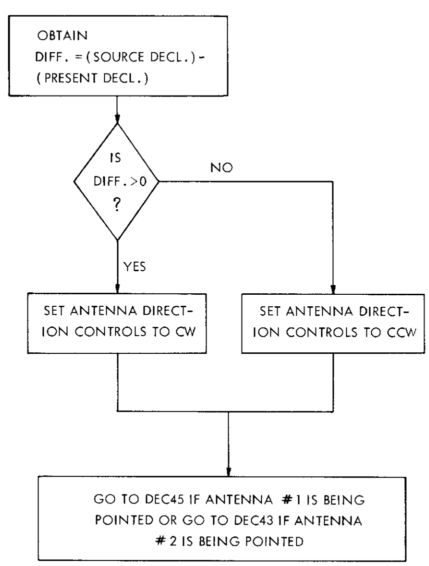

Fig. 30. Pointing the declination axis.

5.15 — DEC45 or DEC43, and PULSEP

The function of this subroutine is presented as a flow chart in Fig. 31.

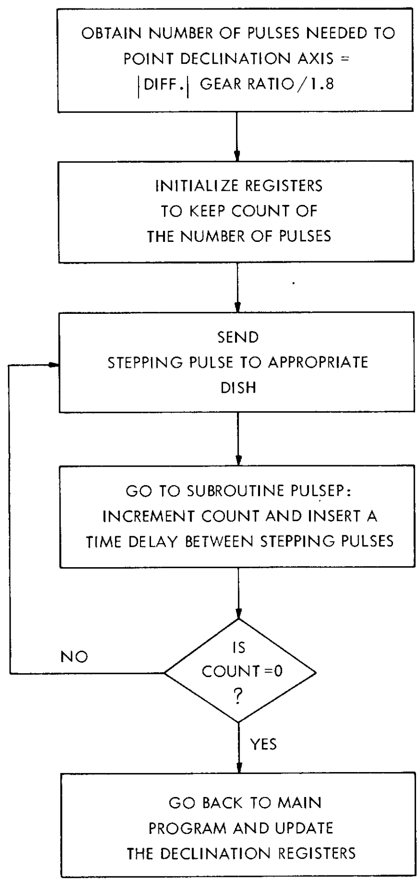

Fig. 31.
Declination pointing subroutines.

5.16 — 1400-1525

The antennas are next pointed on the hour angle axis. They are pointed ahead of the source by a fixed lead time at the end of which tracking begins. Four subroutines are used in pointing the hour angle.

HR12 (2045-2161) — common to both antennas

HR37 (1526-1550) — for antenna No. 1 only

HR36 (1551-1573) — for antenna No. 2 only

PULSEP (5341-5447) — common to both antennas.

The functions performed in this section are presented in Fig. 32.

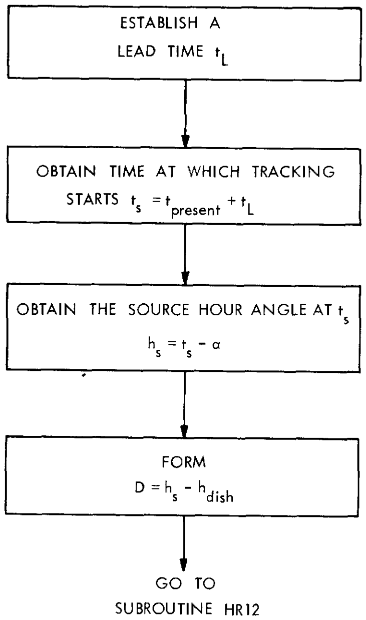

Fig. 32.
Computation of initial hour angle.

5.17 – HR12

This subroutine is presented in Fig. 33.

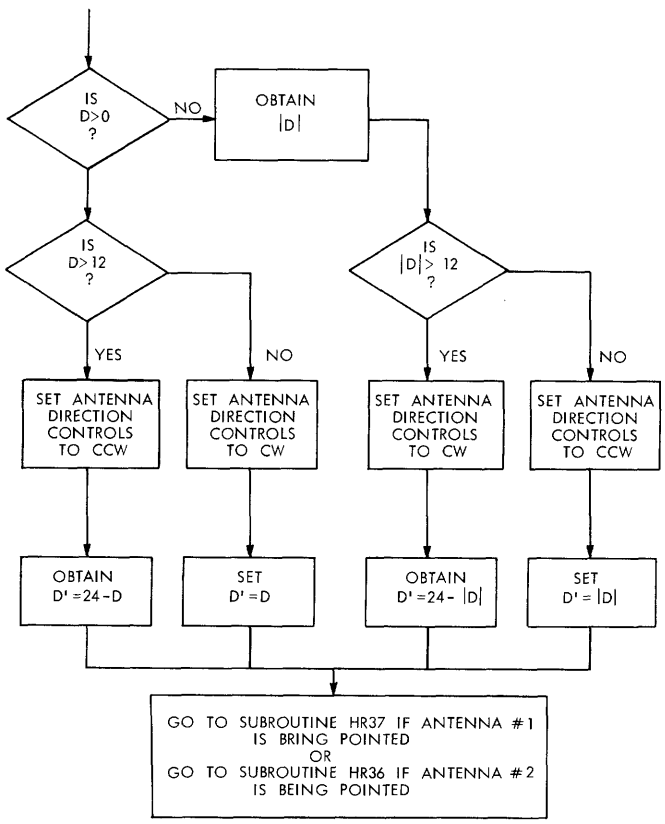

Fig. 33. Determination of direction for pointing the hour angle.

5.18 — HR37, HR36

This subroutine is presented in Fig. 34.

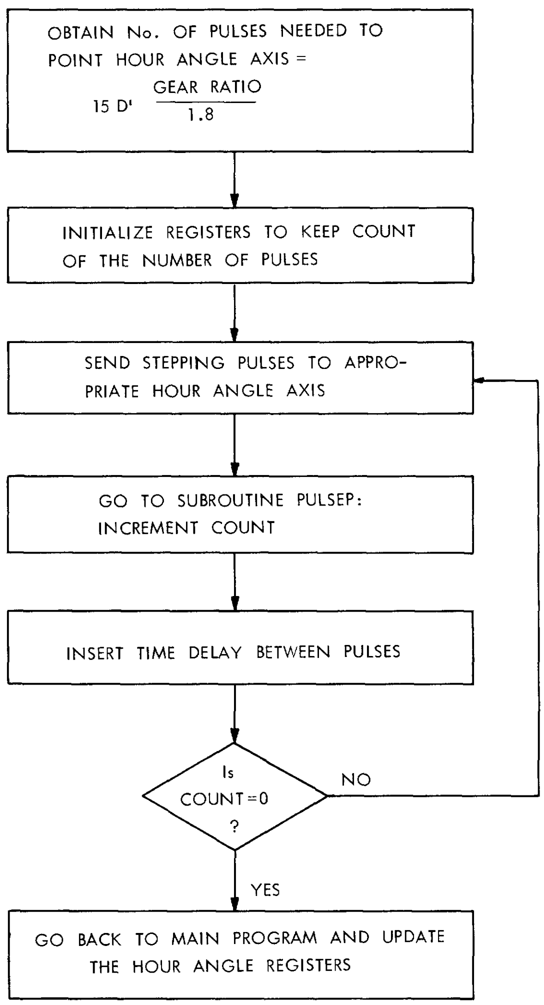

Fig. 34.
Pointing subroutines for the hour angle.

5.19 — 1600-1634

The antennas are pointed ahead of the source at hour angle $h_s = t_s - \alpha$, where $t_s = t_{present} + t_L$. Tracking the source begins when the lead time t_L expires, which is the instant when the source is at the center of the antenna beam. This section of the program receives the 0.2 s clock, increments the time t_p, and checks to see if $t_s = t_p$. If t_p is less than t_s, the program goes back and waits for the next clock. If $t_s = t_p$, the program exits the loop and goes on to set the hour angle direction controls to CW (instruction 6434) to activate the interrupt mechanism for tracking.

5.20 — 1635-1657

This section contains a loop that the program enters or exits at the command of the observer by means of the switch register. For instance, if there is a temporary

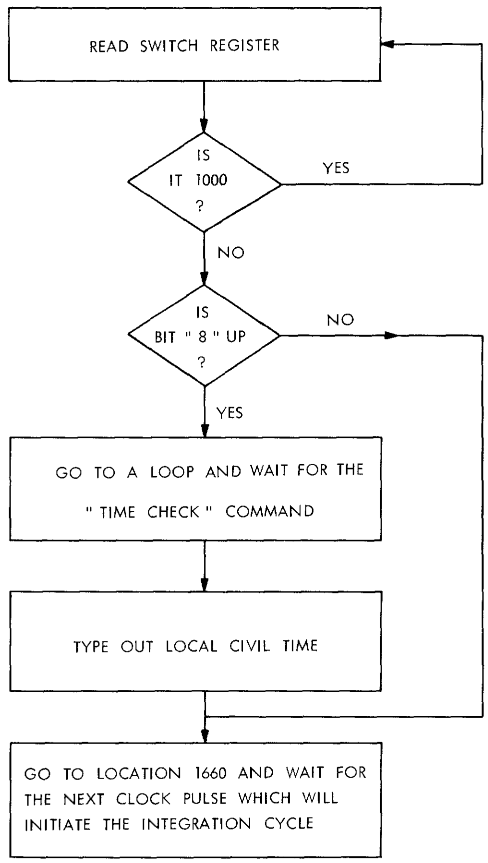

Fig. 35. Functions of Section 5.20.

malfunction in the system that would make the data meaningless, the observer orders the program to wait until the malfunction has been corrected. Another function accomplished in this section is the "time check"; that is, while the program is in this waiting loop the operator may command it to type out the local civil time. The way in which these functions are accomplished is demonstrated in the flow chart of Fig. 35.

5.21 – 1660-1720 and 2200-2442

The program goes through this section before it starts the integration cycle. It enters a loop like that described in Section 5.10 and waits for the 0.2 s clock. Let us call the time when the clock arrives t_{begin}. The program then proceeds to compute $\cos[(\pi/12)(H+\alpha-t_b)]$ and $\sin[(\pi/12)(H+\alpha-t_b)]$ by means of the cosine and sine subroutines.

These two functions are then used to compute the transform plane components u, v given by Eq. 7. These numbers are computed for a time $t = t_{begin} + \frac{T_{integr}}{2}$, where T_{integr} is the length of the integration cycle. The flow chart of Fig. 36 explains the sequence of these computations.

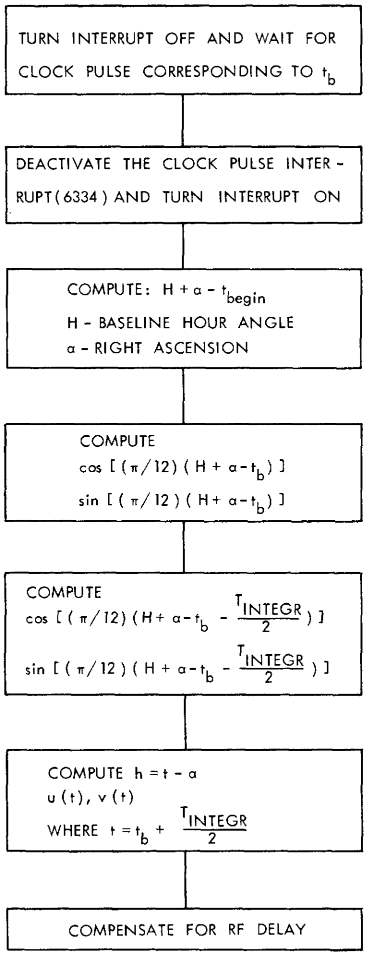

Fig. 36. Sequence of computations in Section 5.21.

5.22 — 2443-3154, 3155-3254

This section of the program accepts data from the four inputs and does the least-squares fit. The data inputs are being sampled sequentially every 0.2 s during the integration cycle. The total number of samples per input depends on the integration time. For instance, for an integration length of 6 min the number of sample will be 1800. At the beginning of each 0.2 s cycle the program waits for the clock pulse. Once the clock pulse arrives it exits the waiting loop and scans by means of IOT instructions (6743, 6703, 6643, and 6603) the four inputs. While the program is waiting for the clock pulse and during scanning of the inputs the interrupt is off. At the end of the scanning the data processing section follows, during which the interrupt is turned on so that the tracking pulses will be serviced. The clock pulse cannot cause an interrupt during this section because it has already been serviced.

The objective in this section is to compute the fringe components a_1, a_2 given by Eqs. 48 and 49.

$$a_1 = \frac{\Sigma\, y_i \cos \gamma_i - \dfrac{\Sigma \cos \gamma_i \sin \gamma_i}{\Sigma \sin^2 \gamma_i} \Sigma\, y_i \sin \gamma_i}{\Sigma \cos^2 \gamma_i}$$

$$a_2 = \frac{\Sigma\, y_i \sin \gamma_i - \dfrac{\Sigma \cos \gamma_i \sin \gamma_i}{\Sigma \cos^2 \gamma_i} \Sigma\, y_i \cos \gamma_i}{\Sigma \sin^2 \gamma_i},$$

where y_i is the data sample taken every 0.2 s, and $\gamma_i = (2\pi d/\lambda)[\sin\delta \sin D + \cos\delta \cos D \cos((\pi/12)(H+\alpha-t_i))]$. In each 0.2 s cycle the products $y_i \cos \gamma_i$, $y_i \sin \gamma_i$, $\cos^2 \gamma_i$, and $\sin^2 \gamma_i$ are being computed and added to their respective summing registers. The program first computes $\cos[(\pi/12)(H+\alpha-t_i)]$ and

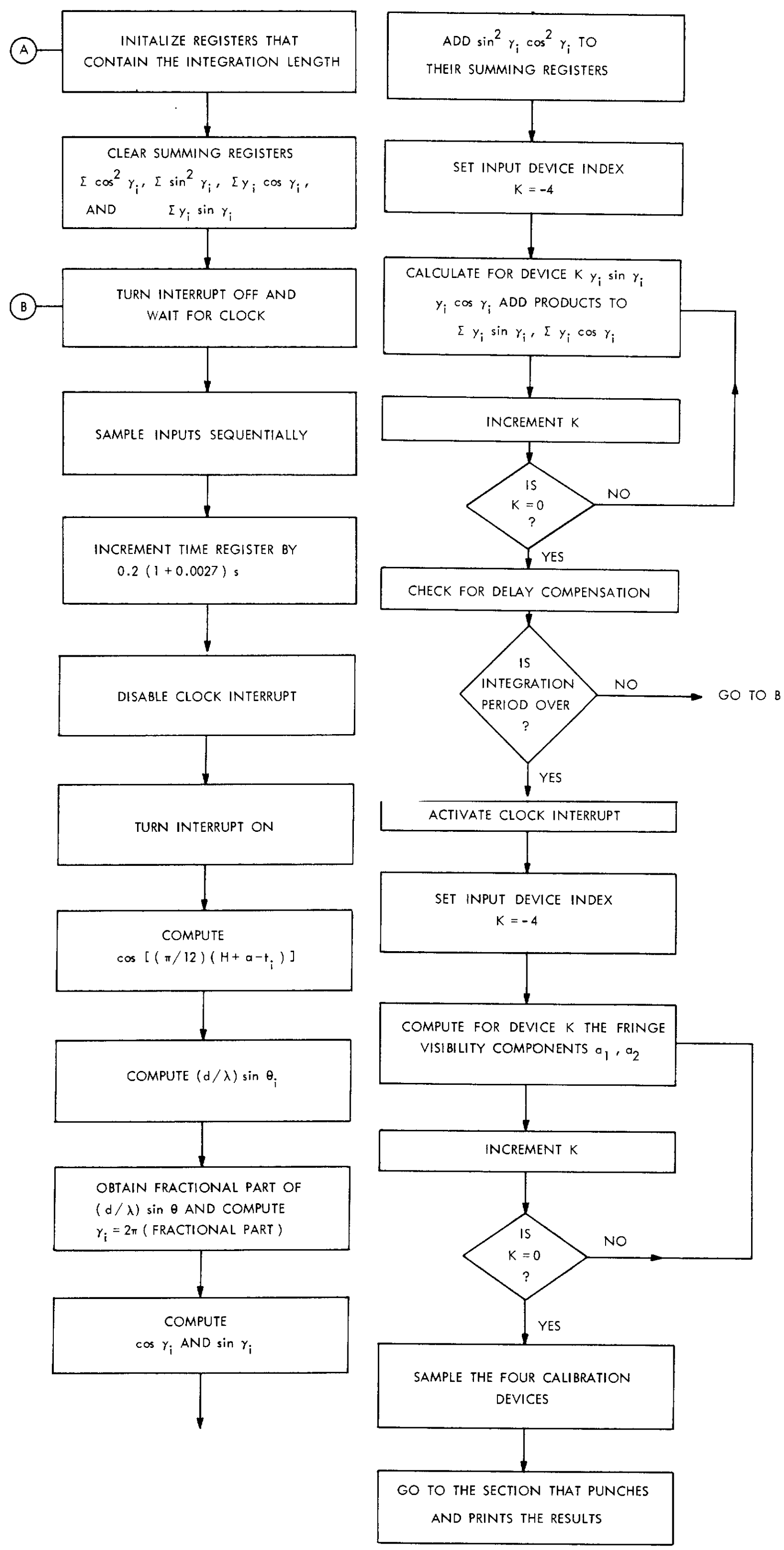

Fig. 37. Least-squares fit processing.

then it calculates $(d/\lambda)\sin\theta_i = (d/\lambda)(\sin\delta\sin D+\cos\delta\cos D\cos[(\pi/12)(H+\alpha-t_i)]$. This number has the following format:

± XXX XXX XXX XXX	XXX	

Integral Part Fractional Part

The fractional part is then separated out with the appropriate sign attached to it and multiplied by 2π. The number that we obtain is γ_i. The program then proceeds to compute $\cos\gamma_i$ and $\sin\gamma_i$, as well as $\cos^2\gamma_i$ and $\sin^2\gamma_i$. These functions are subsequently used in the least-squares fit.

The program was written to sample 4 input devices. The outputs are the circular polarization products $\langle R_1R_2\rangle$, $\langle L_1L_2\rangle$, $\langle R_1L_2\rangle$, and $\langle R_2L_1\rangle$. The least-squares fit routine is then applied sequentially to the data samples from these four inputs.

The sequence of operations in this section is exhibited by means of the flow chart of Fig. 37.

5.23 — 3264-3305

This section contains the "NEGATE" subroutine that gives the 2's complement of a triple precision number.

5.24 — 3306-3362

The subroutine "CHKARG" contained in this section checks to see whether the argument of the cosine and sine functions that must be computed is within the appropriate limits. The flow chart for this subroutine is shown in Fig. 38.

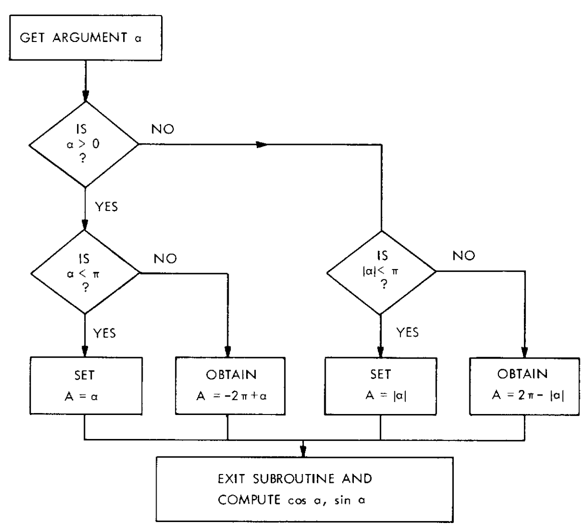

Fig. 38. Subroutine that checks the argument of the cosine and sine functions.

5.25 — 5200-5407

The fringe components a_1, a_2 computed in Section 5.22 are punched on paper tape in binary format and printed out in decimal format. Other quantities that are punched and printed out are the source hour angle, the Fourier plane variables (u, v), as well as the system gain calibration voltages. The DEC subroutine "BPUN" is used for the punching, and the subroutines "DECPRT" and "SSPRNT" are used for the printing. The binary format of the numbers to be output is the following.

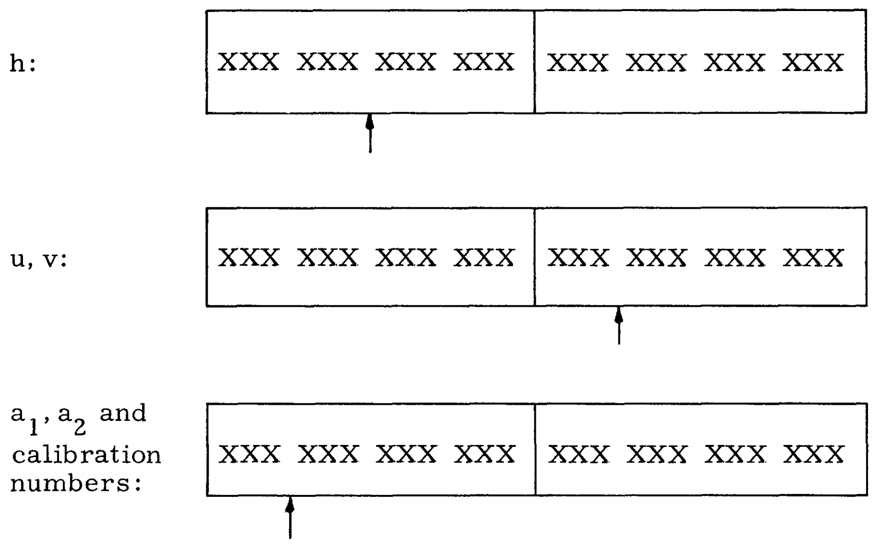

In the decimal print-out, consideration has to be given to the sign and the location of the binary point. Since the set of the (a_1, a_2) components, as well as the calibration numbers, have the same format, a single print-out routine is used for all of them.

The different functions of this section are presented in the flow chart of Fig. 39.

5.26 — 5447-5560

The "COMPEN" subroutine listed in this section generates the digital numbers that control the compensation delays whenever called for by the main program. This is accomplished by computing the difference in the signal RF paths (d/c) sin θ and then converting this difference into a digital number. For instance, if the signal arrives earlier at Antenna No. 1, the program will insert the right amount of delay in device No. 35, which is in series with the IF signal from Antenna No. 1. If Antenna No. 2 receives the radiation earlier, then delay will be inserted in device No. 30, which is in series with the signal from Antenna No. 2. The different delay values are synthesized digitally by means of 8 basic delay units: 1.25 ns, 2.5 ns, 5 ns, 10 ns, 20 ns, 40 ns, 80 ns, and 160 ns.

The flow chart of the compensation routine is presented in Fig. 40.

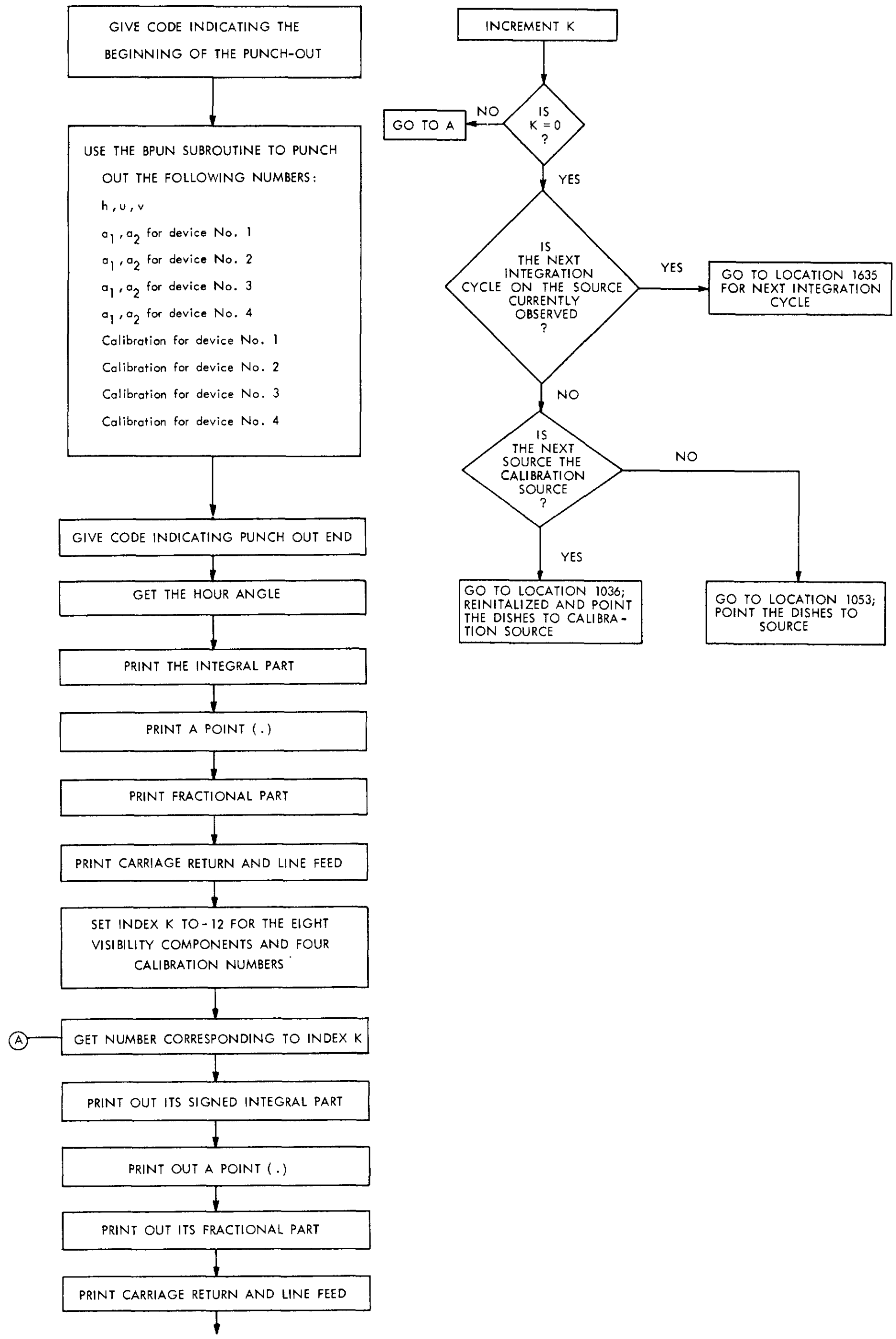

Fig. 39. Punch and print sequence.

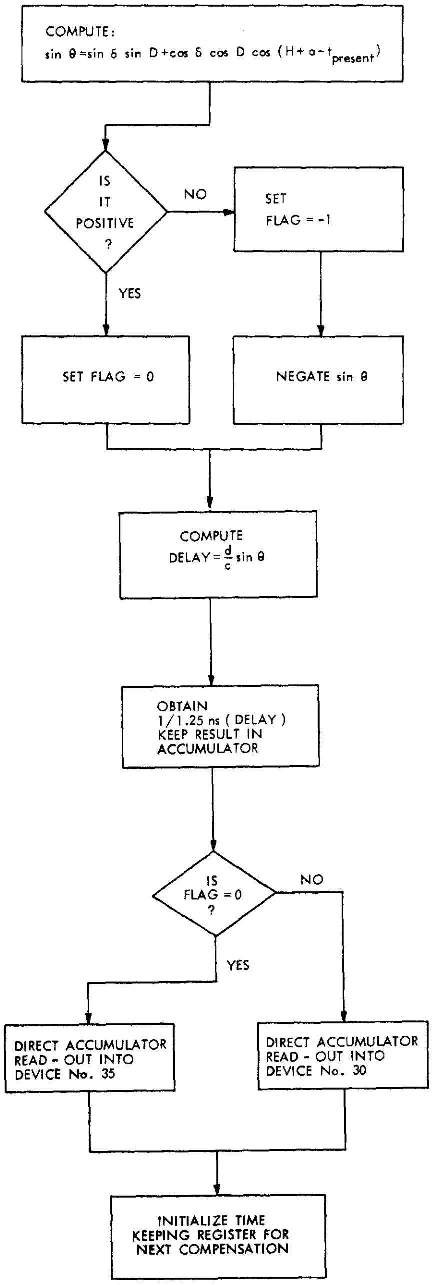

Fig. 40. Delay compensation subroutine.

5.27 — <u>5600-6135</u>

This section checks and services the interrupts. When an interrupt occurs, the location at which the program was interrupted is stored in register "0" and then the program jumps to location 5600. It deposits the contents of the accumulator and the link into auxiliary registers SAVEAC and SAVELK and then proceeds to check to see which device caused the interrupt. Interrupts are caused by the following devices:

Antenna No. 2 tracking pulses	Code No. 36
Antenna No. 1 tracking pulses	Code No. 37
Clock pulses	Code No. 32
Time check	Code No. 33

The sequence of the interrupt servicing is presented in the flow chart of Fig. 41.

5.28 — <u>6143-6464</u>

Most of the subroutines used in this program are listed in this section.

(a) <u>ROT1RT</u>

Rotates the contents of the registers TEMP1, CONTB, CONTC one position to the right. These registers contain the result of a double precision multiplication.

(b) <u>MEGI10</u>

Arranges the dividend for a double precision division in the format:

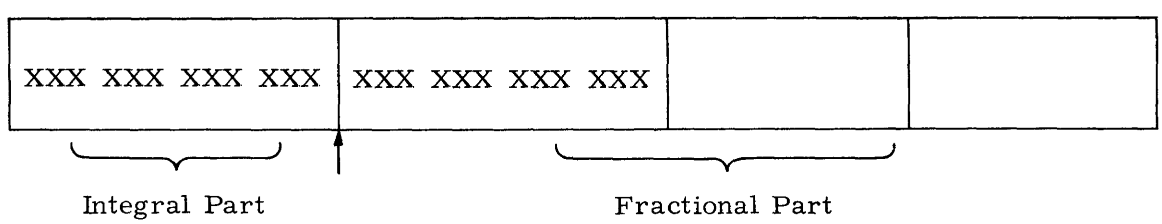

(c) <u>ROT1L</u>

Rotates the contents of the registers TEMP1, CONTB, CONTC one binary position left. As in ROT1RT these registers contain the result of a double precision multiplication.

(d) <u>ROT3RT</u>

Rotates the contents of registers TEMP1, CONTB, CONTC three positions right.

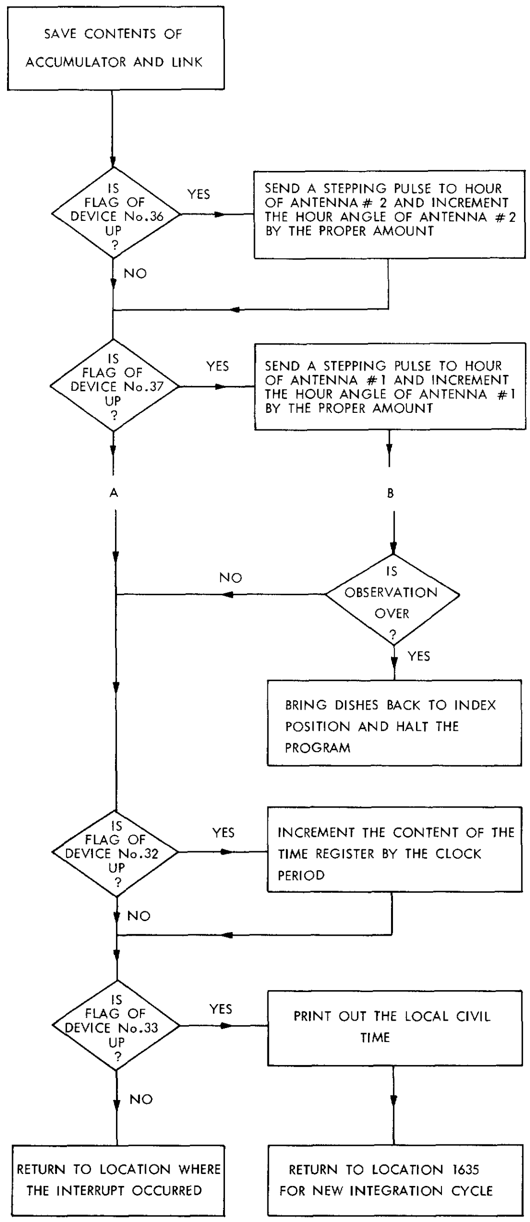

Fig. 41. Sequence of interrupt servicing.

(e) ROT3LF

Rotates the contents of registers TEMP1, CONTB, CONTC three locations left.

(f) TMINCR

Increments the present time by the clock period of $0.2(1+0.0027)/3600$ hours.

(g) ROT6LF

Rotates a triple precision number stored in registers TEMP1, TEMP2, TEMP3 six positions left.

(h) ROT2LF

Rotates the contents of registers TEMP1, CONTB, CONTC two locations left.

(i) PARA

Checks the sign of a number before rotating right.

(j) CRLF

Types carriage return and line feed.

(k) TYPEPT

Types a point (.).

(l) TYPE

Types any character when called.

5.29 – 6400-6463

The source hour angle and the u, v parameters are computed at a time corresponding to the center of the integration interval. This section calculates the functions necessary for the computation of h, u, and v. These are: $T/2$, $\cos[(\pi/12)(T/2)]$ and $\sin[(\pi/12)(T/2)]$, where T is the integration time.

5.30 – 6510-6524

The program begins at location 6510; then it proceeds to clear interrupt flags and reset the timing circuits. After this has been done it jumps back to location 200.

VI. OBSERVATIONS

The interferometer has been operational since the beginning of October 1969. The preliminary observations were made with a baseline spacing of 8 m. The eventual maximum spacing between the two antennas will be 100 m. At this time no other spacing has been tried, primarily because of the persistent problem of interference. The nature of this interference and the difficulties that it causes are discussed in section 6.2. The data are presented in section 6.4 and an interpretation is given in 6.5.

The system in general worked quite well. We achieved most of the engineering goals that we set out to reach. In view of the good phase stability, which was shown in Fig. 16, we may say that this Ku-band interferometer is a successful prototype for interferometric observations at wavelengths less than 2 cm.

With the 8-m baseline length we observed and measured fringes from the Crab Nebula, Cas A, and Cyg A. We did not detect 3C273 because interference limited the integration time.

6.1 OBSERVATIONAL PROCEDURE

The use of the PDP-8 computer made it possible to design the system so that its operation was automatic. The input parameters for starting the observation of a source have been explained in Section 5.3. At the beginning of the observation they are typed in the order listed there. Then the observer starts the clock at the prespecified minute as explained in Section 5.10. At this point the computer assumes control of the system and the observation: It points the antennas, tracks the source, inserts the right compensation delay, performs a least-squares fit on the interferometer output, and at the end of the integration cycle punches out in binary form and prints out in decimal form the source hour angle, the u, v components, the fringe components (a_1, a_2) and the gain calibration constants. At the completion of the punch-out and print-out of data, the program checks whether to continue integrating on the source or switch over to a calibration source. The observer decides whether the calibration source is to be an off-source position or a point source like 3C273 which can be used for flux calibrations.

While the program is cycling the observer cannot interfere with its operation except when he wants to make a time-check. To do that he inserts a number into the switch register of the computer and the program responds by printing out the local civil time at which the command to do so is given. At the end of the observation the antennas are brought back to the index position automatically.

6.2 INTERFERENCE: DIAGNOSTICS AND POSSIBLE SOLUTIONS

Since interference proved to be a very serious impediment, we feel that it is necessary to explain its nature and suggest possible remedies. Its nature is such that it appears only at the output of the correlator (see Fig. 17) and not at the detected IF outputs. The gain of the system is adjusted so that the peak-peak noise fluctuations at the output of the correlator are less than ± 4 V; the DC average, of course, should be zero. Because of interference, this DC level varied from ± 1 V at best to approximately ± 15 V at worst. At the fringe rates of approximately 0.01-0.02 Hz, which we get for the present baseline separation (see Table 6), these DC level variations will destroy the signal coherence for a weak source like 3C273 or upset the phase consistence for the stronger sources.

The diagnostics of the interference may be summarized as follows.

1. It can be picked up in the IF strip; this implies that it is in the IF bandpass range of 50-70 MHz. As a matter of fact, by means of a receiver we picked up 4 frequencies in this range, two of which are television stations.

2. It is present when the klystrons are off, but is much stronger when they are on. It is independent of the reflector voltage setting when the klystrons are in lock, and is still there when the klystrons are out of lock. These diagnostics imply that this is not Ku-band interference and that it is getting in either through the crystals or by amplitude modulation of the local oscillator or both. To modulate the local oscillator it must be picked up by the L. O. power cables. Filters were inserted at the end of these cables just before they go into the klystron. By doing this, we corrected part of the problem but not all of it; that is, before insertion of the filters the correlator DC level was dependent on the setting of the reflector voltage when the klystrons were in lock. That is not so any more.

3. The correlator DC level changes as much as ± 10 V when the antennas move with respect to each other; during tracking the variations are more reasonable. This is to be expected if the interference is IF and it is picked up by cables moving with respect to each other.

From these diagnostics we may say that the interference enters the system through the klystron cables or through a ground loop or both. In the first case it amplitude-modulates the L. O., and in the second case it gets into the crystals or into the input of the IF preamplifier.

Our study of the interference problem suggests both short-term and long-term solutions to the problem. The short-term solutions that we propose are as follows:

(a) Thorough checking of the system for ground loops.

(b) Rebuild all klystron cables so that they are completely shielded.

(c) Use fringe rotation technique; this can be accomplished by off-setting one of the 28 MHz reference signals (see Fig. 15), for instance, by 1 Hz.

The long term solutions that we propose are as follows:

(a) Move the antennas away from the interference.

(b) Improve the signal-to-noise ratio by using larger antennas and/or low-noise front ends.

Because of time limitations, none of these proposals has been implemented.

Table 6. Fringe rates, projected baselines and resolutions.

Baseline	: $H_L = 9^h 44^m 48^s$		$D_L = 42°30'36''$	d = 7.82 m
Crab Nebula	: α = 5 32 40		δ = 21 58 56	(X_c=4 minutes of arc)
CAS A	: α = 23 22 05		δ = 58 39 17	(X_c=4 minutes of arc)
CYG A	: α = 19 58 27		δ = 40 39 08	(X_c=100 seconds of arc)
3C273	: α = 12 27 32		δ = 2 13 08	(Point Source)

Hour Angle	Fringe Rate (Hz)				Projected Baseline ($d/\lambda \cos\theta$)				Resolution (minutes of arc)			
	Crab	CAS A	CYG A	3C273	Crab	CAS A	CYG A	3C273	Crab	CAS A	CYG A	3C273
23	0.007	0.004	0.006	0.008	410	437	445	328	8.35	7.83	7.68	10.4
0	0.013	0.007	0.01	0.014	424	432	447	360	8.05	7.92	7.65	9.49
1	0.017	0.009	0.014	0.018	440	424	445	394	7.76	8.06	7.67	8.67
2	0.02	0.011	0.0167	0.022	446	408	438	426	7.67	8.38	7.8	8.02
3	0.022	0.012	0.0182	0.024	444	387	422	444	7.70	8.84	8.1	7.7
4	0.0222	0.0121	0.0184	0.0241	428	365	400	446	7.98	9.37	8.54	7.67

6.3 FRINGE RATES AND PROJECTED BASELINE LENGTHS

In Table 6 the fringe rates, projected baseline lengths, and resolutions for four sources are listed. The hour angles at which these quantities are computed vary from 23 hours to 4 hours. This hour-angle range is most appropriate for observations with the present baseline orientation, since the fringe rates are largest in this interval; the faster the fringes, the less the effect of interference.

By studying Table 6 we notice that (a) The fringe rates are maximum at 4 h West when the sources are near setting, and (b) Resolutions change very little over an observation period of 4 h; for instance, for the Crab Nebula they change less than 5%.

The best arrangement would be one in which the fringe rates are largest around transit, since the pointing of the antennas is known best there. This arrangement can be achieved with an E-W baseline. Our baseline is almost N-S, which we had to use because of the shape and orientation of the building on which the antennas were placed. The E-W baseline is actually the optimum orientation because with it a larger portion of the u-v plane can be mapped than with an N-S baseline[7]; for instance, for the Crab Nebula, with an E-W baseline, the projected baseline vector would change by at least a factor of 2 in an observation interval of 4 h. Therefore it is clear why an E-W baseline is strongly recommended in a future rearrangement of the interferometer.

6.4 INTERFEROMETER DATA

We shall present some of the interferometric data that we took on Cyg A, Cas A, and the Crab Nebula. The data are listed in Tables 7-21. The quantity A is the fringe amplitude in millivolts, and ϕ is the fringe phase in degrees. They were calculated from the measured fringe components a_1 (in-phase) and a_2 (quadrature). The fringe amplitude is $\sqrt{a_1^2 + a_2^2}$, and the fringe phase is $-\tan^{-1} a_2/a_1$.

The data were taken by integrating 12 min on the source and then 12 min off the source. Interference was there all of the time; its presence is evident from the large fringe components that we obtained on the off-source position. Because of the corruption of the data by interference, no information could be obtained about fringe visibility variations with hour angle, and no accurate estimation of the baseline parameters could be made.

In Figs. 42-49 we show vectorially the data listed in Tables 7-21. The amplitudes of the vectors in each observation were normalized with respect to the maximum signal vector of that particular observation. In each figure we have drawn the signal and noise vectors from two successive observations on the same source. This vector representation makes it easy to discuss the behavior of the fringe amplitude and phase during the course of a single observation and also to compare the phase variations for two successive observations. No comparison, however, should be made of the amplitudes obtained in the two successive observations, because of the way in which they were normalized.

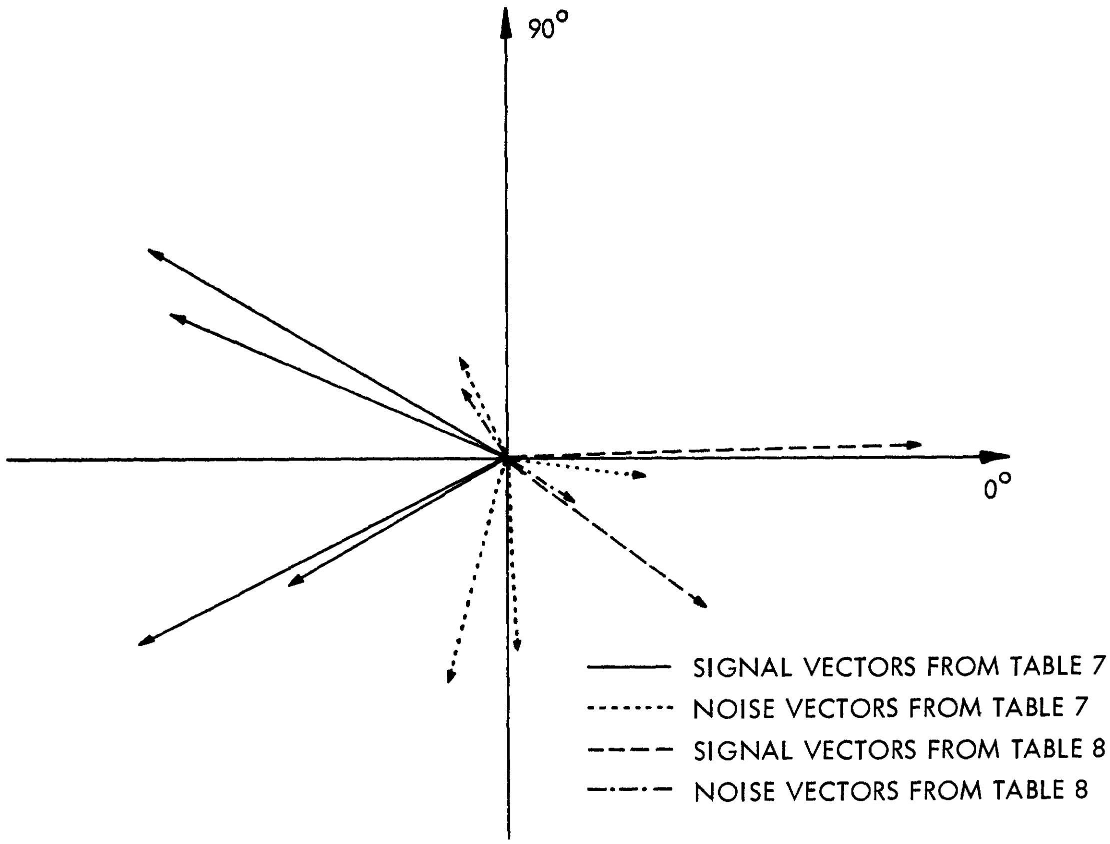

Fig. 42. Vector representation of data in Tables 7 and 8.

Table 7. CYG A – October 12, 1969.

Hour Angle	ON		OFF	
	A (mV)	ϕ (deg)	A (mV)	ϕ (deg)
23.57	91	-150		
0.03			39	114
0.2	135	157		
0.64			50	-6
0.79	152	150		
1.25			86	-105
1.42	151	-153		
1.86			68	-90

Table 8. CYG A – October 16, 1969.

Hour Angle	ON		OFF	
	A (mV)	ϕ (deg)	A (mV)	ϕ(deg)
1.56	48	-35		
0.95			18	119
1.07	83	0		
1.46			16	-35

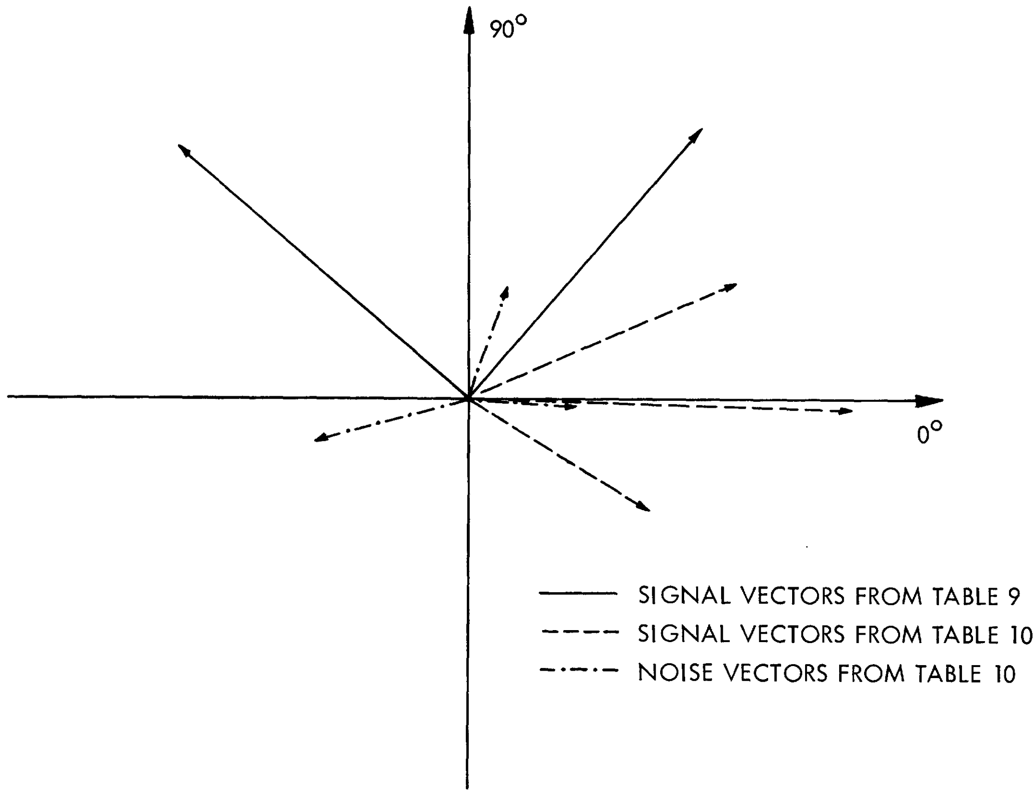

Fig. 43. Vector representation of data in Tables 9 and 10.

Table 9. CAS A — October 21, 1969.

Hour Angle	ON	
	A (mV)	φ (deg)
2.38	89	140
2.70	82	50

Table 10. CAS A — October 26, 1969.

Hour Angle	ON		OFF	
	A (mV)	φ (deg)	A (mV)	φ (deg)
3.37	52	23		
3.80			20	-3
3.90	69	-2		
4.34			31	-167
4.44	38	-32		
4.86			20	70

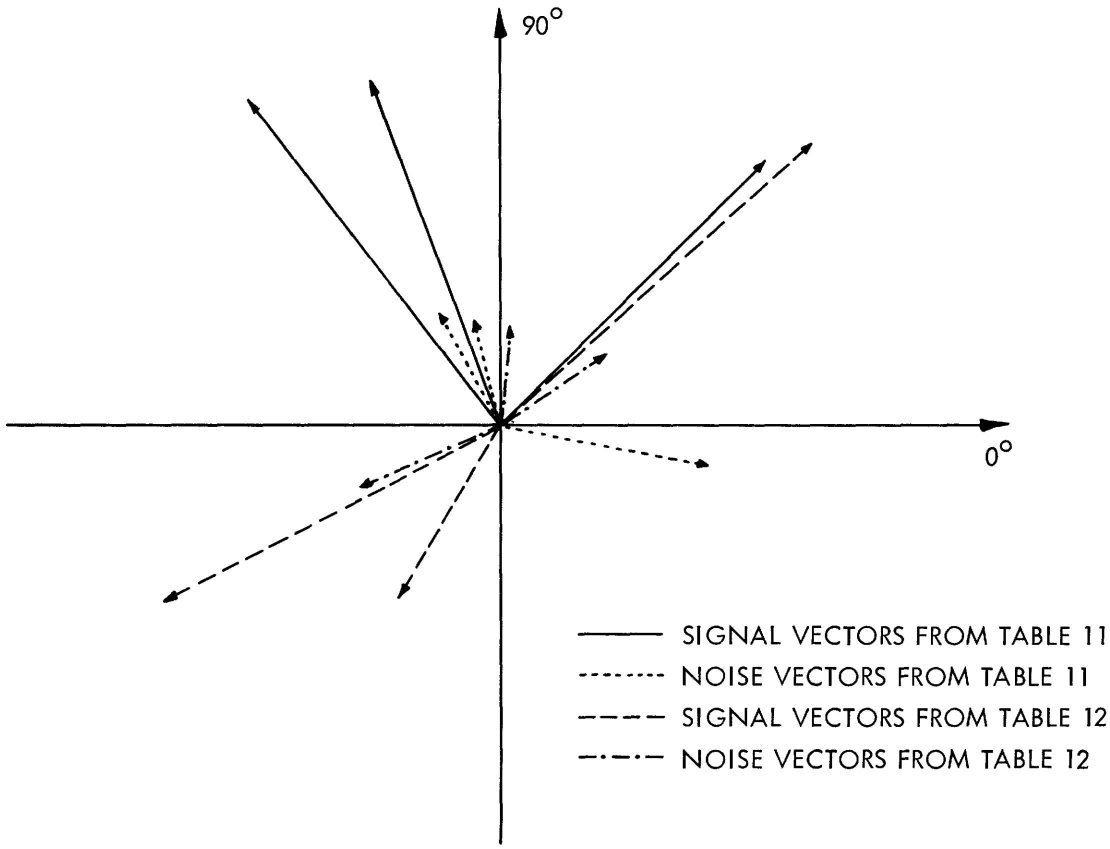

Fig. 44. Vector representation of data in Tables 11 and 12.

Table 11. CAS A – October 30, 1969.

Hour Angle	ON		OFF	
	A (mV)	ϕ (deg)	A (mV)	ϕ (deg)
3.29	56	128		
3.72			15	109
3.79	50	46		
4.22			28	10
4.29	50	111		
4.71			16	120

Table 12. CAS A – November 19, 1969.

Hour Angle	ON		OFF	
	A (mV)	ϕ (deg)	A (mV)	ϕ (deg)
1.01	61	-122		
1.55			27	38
1.69	116	-152		
2.16			29	90
2.3	124	44		
2.79			49	-157

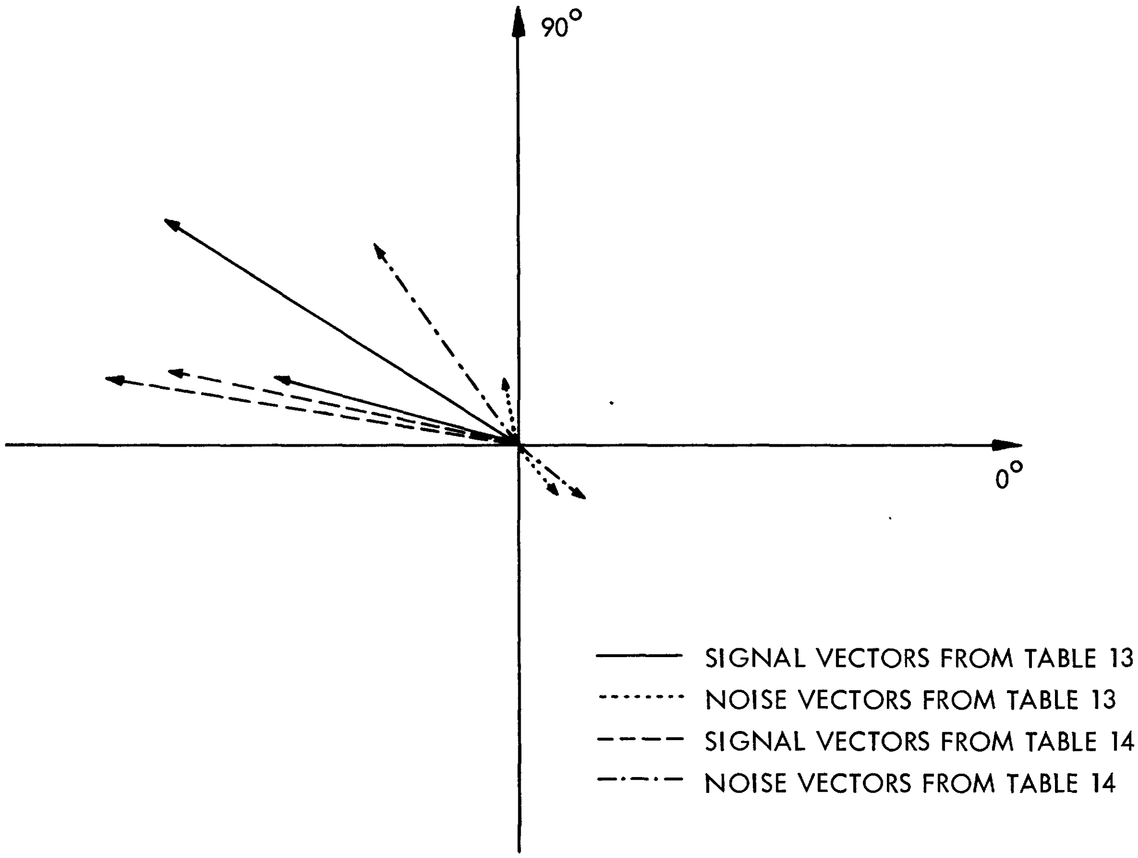

Fig. 45. Vector representation of data in Tables 13 and 14.

Table 13. CAS A — December 3, 1969.

Hour Angle	ON		OFF	
	A (mV)	ϕ (deg)	A (mV)	ϕ (deg)
1.17	22	166		
1.60			6	100
1.70	36	147		
2.14			7	-51

Table 14. CAS A — December 5, 1969.

Hour Angle	ON		OFF	
	A (mV)	ϕ (deg)	A (mV)	ϕ (deg)
1.28	64	170		
1.73			40	126
1.83	53	168		
2.27			4	-45

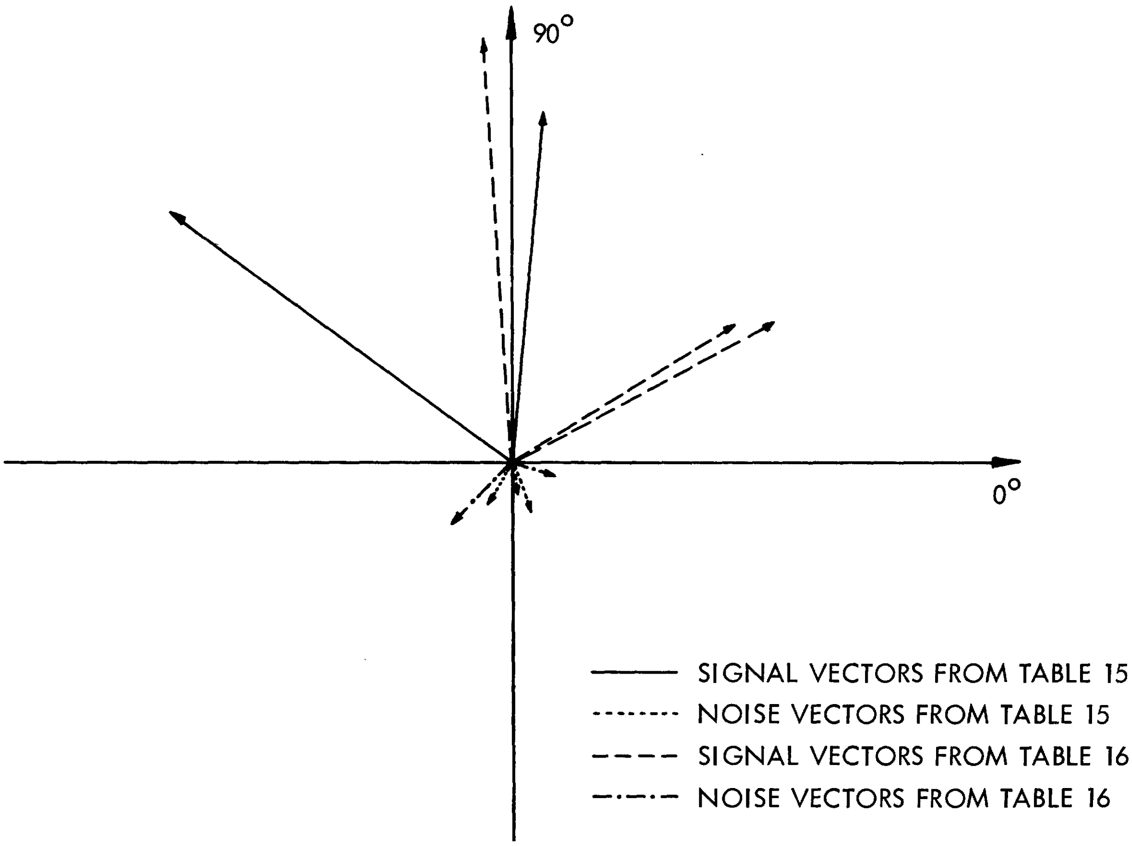

Fig. 46. Vector representation of data in Tables 15 and 16.

Table 15. CRAB NEBULA – October 24, 1969.

Hour Angle	ON		OFF	
	A (mV)	φ (deg)	A (mV)	φ (deg)
0.8	93	86		
1.23			10	-79
1.31	111	144		
1.75			6	-90

Table 16. CRAB NEBULA – October 24, 1969.

Hour Angle	ON		OFF	
	A (mV)	φ (deg)	A (mV)	φ (deg)
1.91	107	30		
2.36			10	-6
2.43	158	+93		
2.88			34	-126
2.96	100	32		
3.4			10	-122

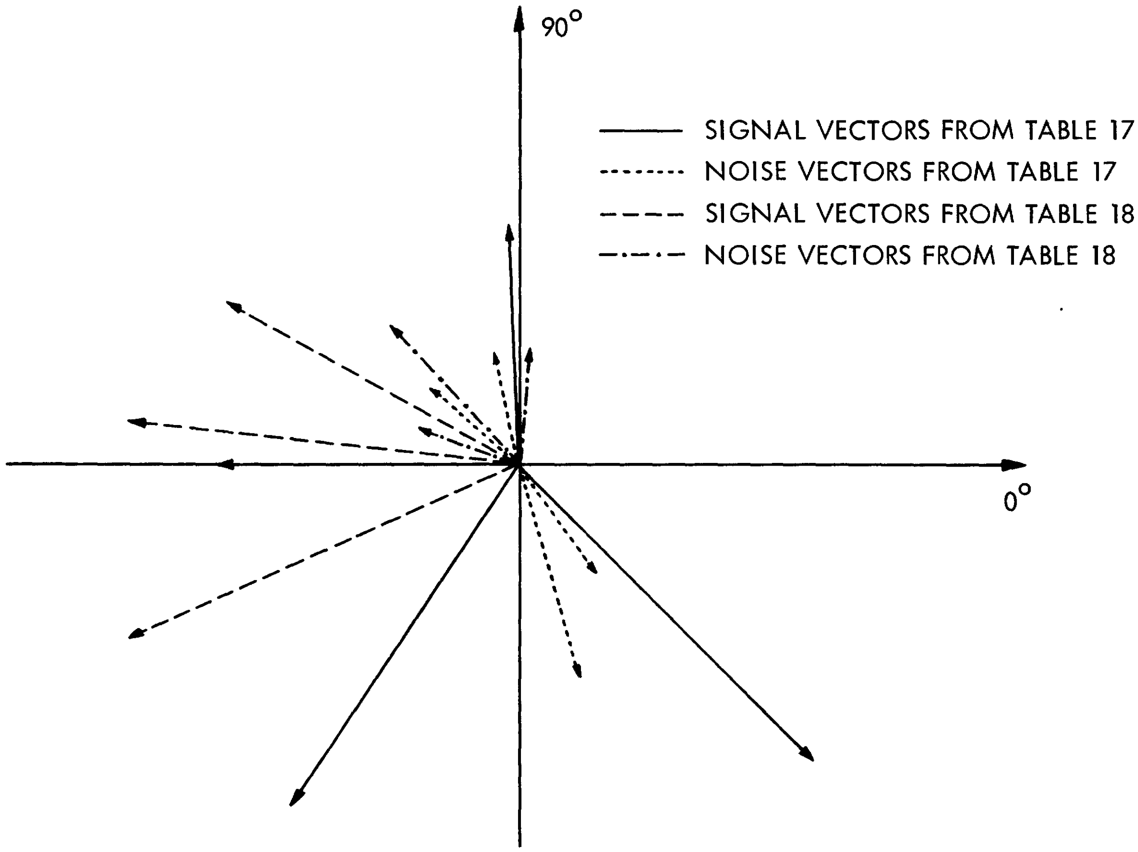

Fig. 47. Vector representation of data in Tables 17 and 18.

Table 17. CRAB NEBULA – October 28, 1969.

Hour Angle	ON		OFF	
	A (mV)	φ (deg)	A (mV)	φ (deg)
0.9	75	180		
1.34			57	-75
1.41	106	-124		
1.86			28	-51
1.93	109	-46		
2.38			28	140
2.45	60	93		
2.90			26	101

Table 18. CRAB NEBULA – October 30, 1969.

Hour Angle	ON		OFF	
	A(mV)	φ (deg)	A (mV)	φ (deg)
1.52	70	150		
1.96			21	157
2.05	91	-156		
2.49			42	136
2.57	85	174		
3.00			25	90

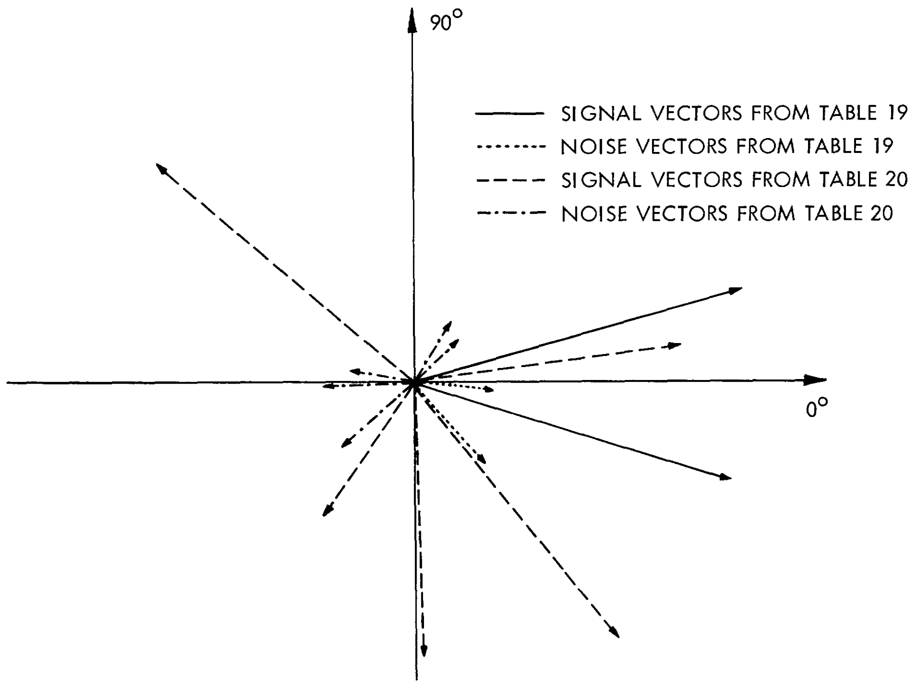

Fig. 48. Vector representation of data in Tables 19 and 20.

Table 19. CRAB NEBULA – December 9, 1969.

Hour Angle	ON		OFF	
	A (mV)	ϕ (deg)	A (mV)	ϕ (deg)
1.6	138	-17		
2.01			42	-50
2.16	141	16		
2.6			39	-6

Table 20. CRAB NEBULA – January 9, 1970.

Hour Angle	ON		OFF	
	A (mV)	ϕ (deg)	A(mV)	ϕ (deg)
1.00	111	-87		
1.05			42	-139
1.6	131	-51		
2.01			33	180
2.12	109	8		
2.57			26	173
2.67	138	140		
3.13			23	45
3.78	66	-124		
4.22			20	53

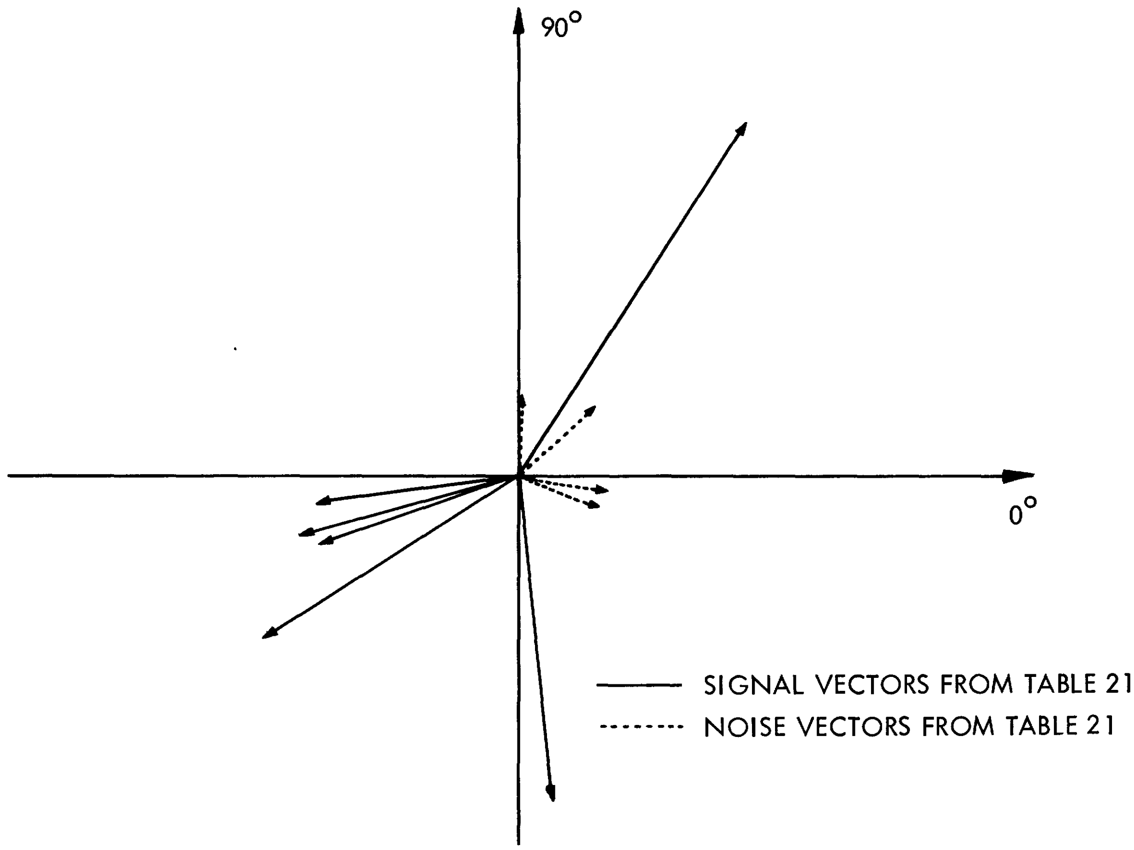

Fig. 49. Vector representation of data in Table 21.

Table 21. CRAB NEBULA – January 11, 1970.

Hour Angle	ON		OFF	
	A (mV)	φ (deg)	A (mV)	φ (deg)
0.74	109	58		
1.2			7	-8
1.84	57	-171		
2.3			5	-11
2.4	81	-147		
2.85			26	43
2.95	54	-162		
3.4			18	90
3.5	84	-85		
3.96			21	-17
4.01	60	-162		
4.5			22	-80

From examination of Figs. 42-49 we may make the following remarks:

(a) The signal vectors are consistently larger than the noise vectors.

(b) The amplitude of the signal vectors rarely varies more that 50% in the course of an observation.

(c) The phase of the signal vectors does not vary more than ±45° for most of the observations.

6.5 INTERPRETATION OF THE DATA

The presence of interference makes it impossible to extract much information from our data. We shall give a short discussion of the methods that can be used to estimate the fringe visibility amplitudes and the uncertainties in the baseline parameters.

6.5.1 Estimated Fringe Visibility for the Crab Nebula

Of the sources observed, the Crab Nebula gave us the most consistent fringes. The fringe amplitude variations were within 20-30% in most cases. To obtain the fringe visibility amplitude experimentally, we would have to measure A, the fringe amplitude of a point source such as 3C273, with the same system gain as in the measurement of the Crab Nebula fringe amplitude, A_{Crab}. Then the fringe visibility, $|V|$, would be

$$|V|_{Crab} = \frac{A_{Crab}/A_{3C273}}{S_{Crab}/S_{3C273}},$$

where S is the flux.

We did not measure any fringes from 3C273; therefore, experimental calculation of the fringe visibility amplitude for the Crab Nebula was impossible. We could, however, obtain an estimate of the fringe visibility amplitude and phase over the useful hour-angle range. We shall do that for a one-dimensional source of uniform brightness temperature with a width of 4 minutes of arc. We make use of Eq. 30, and after simplification and integration we obtain

$$V = \frac{\sin \pi u X_c}{\pi u X_c}. \tag{84}$$

For X_c = 4 minutes of arc and the values of u given in Table 6 we find that V = 0.6 over the 4-h observation interval. The phase is zero because we assumed a uniform brightness temperature distribution. In reality, the distribution is not uniform; therefore, the fringe visibility amplitude is not 0.6, and the phase is not zero. Yet both remain constant over the observation interval, because of the small changes in u.

6.5.2 Baseline Parameters

To estimate the baseline parameters one should measure the phase of a point source for an interval of 2 h. Actually, for our present baseline length and orientation, the Crab Nebula can be used for estimating the baseline parameters, since its intrinsic phase remains essentially constant over an interval of 2 h. Interference, however, corrupted the consistency of the fringe phase that we measured; thus, the Crab Nebula cannot be used, at this time, for the estimation of the baseline parameters.

The baseline parameters used in our observations were obtained from geometrical measurements. The accuracy of these measurements cannot be depended upon for interferometric work; therefore, we can safely say that part of the phase inconsistency in our data is due to baseline errors. This is suggested in one set of our data; specifically, examination of the data in Table 20 reveals that the fringe vector seems to be changing phase in almost consistent fashion. We shall assume that these changes are due entirely to errors in the baseline parameters and proceed to demonstrate the technique by means of which these parameters can be obtained exactly.

The phase error, $\Delta\phi$, attributable to errors Δd, ΔD_L, and ΔH_L in the baseline length, declination, and hour angle, respectively, is given by

$$\Delta\phi = \frac{\partial\phi}{\partial d}\Delta d + \frac{\partial\phi}{\partial D_L}\Delta D + \frac{\partial\phi}{\partial H_L}\Delta H, \tag{85}$$

where

$$\phi = 2\pi\frac{d}{\lambda}\left(\sin\delta\sin D_L + \cos\delta\cos D_L\cos\frac{\pi}{12}(H_L-h_s)\right),$$

and h_s is the source hour angle.

Then

$$\begin{aligned}\Delta\phi &= 2\pi\frac{d}{\lambda}\left(\sin\delta\sin D_L + \cos\delta\cos D_L\cos\frac{\pi}{12}(H_L-h_s)\right)\frac{\Delta d}{d}\\ &+ 2\pi\frac{d}{\lambda}\left(\sin\delta\cos D_L - \cos\delta\sin D_L\cos\frac{\pi}{12}(H_L-h_s)\right)\frac{\Delta D_L}{57}\\ &- 2\pi\frac{d}{\lambda}\left(\cos\delta\cos D_L\sin\frac{\pi}{12}(H_L-h_s)\right)\frac{\pi}{12}\Delta H_L,\end{aligned} \tag{86}$$

where ΔD_L is in degrees, and ΔH_L is in hours.

If we now separate the constant and time-variant terms, we obtain

$$\begin{aligned}\Delta\phi &= 2\pi\frac{d}{\lambda}\left(\sin\delta\sin D_L\frac{\Delta d}{d} + \sin\delta\cos D_L\frac{\Delta D_L}{57}\right)\\ &+ 2\pi\frac{d}{\lambda}\left(\cos\delta\cos D_L\frac{\Delta d}{d} - \cos\delta\sin D_L\frac{\Delta D_L}{57}\right)\cos\frac{\pi}{12}(H_L-h_s)\\ &- 2\pi\frac{d}{\lambda}\left(\cos\delta\cos D_L\frac{\pi}{12}\Delta H_L\right)\sin\frac{\pi}{12}(H_L-h_s).\end{aligned} \tag{87}$$

Equation 87 can be written

$$\Delta\phi = A(\Delta d, \Delta D_L) + B(\Delta d, \Delta D_L)\cos\frac{\pi}{12}(H_L - h_s) - C(\Delta H_L)\sin\frac{\pi}{12}(H_L - h_s).$$

Thus, by measuring the phase over 2 h, we can compute the coefficients A, B and C; then we can solve for Δd, ΔD_L, and ΔH_L.

Another method that is not sensitive to the instrumental phase and to the intrinsic phase of the source is to differentiate $\Delta\phi$ with respect to h_s. The derivative is called $\delta(\Delta\phi)$ and corresponds to the difference between 2 successive phase measurements, provided the hour angle change is reasonably small.

If we differentiate Eq. 86 with respect to h_s, we obtain

$$\delta(\Delta\phi) = \left[2\pi\frac{d}{\lambda}\cos\delta\cos D_L\sin\frac{\pi}{12}(H_L - h_s)\left(\frac{\pi}{12}\Delta h_s\right)\right]\frac{\Delta d}{d}$$

$$- \left[2\pi\frac{d}{\lambda}\cos\delta\sin D_L\sin\frac{\pi}{12}(H_L - h_s)\left(\frac{\pi}{12}\Delta h_s\right)\right]\frac{\Delta D_L}{57}$$

$$+ \left[2\pi\frac{d}{\lambda}\cos\delta\cos D_L\cos\frac{\pi}{12}(H_L - h_s)\left(\frac{\pi}{12}\Delta h_s\right)\right]\frac{\pi}{12}\Delta H_L. \tag{88}$$

To compute Δd, ΔD_L, and ΔH_L, we must form a system of 3 equations by measuring 3 successive phase changes; each measurement is separated from the next by a reasonable hour interval. From the data in Table 20 we can form Table 22, which shows the hour angles at which the measurements were taken, the hour angle intervals, and the phase changes.

Table 22. Parameters used to solve for Δd, ΔD_L, and ΔH_L, obtained from Table 21.

Source Hour Angle (h) h_s	Hour Angle Change (h) Δh_s	Phase Change (deg) $\delta(\Delta\phi)$
1.3	0.6	36.5
1.86	0.52	58.5
2.4	0.55	132

If we use Eq. 88 and the values given in Table 22, we obtain the following system of equations:

$$30.9\Delta d - 3.88\Delta D_L - 47.2\Delta H_L = 0.68$$

$$29.4\Delta d - 3.69\Delta D_L - 32.4\Delta H_L = 1.02$$

$$33.15\Delta d - 4.17\Delta D_L - 24.9\Delta H_L = 2.30$$

The solution of this system yields

$$\Delta d = 1101 \text{ m}, \ \Delta D_L = 8045°, \ \Delta H_L = 0.056 \text{ h}.$$

These values are not realistic. We then proceed to solve the first two equations of the system by setting $\Delta d = 0$. This assumption is reasonable because the baseline length was measured rather accurately. Then the solution of the new system gives

$$\Delta D_L = -0.55° = -33 \text{ minutes of arc.}$$

$$\Delta H_L = 0.03 \text{ h} = 27 \text{ minutes of arc.}$$

These uncertainties in the baseline declination and hour angle are quite possible.

VII. CONCLUSION

When work began on the Ku-band interferometer three years ago, there was not much to it except two antennas, an available roof, and our determination and enthusiasm. Today, we have a working prototype for interferometric work at a wavelength of 1.75 cm. With some more work, especially on the problem of interference, and with the improvement of the signal-to-noise ratio, we believe that this interferometer will add to our knowledge of some discrete radio sources like the Crab Nebula, Venus, Cas A, Cyg A, and possibly some H II regions.

Possible solutions for the interference problem have been discussed in section 6.3. The signal-to-noise ratio can be improved by using larger antennas or low-noise front ends as parametric amplifiers, or both. As we have pointed out, in any future rearrangement of the interferometer an E-W baseline is strongly recommended.

With the discovery of strong H_2O sources, use of the interferometer for H_2O line work becomes possible. For instance, at the maximum baseline spacing of 100 m the interferometer will be able to resolve features separated by 10^s of arc. As well as relative position measurements, we can study the atmospheric phase effects at different baseline spacings by monitoring H_2O sources. The conversion of the continuum Ku-band interferometer to an H_2O spectral-line interferometer would be simple, since we already have two phase-locked front ends. For the back end we recommend 30 channels each with a 20-kHz bandwidth. This would give us a total bandwidth of 600 kHz. Each channel would consist of a FET multiplier. The H_2O line sources have features that spread over a bandwidth of 10 MHz. Thus, a synthesizer would have to be used as a second local oscillator. Real-time data processing for all 30 channels will be feasible if we add an arithmetic element to the PDP-8 computer.

APPENDIX A

Circuits

We shall now show the circuits that were used to generate the 28-MHz and 300-MHz local-oscillator synchronizing signals of the Ku-band interferometer. The 28-MHz signal is generated from the 1-MHz standard in two steps: 1-7 and 7-28. Step-recovery diodes were used to generate the harmonics (see Figs. A-1, A-2 and A-3). The 300-MHz signal is generated from a 100-MHz crystal oscillator (see Fig. A-4). Figure A-5 shows the circuit of the 300-MHz Class B power amplifier.

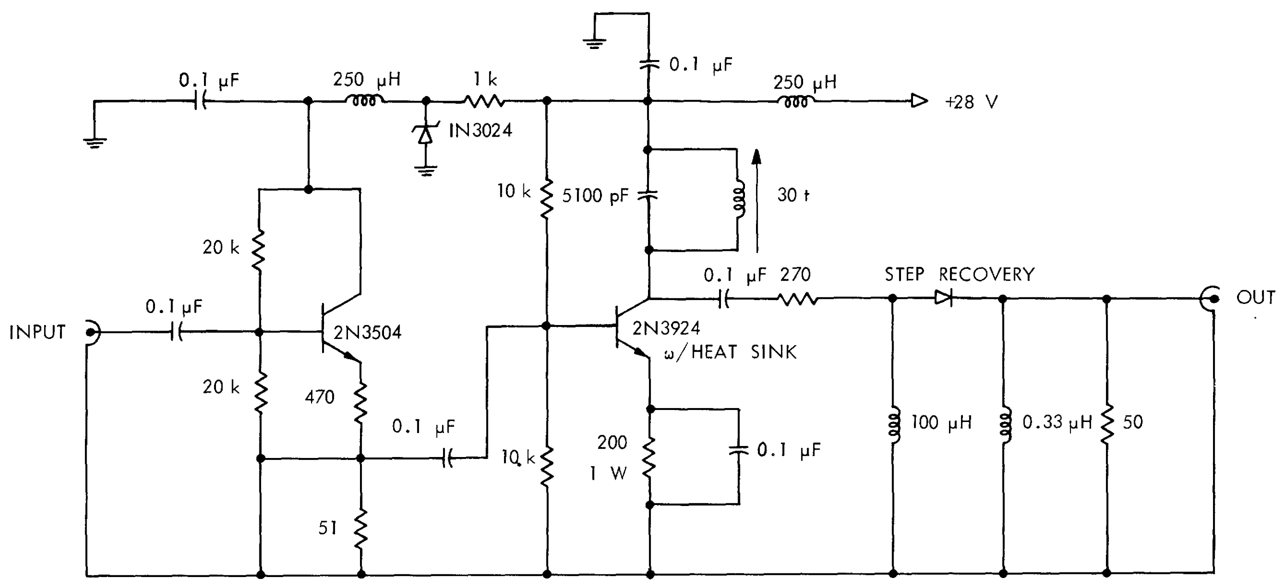

Fig. A-1. Harmonic multiplier (1-7 MHz).

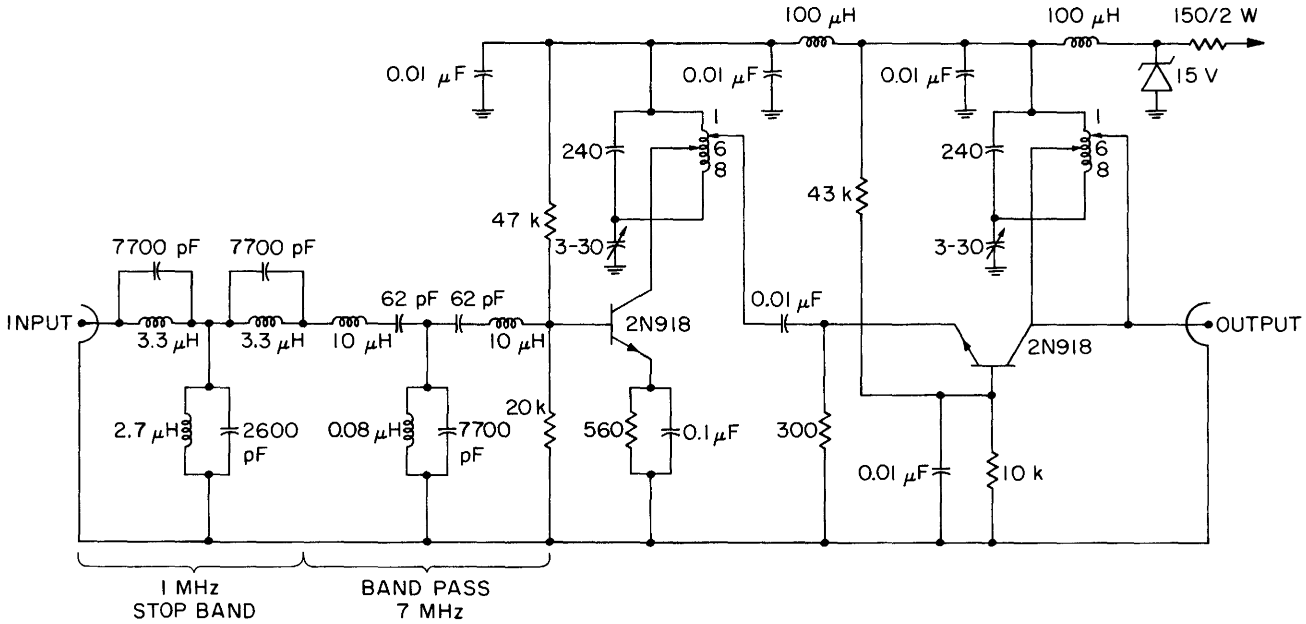

Fig. A-2.

Amplifier (7 MHz). Output ~0.2 V p-p. Input from harmonic mixer.

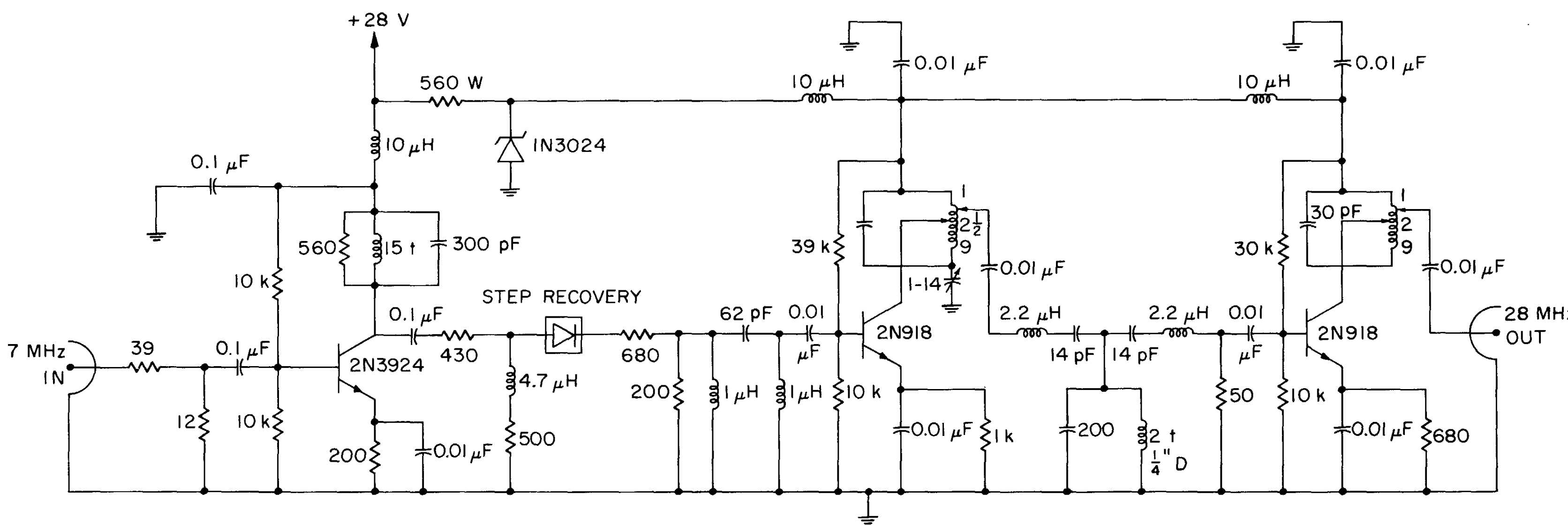

Fig. A-3. Multiplier (7-28 MHz).

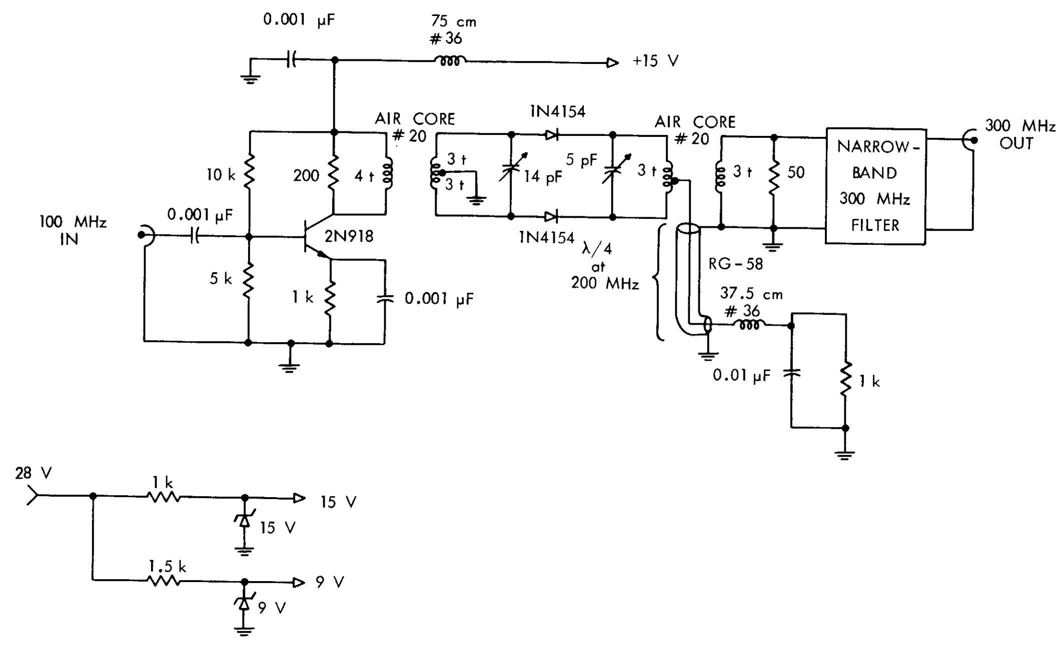

Fig. A-4.
Multiplier (100-300 MHz).

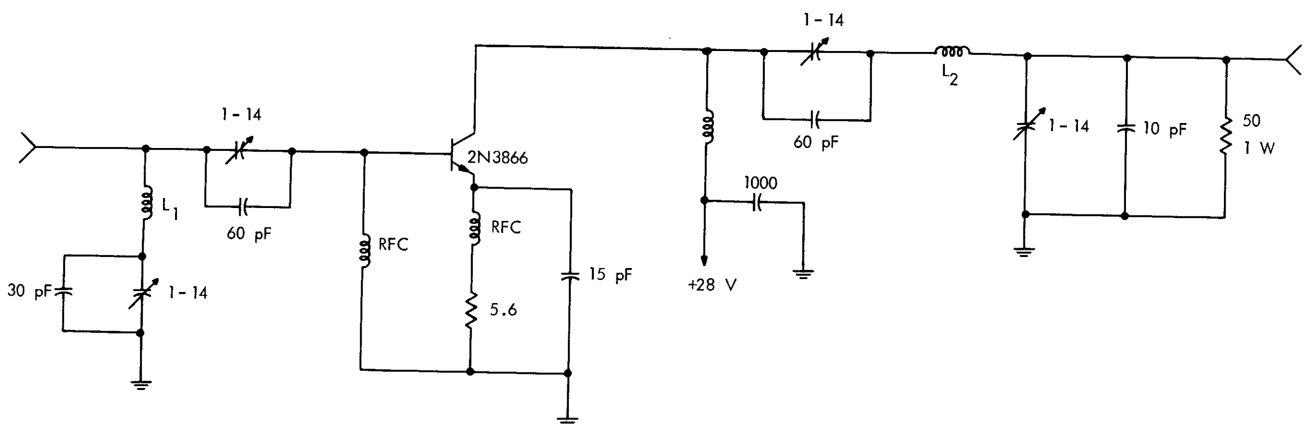

Fig. A-5.
Power amplifier
(300 MHz).

L_1 2 3/4 TURNS No. 18
1/4" DIAMETER
1/8" LONG

L_2 3 3/4 TURNS No. 18
1/4" DIAMETER
3/16" LONG

APPENDIX B

Computer Organization

The PDP-8 4K memory is divided into 32 pages. Each page consists of 128 registers. The registers of page "0' can be addressed from any other page directly; indirect instructions must be used when addressing a register of a certain page from a register of another page.

The most important instructions are presented and explained as follows.

INSTRUCTION	CODE	FUNCTION
AND	0000	logical and
TAD	1000	2's complement add
ISZ	2000	increment and skip if zero
DCA	3000	deposit and clear Accumulator
JMS	4000	jump to subroutine
JMP	5000	jump
IOT	6000	in/out transfer
NOP	7000	no operation
CLA	7200	clear AC
CLL	7100	clear link
CMA	7040	complement AC
CML	7020	complement link
RAR	7010	rotate AC and link one location to the right
RAL	7004	rotate AC and link one location to the left
RTR	7012	rotate AC and link two locations to the right
RTL	7006	rotate AC and link two locations to the left
IAC	7001	increment AC
SMA	7500	skip on minus AC
SZA	7440	skip on zero AC
SPA	7510	skip on plus AC
SNA	7450	skip on non-zero AC
SNL	7420	skip on zero link
SKP	7410	skip
OSR	7404	inclusive OR, switch register with AC
HLT	7402	halt program
CIA	7041	complement and increment AC
LAS	7604	load AC with switch register
STL	7120	set link to 1
ION	6001	interrupt on
IOF	6002	interrupt off

The DEC subroutines used in conjunction with the main program are the following.

SICONV	single precision decimal-to-binary conversion and input ASR-33; signed or unsigned
DMUL	double precision multiplication
DUBDIV	double precision division
DSIN	double precision sine
DCOS	double precision cosine
BPUN	binary punch
DECPRT	unsigned decimal print, single precision
SSPRNT	signed decimal print, single precision

APPENDIX C

Program Language

The program was written in machine language and is listed in the following pages. On the first page the user's symbols are defined. The program uses up 29 out of the 32 computer pages that were defined in Appendix B. Although efficiency was one of our concerns, it was not the primary one. In a new edition of the program use of the Marco-8 machine language is recommended instead of the PAL-III machine language that we used.

SYMBOLS

```
ADRES   Ø16Ø
ALFLG   ØØ2Ø
ALPHS   ØØ33
ARCHI   1635
ARG     3742
ARHI    166Ø
ARXI    617Ø
B       4141
BASL    ØØ61
BASLD   6647
BINP    4451
BPUN    44ØØ
BPUNCH  5365
BSLAMD  1157
C       4142
CHKARG  33Ø6
CKARG   Ø123
CKSM    4476
CLABCD  5267
CMINTG  Ø14Ø
CM3ØØ   Ø125
CNANO   5555
CNTDEV  Ø144
CNTIN   Ø37Ø
CNTM2   ØØ22
CNTM3   ØØ24
CNTM6   Ø12Ø
CNTN    Ø121
COMPE   Ø124
COMPEN  5447
CONPNT  54Ø6
CONSTØ  1357
CONST1  Ø1Ø5
CONST2  1355
CONST3  1361
CONST4  Ø1Ø7
CONST5  1363
CONST9  Ø112
CONS1Ø  2165
CONTB   ØØ55
CONTC   ØØ56
CONTD   ØØ57
CONVER  Ø57Ø
COSDDE  1166
COSDIF  236Ø
COSGAM  277Ø
COSIM1  Ø132
COSMDT  646Ø
COSTI   Ø126
CRLF    6344
CRLFP   Ø166
CTR1    45Ø3
CYCL36  1562
CYCL37  1537
CYCL43  6473
CYCL45  5417
C2ØØ    45Ø4
D       4143
DATA    2467
DATAC   3167
DAYS    661Ø
DAYX24  5761
DAY24   Ø537
DCOS    5Ø6Ø
DCOSP   ØØ76
DCPRNT  Ø17Ø
DC43    137Ø
DC45    1367
DDIVP   ØØ47
DECAL   6663
DECB    6643
DECL    6633
DECLB   6667
DECPNT  1366
DECPRT  5ØØØ
DECS    6637
DEC1    6727
DEC1Z   6711
DEC12   2ØØØ
DEC12P  5756
DEC2    6732
DEC2Z   6715
DEC43   6464
DEC43P  576Ø
DEC45   541Ø
DEC45P  5757
DEGR    Ø564
DEGRS   Ø274
DELTS   6665
DIVND4  4335
DIXE    Ø157
DMEGA   3255
DMINS   Ø277
DMUL    4ØØØ
DMULTP  ØØ54
DSECS   Ø317
DSIN    34ØØ
DSINP   ØØ77
DUBDIV  42ØØ
D1ØØ    5561
EN      1161
ENTER   Ø366
EXI     3166
FA      45Ø1
FERE1   Ø572
FERE2   Ø573
FINADR  Ø164
FLGCHK  56ØØ
FLGCK   Ø171
FRCNL   5334
FREQU   Ø766
GET1    Ø757
GET2    1523
GET3    5751
GET4    5752

HARG    Ø13Ø
HOURB   6627
HRANGL  6735
HRBSL   ØØ36
HRDEC   Ø651
HRJAN   6671
HRPNT   1524
HRS     Ø227
HR1     6721
HR1P    5744
HR17    6731
HR12    2745
HR12P   5753
HR2     6724
HR2P    5737
HR27    67Ø5
HR36    1551
HR36P   5755
HR37    1526
HR37P   5754
IA      45ØØ
INCHR   6273
INTADR  Ø163
INTEGR  Ø136
KCR     6351
KLF     6354
KRIK    ØØØ2
K244    5364
K246    5361
LARG    Ø191
LCT     6613
LCTP    1165
LONGI   ØØ63
LOJOT   Ø353
LSQFIT  3Ø47
MALF    2364
MALPH   152Ø
MEGA    ØØ42
MEGA1   ØØ41
MEGI    3171
MEGI1Ø  6156
MEGROT  1ØØ1
MIDDL   64ØØ
MIDI    3771
MIDLTM  Ø172
MINS    Ø231
MPLOT   3362
MS4ØØ   1716
MS7ØØØ  Ø145
MS77ØØ  ØØ75
MS777Ø  5367
M15OPT  3366
M2      ØØ21
M212    4532
M24     ØØ74
M3      ØØ23
M3ØØ    5554
M6      Ø117
N       6611
NH      4477
NDAYS   Ø565
NDVICE  Ø143
NEGAT   ØØ66
NEGATF  3264
NEXCLE  54Ø5
NUMBIN  Ø367
NXHL    441Ø
N1ØØ    5563
N1ØØØ   66Ø2
N125    5557
N17     1756
N17P    317Ø
N22     175Ø
N22P    Ø761
N226    Ø574
N36ØØ   66Ø4
N5338   176Ø
N5371   1762
N5416   1754
N5442   1752
N6Ø     66ØØ
N63ØØ   5446
N73ØØ   Ø566
NR64ØØ  66Ø6
PAGE1Ø  24ØØ
PAGE11  26ØØ
PAGE12  3ØØØ
PAGE13  32ØØ
PAGE2   Ø4ØØ
PAGE21  52ØØ
PAGE22  54ØØ
PAGE24  6ØØØ
PAGE3   Ø6ØØ
PAGE4   1ØØØ
PAGE5   12ØØ
PAGE6   14ØØ
PAGE9   22ØØ
PAG1Ø   2367
PAG11   2576
PAG12   2774
PAG13   3172
PAG2    Ø375
PAG21   3254
PAG22   537Ø
PAG24   5762
PAG3    Ø576
PAG4    Ø772
PAG5    117Ø
PAG6    1371
PAG7    1525
PAG9    172Ø
PA1     2161
PARA    6331
PARF    Ø161
PGMBEG  42[illegible]
P112    2163

PLOT    444Ø
PNT1    6456
POINTP  1Ø53
POSARG  3334
POSD    2114
PROSO1  ØØ51
PROSO2  ØØ52
PROSO3  ØØ53
PT256   6362
PULSE   Ø122
PULSEP  5431
PUN     4471
PUNCT   Ø167
PUNL    4417
PUT1    Ø372
PUT1P   1162
PUT2    Ø373
PUT2P   1163
PUT3    Ø374
PUT3P   1164
PUT4    Ø76Ø
PUT4P   1365
RACAL   ØØ3Ø
RACL    6617
RAS     6623
REDIVD  3137
RESET   1Ø36
RESETP  54Ø7
ROTP    5355
ROT1L   ØØ6Ø
ROT1LF  62ØØ
ROT1R   Ø146
ROT1RT  6143
ROT2L   Ø147
ROT2LF  6314
ROT3L   Ø1Ø2
ROT3LF  6231
ROT3R   ØØ7Ø
ROT3RT  6212
ROT6L   Ø116
ROT6LF  6275
SAVEAC  5736
SAVERL  2572
SECS    Ø24Ø
SICON   Ø371
SICONV  46ØØ
SIDHRØ  ØØ71
SIFTL   3352
SILLY   6136
SILY    1717
SINDDE  Ø1Ø3
SINDIF  2362
SINGAM  2772
SINIM1  Ø134
SINMDT  6462
SINTI   Ø13Ø
SL6     45Ø7
SL7     45Ø6
SPRNT   5366
SR32    57Ø4
SR33    57Ø6
SR36    562Ø
SR37    564Ø
SSADDR  4554
SSBOX   4561
SSCNT   4562
SSCNTR  456Ø
SSCON   4564
SSMNS   4557
SSOUT   4545
SSPLUS  4556
SSPRNT  451Ø
SSTWO   4555
SSVAL   4563
SSXYZ   4526
STDECL  6654
STDECS  6657
STEP1   Ø764
STEP1P  5747
STEP2   Ø762
STEP2P  5742
STIME   1515
STORE   Ø142
STPNT   2133
SUMPEL  6743
SUM1    Ø15Ø
SUM2    Ø153
TEMPO   ØØØ3
TEMP1   ØØØ5
TEMP2   ØØØ6
TEMP3   ØØØ7
TEP1    45Ø5
TIME    ØØ25
TMINC   Ø115
TMINCR  625Ø
TOPOS   Ø156
TRANPR  5725
TRANSF  1721
TRANSX  ØØ67
TRIA    Ø162
TS      1713
TWOPI   3364
TYPE    6363
TYPEPT  6355
TYPO    Ø165
VEL     Ø77Ø
V1      6741
WAIT    1643
WAITST  16ØØ
WLONG   6675
YU      6737
DUBDIV=42ØØ
DDIVND4=4335
DMUL=4ØØØ
B     =4141
C     =4142
D     =4143
SICONV=46ØØ
DECPRT=5ØØØ
DSIN=34ØØ
DCOS=5Ø6Ø
ARG=3742
```

```
*1
JMP I FLGCK
KRIK,0
TEMPO,0
*5
TEMP1,0
TEMP2,0
TEMP3,0
*20
ALFLG,0
M2,-2
CNTM2,0
M3,-3
CNTM3,0
TIME,0
0
0
RACAL,0
0
0
ALPHS,0
0
0
HRBSL,0
0
0
MEGA1,DMEGA
MEGA,.+1
0
0
0
0
DDIVP,DUBDIV
LQUOT,DIVND4
PROSO1,0
PROSO2,0
PROSO3,0
DMULTP,DMUL
CONTB,B
CONTC,C
CONTD,D
ROT1L,ROT1LF
BASL,0
0
LONGI, 0
0
0
NEGAT, NEGATE
TRANSX, TRANSF
ROT3R,ROT3RT
SIDHR0,0
0
0
M24,7750
MS7700,7700
DCOSP,DCOS
DSINP,DSIN
HARG,ARG
LARG,ARG+1
ROT3L,ROT3LF
SINDDE,0
0
CONST1,0
0
CONST4,0
0
0
CONST9, 0
0
0
TMINC,TMINCR
ROT6L,ROT6LF
M6,-6
CNTM6,0
CNTN, 0
PULSE, PULSEP
CKARG, CHKARG
COMPE, COMPEN
CM300,0
COSTI,0
0
SINTI,0
0
COSIM1,0
0
SINIM1,0
0
INTEGR,7777
4367
CMINTG,0
0
STORE,SAVERL
NDVICE,-4
CNTDEV,0
MS7000,7000
ROT1R, ROT1RT
ROT2L,ROT2LF
SUM1,0
0
0
SUM2,0
0
0
TOPOS,SUMPEL
DIXE,0
ADRES,0
PARE,PARA
TRIA,3
INIADR,HRANGL
FINADR,SUMPEL+27
TYPO,TYPE
CRLFP,CRLF
PUNCT,TYPEPT
DCPRNT,DECPRT
FLGCK,FLGCHK
MIDLTM,0
0
*177
6540
$
```

```
    *200
    PGMBEG,CLA CLL      /CLEAR LINK AND ACCUMULATOR
    TAD ENTER           /INITIALIZE THE REGISTERS IN WHICH THE INPUT
                        /PARAMETERS GO
    DCA 10              /DEPOSIT IT IN REGISTER 10
    TAD NUMBIN          /INITIALIZE COUNT OF THE NUMBER OF
    DCA CNTIN           /PARAMETERS TO BE TYPED IN
    JMS I SICON         /TYPE PARAMETER
    DCA I 10            /DEPOSIT IT BY MEANS OF THE SELF-INDEXING REGISTER 10
    ISZ CNTIN           /HAVE ALL THE PARAMETERS TYPED IN?
    JMP .-3             /NO, JUMP 3 LOCATIONS BACK AND TYPE NEXT
    TAD ENTER           /YES, GET THE FIRST OF THE REGISTERS IN WHICH THE
    TAD TRIA            /INPUT PARAMETERS ARE STORED
    DCA 10              /DEPOSIT IT IN 10
    TAD PUT1            /INITIALIZE REGISTERS IN WHICH THE TIME, THE RIGHT
    DCA 11              /ASCENSIONS AND
    TAD PUT2            /DECLINATIONS ARE TO BE DEPOSITED
    DCA 12              /AFTER THEY HAVE BEEN CONVERTED
    TAD PUT3
    DCA 13              /INTO THE APPROPRIATE UNITS
    CMA
    TAD M3
    DCA CNTM2           /SET COUNT TO -4 FOR THE HOUR PARAMETERS
    TAD M3
    DCA CNTM3           /SET COUNT TO -3 FOR THE DECLINATION PARAMETERS
227 HRS, TAD I 10       /CONVERT FIRST THE HOUR PARAMETERS; OBTAIN THE
    DCA I 11            /HOURS, DEPOSIT INTO THE HOUR REGISTER
    MINS,TAD I 10       /OBTAIN THE MINUTES
    JMS I MEGA1
    JMS I DDIVP         /DIVIDE BY 60
    N60
    DCA TEMP2           /PLACE QUOTIENT IN TEMPORARY REGISTERS
    TAD I LQUOT         /TEMP2 AND TEMP3
    DCA TEMP3
    SECS,TAD I 10       /OBTAIN THE SECONDS
    DCA PROSO3
    TAD I 10            /OBTAIN THE FRACTIONAL SECONDS
    JMS I MEGA1
    JMS I DDIVP         /DIVIDE BY 1000
    N1000
    DCA MEGA+3
    TAD I LQUOT
    DCA MEGA+4
    TAD PROSO3
    DCA MEGA+2
    DCA MEGA+1
    TAD MEGA
    JMS I DDIVP         /DIVIDE SECONDS BY 3600
    N3600
    DCA PROSO2
    CLL
    TAD I LQUOT         /ADD MINS/60 TO SECS/3600
    TAD TEMP3
    DCA TEMP3
    RAL
    TAD PROSO2
    TAD TEMP2
    DCA I 11            /DEPOSIT INTO THE HOUR REGISTER (TRIPPE PRECISION)
    TAD TEMP3
    DCA I 11            /DEPOSIT INTO THE HOUR REGISTER (TRIPPE PRECISION)
    ISZ CNTM2           /IS COUNT 0
    JMP HRS             /NO, JUMP BACK AND CONVERT THE NEXT PARAMETER
274 DEGRS,TAD I 10      /YES, OBTAIN DEGREES COMPONENT OF THE DECLINATION
    DCA TEMPO           /DEPOSIT IN TEMPO
    DCA ALFLG           /CLEAR FLAG
    DMINS,TAD I 10      /OBTAIN MINUTES
    DCA TEMP2           /DEPOSIT IN TEMP2
    TAD TEMP2
    SMA CLA             /IS DECLINATION NEGATIVE
    JMP .+3             /NO, JUMP 3 LOCATIONS AHEAD
    CMA                 /YES
    DCA ALFLG           /SET FLAG TO -1
    TAD TEMP2
    JMS I MEGA1
    JMS I DDIVP         /DIVIDE MINS BY 60
    N60
    DCA TEMP2           /DEPOSIT MINS/60 IN REGISTERS TEMP2, TEMP3
    TAD I LQUOT
    DCA TEMP3
    TAD ALFLG
    DCA TEMP1
    DSECS,TAD I 10      /OBTAIN SECONDS
    DCA PROSO1
    TAD I 10            /OBTAIN FRACTIONAL SECONDS
    JMS I MEGA1
    JMS I DDIVP         /DIVIDE FRACTIONAL SECONDS BY 1000
    N1000
    DCA MEGA+3
    TAD I LQUOT
    DCA MEGA+4
    TAD PROSO1
    TAD ALFLG
    DCA MEGA+2
    TAD ALFLG
    DCA MEGA+1
    TAD MEGA
    JMS I DDIVP         /DIVIDE SECONDS BY 3600
    N3600
    DCA PROSO2
    TAD I LQUOT
    DCA PROSO3
    TAD ALFLG
    DCA PROSO1
    CLL
    TAD PROSO3          /OBTAIN MINS/60 + SECONDS/3600
    TAD TEMP3
    DCA I 12
    RAL
    TAD PROSO2
    TAD TEMP2
    DCA I 12            /DEPOSIT DECLINATION INTO A TRIPPLE PRECISION
    RAL                 /REGISTER, BY MEANS OF THE SELF-INDEXING REGISTER
    TAD TEMPO           /12. THE UNITS ARE IN DEGREES
    TAD PROSO1
    TAD TEMP1
    DCA I 12
    TAD 12              /RE-INITIALIZE REGISTER 12
    TAD M3
    DCA 12
    JMP I PAG2          /JUMP TO PAGE 2
    ENTER,DAYS-1
    NUMBIN,-42
    CNTIN,0
    SICON,SICONV
    PUT1,TIME-1
    PUT2,STDECL-3
    PUT3, DECAL-1
    PAG2,PAGE2
    PAUSE
```

```
*400
PAGE2,DCA MEGA+4
TAD I 12
DCA MEGA+3
TAD I 12
DCA MEGA+2
TAD  I 12
DCA MEGA+1
TAD MEGA
JMS I DDIVP          /DIVIDE DECLINATION (IN DEGREES) BY 180
D180
DCA TEMP1
TAD I LQUOT
DCA TEMP2
JMS I DMULTP         /MULTIPLY QUOTIENT BY PAI (π)
TEMP1
PAI
DCA TEMP1
JMS I ROT1L
DCA I 13             /DEPOSIT DOUBLE-PRECISION DECLINATION (IN RADIANS)
TAD I CONTB          /BY MEANS OF THE SELF INDEXING REGISTER 13
DCA I 13
ISZ CNTM3            /HAVE ALL THE DECLINATION COORDINATES BEING CONVERTED
JMP I DEGR           /NO, JUMP BACK AND CONVERT THE NEXT
427 TAD I 10         /YES, OBTAIN THE METER COMPONENT OF THE BASELINE
DCA BASL
TAD I 10             /OBTAIN THE CENTIMETER COMPONENT OF THE BASELINE
JMS I MEGA1
JMS I DDIVP          /DIVIDE BY 100
N100
DCA TEMP1
TAD I 10             /OBTAIN THE MILLIMETER CONPONENT
JMS I MEGA1
JMS I DDIVP          /DIVIDE BY 1000
N1000
TAD TEMP1
DCA BASL+1
444 TAD FERE1        /OBTAIN THE GREENWICH SIDEREAL TIME AT JANUARY 0
DCA 10
JMS I TRANSX         /CONVERT IT INTO HOUR UNITS AND DEPOSIT IT
TAD PROSO3           /IN THE TRIPPLE PRECISION REGISTER SIDHR0
DCA SIDHR0+2
RAL
TAD TEMPO
TAD PROSO2
DCA SIDHR0+1
RAL
TAD PROSO1
DCA SIDHR0
JMS DAY24            /GO TO SUBROUTINE DAY24
TAD TIME             /OBTAIN GREEWICH CIVIL TIME (GCT) AND MULTIPLY IT BY
DCA MEGA+2           /THE CONVERSION FATOR C1=9.857/3600
TAD TIME+1
DCA MEGA+3
TAD TIME+2
DCA MEGA+4
DCA MEGA+1
TAD MEGA
JMS I DDIVP          /DEVIDE BY 3600
N7020
DCA PROSO1
TAD I LQUOT
DCA PROSO2
JMS I DMULTP         /MULTIPLY BY 9.857
CONVER
PROSO1               /PRODUCT REGISTERS B AND C CONTAIN GCT*C1
CLL
TAD TEMP3            /ADD GCT+(DAYS)*24*C1
TAD TIME+2
DCA TEMP3
RAL
TAD TEMP2
TAD TIME+1
DCA TEMP2
RAL
TAD TEMP1
TAD TIME
DCA TEMP1            /REGISTERS TEMP1, TEMP2, TEMP3 CONTAIN THE ABOVE SUM
CLL
JMP I TO7215
TO7215, 7215
*522
TAD FERE2            /OBTAIN THE LONGITUDE COMPONENTS
DCA 10
JMS I TRANSX         /CONVERT THEM INTO A SINGLE UNIT (HOURS) NUMBER
TAD PROSO3           /CONTAINED IN REGISTER LONGI, +1, +2
DCA LONGI+2
RAL
TAD TEMPO
TAD PROSO2
DCA LONGI+1
RAL
TAD PROSO1
DCA LONGI
JMP I PAG3           /JUMP TO PAGE 3
DAY24,0              /MULTIPLY THE NUMBER OF DAYS THAT HAVE ELLAPSED
TAD I NDAYS          /SINCE JAN. 0 BY 24*9.857/3600=9.857/150
DCA MEGA+2
DCA MEGA+3
DCA MEGA+4
DCA MEGA+1           /PUT THE NUMBER OF DAYS IN THE DIVIDEND
TAD MEGA
JMS I DDIVP          /DIVIDE BY 150
N226
DCA TEMP1
TAD I LQUOT
DCA TEMP2
JMS I DMULTP         /MULTIPLY QUOTIENT BY 9.857
TEMP1
CONVER
DCA TEMP1            /DEPOSIT CONTENTS IN REGISTERS TEMP1, TEMP2
TAD I CONTB          /AND TEMP3
DCA TEMP2
TAD I CONTC
DCA TEMP3
JMP I DAY24
DEGR,DEGRS
NDAYS,DAYS
N7020,0070
2000
CONVER,1166
6416
FERE1,HRJAN-1
FERE2,WLONG-1
N226,0002
2600
PAG3,PAGE3
PAUSE
```

```
*600
PAGE3,CLL
TAD LONGI+2          /NEGATE LONGITUDE
CIA
DCA PROSO3
RAL
DCA KRIK
TAD LONGI+1
CMA
TAD KRIK
DCA PROSO2
RAL
DCA KRIK
TAD LONGI
CMA
TAD KRIK
DCA PROSO1
CLL
TAD PROSO3           /OBTAIN (GST-LONGITUDE) AND DEPOSIT IT
TAD TEMP3            /IN THE TRIPPLE PRECISION REGISTER TIME, +1, +2
DCA TIME+2
RAL
TAD PROSO2
TAD TEMP2
DCA TIME+1
RAL
TAD PROSO1
TAD TEMP1
DCA TIME
TAD TIME
TAD M24              /OBTAIN THE DIFFERENCE (TIME-24)
SPA                  /IS DIFFERENCE POSITIVE?
JMP.+2               /NO, JUMP 2 LOCATIONS AHEAD
DCA TIME             /YES, DEPOSIT DIFFERENCE IN THE REGISTER TIME
641 CLA CLL          /CONVERT THE ANTENNA COORDINATES
TAD GET1             /OBTAIN THE INDEX POSITIONS OF THE HOUR AND DECLINATION
DCA 10               /AXES OF THE DISHES BY MEANS OF THE SELF INDEXING
TAD PUT4             /REGISTER 10.  INITIALIZE LOCATIONS AT WHICH THE
DCA 11               /INDEX POSITIONS ARE TO BE DEPOSITED AFTER THEY
CMA                  /ARE CONVERTED
TAD M3
DCA CNTM2            /SET COUNT TO -4
HRDEC,JMS I TRANSX/THE HOUR INDEX POSITIONS ARE IN UNITS OF HOURS,
TAD PROSO3           /MINS, SECS AND THE DECLINATION ONES IN DEGREES, MINS,
DCA PROSO3           /SECS; THE TRANSX SUBROUTINE CONVERTS THEM INTO SINGLE
RAL                  /UNIT NUMBERS: HOURS FOR THE HOUR ANGLES AND DEGREES
TAD PROSO2           /FOR THE DECLINATIONS
TAD TEMPO
DCA PROSO2
TAD PROSO1           /DEPOSIT CONVERTED INDEX COORDINATES BY MEANS OF
DCA I 11             /THE SELF-INDEXING REGISTER 11
TAD PROSO2
DCA I 11
TAD PROSO3
DCA I 11
ISZ CNTM2            /HAVE ALL THE INDEX POSITIONS BEEN CONVERTED?
JMP HRDEC            /NO, JUMP BACK TO HRDEC
670 TAD N22P         /YES, COMPUTE HOUR ANGLE STEPPING INTERVALS
DCA MEGA+2           /EACH STEPPING PULSE INCREMENTS THE HOUR ANGLE
DCA MEGA+1           /OF ANT. #2 BY STEP2=(1.8/537.1)*1/15
DCA MEGA+3
DCA MEGA+4
TAD MEGA
JMS I DDIVP            /OBTAIN 1.8/537.1
N5371
DCA MEGA+2
TAD I LQUOT
DCA MEGA+3
DCA MEGA+1
DCA MEGA+4
TAD MEGA
JMS I DDIVP            /DIVIDE QUOTIENT BY 15
N17
DCA STEP2
TAD I LQUOT
DCA STEP2+1
TAD N22P
DCA MEGA+2             /STEP1=(1.8/533.8)*1/15
DCA MEGA+1
DCA MEGA+3
DCA MEGA+4
TAD MEGA
JMS I DDIVP            /OBTAIN (1.8/533.8)
N5338
DCA MEGA+2
TAD I LQUOT
DCA MEGA+3
DCA MEGA+1
DCA MEGA+4
TAD MEGA
JMS I DDIVP            /DIVIDE BY 15
N17
DCA STEP1
TAD I LQUOT
DCA STEP1+1
JMS I MIDL             /GO TO SUBROUTINE MIDL
TAD VEL                /OBTAIN VELOCITY OF LIGHT
DCA TEMP1              /DEPOSIT IT IN REGISTERS TEMP1, TEMP2
DCA TEMP2
CLL
JMS I DMULTP           /FORM PRODUCT OF (FREQ.)*(BASELINE)=ν* d
BASL
FREQU
DCA MEGA+1             /DEPOSIT PRODUCT IN DIVIDEND
TAD I CONTB
DCA MEGA+2
TAD I CONTC
DCA MEGA+3
TAD I CONTD
DCA MEGA+4
NOP
JMP I PAG4             /JUMP TO PAGE 4
GET1, HR1Z-1
PUT4,HR1-1
N22P,2200
STEP2,0
0
STEP1,0
0
FREQU,2532
3146
VEL,300
MIDL, MIDDL
PAG4,PAGE4
PAUSE
```

```
*1000
PAGE4, CLL
NOP                 /THESE NOP INSTRUCTIONS WERE INSERTED
NOP                 /AFTER A CORRECTION WAS INTRODUCED
NOP                 /IN THIS SECTION OF THE PROGRAM
NOP
NOP
NOP
NOP
NOP
NOP
NOP
NOP
TAD MEGA
JMS I DDIVP         /OBTAIN (ν*d)/C
TEMP1
DCA BSLAMD          /DEPOSIT QUOTIENT (d/λ) IN THE DOUBLE-PRECISION
TAD I LQUOT         /REGISTER BSLAMD
DCA BSLAMD+1        /START CLOK
TLS
HLT                 /PROGRAM HALTS
023 6311            /RESET SKIP FLIP-FLOP
6312                /HAS CLOCK ARRIVED?  YES, SKIP
JMP.-1              /NO, JUMP ONE LOCATION BACK
6321                /CLEAR CLOCK INTERRUPT
6331                /CLEAR TIME-CHECK INTERRUPT
6324                /ACTIVATE CLOCK INTERRUPT
6361                /CLEAR TRACKING PULSE (#2) INTERRUPT
6371                /CLEAR TRACKING PULSE (#1) INTERRUPT
6374                /DEACTIVE TRACKING INTERRUPTS
ION                 /TURN INTERRUPT ON
1036 RESET, 6374
CLA
CMA                 /GET REGISTER THAT CONTAINS THE NUMBER OF
TAD EN              /INTGRATION CYCLES ON THE CALIBRATION SOURCE
DCA 12              /DEPOSIT IT IN THE SELF-INDEXING REGISTER 12
TAD PUT1P           /INITIALIZE REGISTERS CONTAINING THE RIGHT ASCENSIONS
DCA 13              /OF THE TWO SOURCES; DEPOSIT INITIAL REGISTER IN 13
TAD PUT3P           /INITIALIZE REGISTERS CONTAINING THE DECLINATIONS
DCA 14              /OF THE TWO SOURCES IN RADIANS; DEPOSIT IN 14
TAD PUT2P           /INITIALIZE REGISTERS CONTAINING THE DECLINATIONS OF
DCA 15              /THE TWO SOURCES IN DEGREES; DEPOSIT IN 15
TAD M2              /SET SOURCE IDENTIFICATION INDEX TO -2; -2 CORRESPONDS
DCA 16              /TO THE CALIBRATION SOURCE AND -1 TO THE REGULAR
1053 POINTP, 6374   /SOURCE
TAD I 12            /GET THE NUMBER OF INTEGRATION CYCLES FOR THE SOURCE
DCA CNTN            /UNDER EXAMINATION; DEPOSIT IT IN REGISTER CNTN
TAD I 13            /GET THE RIGHT ASCENSION
DCA TEMP1           /DEPOSIT IT IN REGISTERS TEMP1, TEMP2, TEMP3
TAD I 13
DCA TEMP2
TAD I 13
DCA TEMP3
CLL
TAD TEMP3           /OBTAIN H+α=(HOUR ANGLE OF BASELINE)+(R. ASCENSION OF
TAD HRBSL+2         /SOURCE)
DCA CONST9+2
RAL
TAD TEMP2
TAD HRBSL+1
DCA CONST9+1
RAL

TAD TEMP1
TAD HRBSL
DCA CONST9          /REGISTER CONST9, +1, +2 CONTAINS (H+α)
TAD LCTP            /INITIALIZE REGISTERS FOR SCRAP CALCULATIONS
DCA 10              /DEPOSIT INITIAL REGISTER LCT INTO 10
TAD I 14            /OBTAIN HIGH ORDER DECLINATION IN RADIANS
DCA I 10            /DEPOSIT IT INTO LCT
TAD I 14            /OBTAIN LOW-ORDER DECLINATION IN RADIANS
DCA I 10            /DEPOSIT IT INTO LCT+1
JMS I DCOSP         /OBTAIN COSINE OF THE BASELINE DECLINATION (COS D)
DECLB
TAD I HARG
DCA I 10            /DEPOSIT HIGH ORDER COSINE IN LCT+2
TAD I LARG
DCA I 10            /DEPOSIT LOW ORDER COSINE IN LCT+3
JMS I DSINP         /OBTAIN COSINE OF THE BASELINE DECLINATION (SIN D)
DECLB
TAD I HARG          /DEPOSIT IN LCT+4
DCA I 10
TAD I LARG
DCA I 10            /DEPOSIT IN LCT+5
JMS I DCOSP         /OBTAIN COSINE OF THE SOURCE DECLINATION (COSδ)
LCT
TAD I HARG
DCA I 10            /DEPOSIT INTO LCT+6
TAD I LARG
DCA I 10            /DEPOSIT INTO LCT+7
JMS I DSINP         /OBTAIN SINE OF THE SOURCE DECLINATION (SINδ)
LCT
TAD I HARG
DCA I 10            /DEPOSIT INTO LCT+8
TAD I LARG
DCA I 10            /DEPOSIT INTO LCT+9
JMS I DMULTP        /MULTIPLY COSδCOSD
LCT+2
LCT+6
DCA TEMP1
JMS I ROT1L         /ROTATE CONTENTS OF TEMP1, CONTB, CONTC BY ONE LEFT
DCA COSDDE          /REGISTERS COSDDE, +1 CONTAIN COSδCOSD
TAD I CONTB
DCA COSDDE+1
JMS I DMULTP        /MULTIPLY SINδSIND
LCT+4
LCT+8
DCA TEMP1
JMS I ROT1L
DCA SINDDE          /REGISTERS SINDDE, +1 CONTAIN SINδSIND
TAD I CONTB
DCA SINDDE+1
JMP I PAG5          /JUMP TO PAGE 5
BSLAMD, 0
0
EN, N
PUT1P, RACAL-1
PUT2P, STDECL-3
PUT3P, DECAL-1
LCTP, LCT-1
COSDDE,0
0
PAG5, PAGE5
PAUSE
```

```
*1200
PAGE5, JMS I DMULTP  /MULTIPLY COSδSIND
LCT+6
LCT+4
DCA TEMP1
JMS I ROT1L
DCA CONST1          /REGISTERS CONST1, +1 CONTAIN COSδSIND
TAD I CONTB
DCA CONST1+1
JMS I DMULTP        /MULTIPLY COSDSINδ
LCT+2
LCT+8
DCA TEMP1
JMS I ROT1L
DCA CONST2          /REGISTER CONST2, +1 CONTAIN COSDSINδ
TAD I CONTB
DCA CONST2+1
JMS I DMULTP        /OBTAIN d/λ COSδSIND
BSLAMD
CONST1
DCA TEMP1
JMS I ROT1L
DCA CONST1          /CONST1, +1 CONTAIN d/λ COSδSIND
TAD I CONTB
DCA CONST1+1
JMS I DMULTP        /OBTAIN d/λ COSDSINδ
BSLAMD
CONST2
DCA TEMP1
JMS I ROT1L
DCA CONST2          /REGISTERS CONST2, +1 CONTAIN d/λ COSDSINδ
TAD I CONTB
DCA CONST2+1
JMS I DMULTP        /FORM PRODUCT 2π d/λ
PAI
BSLAMD
DCA MEGA+1          /PUT PRODUCT INTO DIVIDEND
TAD I CONTB
DCA MEGA+2
TAD I CONTC
DCA MEGA+3
TAD I CONTD
DCA MEGA+4
TAD MEGA
JMS I DDIVP          /DIVIDE BY 86,400
N86400
DCA CONST0
TAD I LQUOT          /CONST0, +1 CONTAIN (2π/86400)*(d/λ)
DCA CONST0+1
JMS I DMULTP         /MULTIPLY (CONST0)*COSDDE
CONST0
COSDDE
DCA TEMP1
JMS I ROT1L
DCA CONST0           /REGISTERS CONST0, +1 CONTAIN (2π/86400)*(d/λ)*COSδCOSD
TAD I CONTB
DCA CONST0+1
JMS I DMULTP         /OBTAIN (d/λ)*COSD
BSLAMD
LCT+2
DCA TEMP1
JMS I ROT1L
DCA CONST3           /REGISTERS CONST3, +1 CONTAIN (d/λ)*COSD
TAD I CONTB
DCA CONST3+1
JMS I DMULTP        /OBTAIN (d/λ)*SINδSIND
BSLAMD
SINDDE
DCA TEMP1
JMS I ROT1L
DCA CONST4          /REGISTERS CONST4, +1, +2 CONTAIN (d/λ)*SINδSIND
TAD I CONTB
DCA CONST4+1
TAD I CONTC
DCA CONST4+2
JMS I DMULTP        /MULTIPLY (d/λ)*COSδCOSD
BSLAMD
COSDDE
DCA TEMP1
JMS I ROT1L
DCA CONST5          /PRODUCT IS DEPOSITED IN REGISTERS CONST5, +1
TAD I CONTB
DCA CONST5+1        /POINT DECLINATION
1322 TAD PUT4P      /INITIALIZE THE REGISTERS CONTAINING THE DECLINATION
DCA 11              /AT WHICH THE DISHES ARE POINTING; DEPOSIT INITIAL
TAD I 15            /REGISTER IN 11, GET DECLINATION OF THE SOURCE
DCA PROSO3
TAD I 15
DCA PROSO2
TAD I 15
DCA PROSO1          /REGISTERS PROSO1, 2, 3 CONTAIN THE SOURCE DECLINATION
JMS I DECPNT        /GO TO SUBROUTINE DEC12
JMS I DC45          /GO TO SUBROUTINE DEC45, POINT DECL. OF ANT. #1
JMS I DECPNT        /GO TO SUBROUTINE DEC12
JMS I DC43          /GO TO SUBROUTINE DEC43, POINT DECL. AXIS OF ANT. #2
TAD PUT4P           /RE-INITIALIZE THE REGISTERS CONTAINING THE DECLINATION
DCA 11              /AT WHICH THE DISHES ARE POINTING
TAD PROSO1          /DEPOSIT THE NEW DECLINATION POSITION OF DISHES
DCA I 11            /BY MEANS OF THE SELF-INDEXING REGISTER11
TAD PROSO2          /INTO REGISTERS DEC1, +1, +2
DCA I 11            /FOR DISHES #1 AND #2 RESPECTIVELY
TAD PROSO3
DCA I 11
TAD PROSO1
DCA I 11
TAD PROSO2
DCA I 11
TAD PROSO3
1353 DCA I 11
JMP I PAG6          /JUMP TO PAGE 6
CONST2,0
0
CONST0,0
0
CONST3,0
0
CONST5,0
0
PUT4P,DEC1-1
DECPNT,DEC12
DC45, DEC45
DC43,DEC43
PAG6,PAGE6
PAUSE
```

```
*1400                   /POINT HR ANGLE
PAGE6, TAD TRIA
TAD TRIA                /ESTABLISH A 10 MIN. LEAD TIME
TAD TRIA
IAC
JMS I MEGA1
JMS I DDIVP             /DIVIDE IT BY 60
N60
DCA TEMP2
TAD I LQUOT
DCA TEMP3
CLL
TAD TIME+2              /ADD 10/60 TO PRESENT TIME
TAD TEMP3
DCA STIME+2             /REGISTERS STIME, +1, +2 CONTAIN THE TIME
RAL
TAD TIME+1              /AT WHICH TRACKING IS TO START
TAD TEMP2
DCA STIME+1
RAL
TAD TIME
JMP I 1576              /JUMP TO A ROUTINE TO CHECK IF STIME<24
TAD 13                  /REINITIALIZE THE REGISTERS CONTAINING THE RIGHT
TAD M3                  /ASCENSION AT WHICH THE DISHES ARE TO BE POINTED
DCA 13
TAD I 13                /DEPOSIT THE RIGHT ASCENSION α IN REGISTERS
DCA TEMP1               /TEMP1, TEMP2, TEMP3
TAD I 13
DCA TEMP2
TAD I 13
DCA TEMP3
JMS I NEGAT             /NEGATE RIGHT ASCENSION
TAD TEMP1
DCA MALPH               /REGISTERS MALPH, +1, +2 CONTAIN (-α)
TAD TEMP2
DCA MALPH+1
TAD TEMP3
DCA MALPH+2
CLL
TAD TEMP3               /FORM (STIME -α); THIS DIFFERENCE
TAD STIME+2             /IS THE HOUR ANGLE AT WHICH THE DISHES MUST
DCA PROSO3              /POINT; THIS HOUR ANGLE IS STORED IN
RAL                     /REGISTERS PROSO1, PROSO2, AND PROSO3
TAD TEMP2
TAD STIME+1
DCA PROSO2
RAL
TAD TEMP1
TAD STIME
DCA PROSO1
TAD PROSO1              /OBTAIN INTEGRAL PART OF   THIS HOUR ANGLE
SMA CLA                 /IS IT NEGATIVE
JMP.+5                  /NO, JUMP FIVE POSITIONS AHEAD
TAD M24                 /YES, ADD TO IT 24
CIA
TAD PROSO1              /FORM PROSO1 + 24
DCA PROSO1              /DEPOSIT IT IN PROSO1
TAD GET2                /INITIALIZE AGAIN THE REGISTERS THAT CONTAIN THE
DCA 11                  /HOUR ANGLEAT WHICH THE DISHES ARE TO BE POINTED
JMS I HRPNT             /JUMP TO SUBROUTINE HR12
JMS HR37                /JUMP TO SUBROUTINE HR37, POINT HOUR AXIS OF ANT. #1
JMS I HRPNT             /JUMP TO SUBROUTINE HR12
JMS HR36                /JUMP TO SUBROUTINE HR36, POINT HOUR AXIS OF ANT#2
TAD GET2                /REINITIALIZE HOUR ANGLE REGISTERS
DCA 11
TAD PROSO1              /OBTAIN THE NEW HOUR ANGLE POSITION OF DISH #1
DCA I 11                /DEPOSIT IT IN HOUR1 (TRIPPLE PRECISION)
TAD PROSO2
DCA I 11
TAD PROSO3
DCA I 11
TAD PROSO1              /OBTAIN THE NEW HOUR ANGLE OF DISH #2
DCA I 11                /DEPOSIT IT IN HOUR2 (TRIPPLE PRECISION)
TAD PROSO2
  A I 11
TAD PROSO3
DCA I 11
JMP I PAG7              /JUMP TO PAGE 7
STIME,0
0
0
MALPH,0
0
0
GET2,HR1-1
HRPNT,HR12
1525 PAG7,WAITST
HR37,0                  /SUBROUTINE FOR POINTING ANT. #1
JMS I DMULTP            /MULTIPLY (SOURCE HOUR - DISH HOUR)*15*(533.8/1.8)
TEMP1
N5338
DCA TEMP1               /TEMP1, TEMP2, TEMP3 NOW CONTAIN THE NUMBER OF PULSES
TAD I CONTB             /NEEDED TO POINT THE HOUR OF ANT. #1
DCA TEMP2
DCA TEMP3
JMS I NEGAT             /INITIALIZE PULSE COUNT (NEGATIVE NUMBER)
CYCL37,CLA
6411
6372                    /SEND STEPPING PULSE TO ANT.#1
6412                    /WAIT FOR RETURN PULSE
JMP.-1
JMS I PULSE             /GO TO SUBROUTINE WHICH INCREMENTS COUNT OF PULSES
TAD TEMP1               /GET THE PULSE COUNT
SPA CLA                 /IS IT LESS THAN ZERO?
JMP CYCL37              /YES, SEND NEXT STEPPING PULSE
JMP I HR37              /NO, JUMP OUT OF THE SUBROUTINE
HR36,0                  /SUBROUTINE FOR POINTING HOUR OF ANT. #2; SIMILAR
JMS I DMULTP            /TO HR37 EXCEPT FOR GEAR RATIO
TEMP1
N5371
DCA TEMP1
TAD I CONTB
DCA TEMP2
DCA TEMP3
JMS I NEGAT
CYCL36,CLA
6411
6362
6412
JMP.-1
JMS I PULSE
TAD TEMP1
SPA CLA
JMP CYCL36
JMP I HR36
*1576
6550
PAUSE
```

```
*1600
WAITST,6334             /DEACTIVATE CLOCK INTERRUPT
6311                    /CLEAR SKIP FLIP-FLOP
6312                    /HAS CLOCK ARRIVED?
JMP.-1                  /NO, JUMP ONE BACK
JMS I TMINC             /YES, INCREMENT TIME
6321                    /CLEAR CLOCK INTERRUPT FLAG
JMS I 177               /DEPOSIT PRESENT TIME IN REGISTERS TEMP1, TEMP2,&TEMP3
6324                    /ACTIVATE CLOCK INTERRUPT
JMS I NEGAT             /NEGATE TIME
CLL
TAD TEMP3               /FORM DIFF.=(STARTING TIME)-(PRESENT TIME)
TAD I TS+2
DCA TEMP3               /THE DIFFERENCE IS DEPOSITED IN TEMP1,TEMP2,&TEMP3
RAL
TAD TEMP2
TAD I TS+1
DCA TEMP2
RAL
TAD TEMP1
TAD I TS
DCA TEMP1
TAD TEMP1               /GET THE INTEGRAL PART OF DIFFERENCE
SMA CLA                 /IS IT NEGATIVE?
JMP WAITST              /NO, JUMP TO WAITST
6361                    /YES, CLEAR TRACKING INTERRUPTS #36 & #37
6371
6304                    /CLEAR COUNTERS GENERATING TRACKING PULSES
6434                    /SET DIRECTION TO CW
1634 6364               /ACTIVATE TRACKING PULSE INTERRUPT
ARCHI,CLA
LAS                     /DEPOSIT SWITCH REGISTER IN AC
TAD MS7000              /ADD 7000
SNA                     /IS AC ZERO?
JMP WAIT                /YES, JUMP TO WAIT
JMP ARHI                /NO, JUMP TO ARHI
WAIT,CLA                /THIS IS A WAITING LOOP IN CASE THERE IS A BREAKDOWN
DCA TEMPO
IS7 TEMPO               /IN THE SYSTEM; ENTER IT BY MAKING THE
JMP.-1                  /SWITCH REGISTER 1000
CLA                     /CLEAR AC
LAS                     /READ SWITCH REGISTER AGAIN
TAD MS7000              /ADD 7000
SNA                     /IS THE AC NON-ZERO
JMP WAIT                /NO, JUMP BACK TO WAIT
AND MS400               /YES, MASK AC WITH 400
SNA                     /IS AC NON-ZERO
JMP ARHI                /NO, JUMP TO ARHI
JMP I SILY              /YES, DO TIME-CHECK
1660 ARHI,IOF           /TURN INTERRUPT OFF
6311
6312                    /WAIT FOR CLOCK
JMP.-1
JMS I TMINC             /INCREMENT TIME
6334                    /DEACTIVATE CLOCK INTERRUPT
ION                     /TURN INTERRUPT ON
TAD TIME                /DEPOSIT THE PRESENT TIME IN REGISTERS
DCA TEMP1               /TEMP1, TEMP2, &TEMP3
TAD TIME+1
DCA TEMP2
TAD TIME+2
DCA TEMP3
JMS I NEGAT             /NEGATE THE TIME
CLL
TAD TEMP3               /COMPUTE H+α-t; DEPOSIT IT IN TEMP1, TEMP2, &TEMP3
TAD CONST9+2
DCA TEMP3
RAL
TAD TEMP2
TAD CONST9+1
DCA TEMP2
RAL
TAD TEMP1
TAD CONST9
DCA TEMP1
JMP I PAG9              /JUMP TO PAGE 9
TS,STIME
STIME+1
STIME+2
MS400,400
SILY,SILLY
1720 PAG9,PAGE9
TRANSF,0                /THIS SUBROUTINE CONVERTS HOUR ANGLES GIVEN
TAD I 10                /IN HOURS, MINS., SECS., &FRACTIONAL SECS.
DCA PROSO1              /AND DECLINATIONS GIVEN IN DEG.,MINS.,SECS.,&FR. SECS
TAD I 10                /INTO SINGLE UNIT TRIPPLE PRECISION NUMBERS
JMS I MEGA1
JMS I DDIVP
N60
DCA PROSO2
TAD I LQUOT
DCA PROSO3
TAD I 10
DCA MEGA+2
DCA MEGA+1
TAD I 10
DCA MEGA+3
DCA MEGA+4
TAD MEGA
JMS I DDIVP
N3600
DCA TEMPO
CLL
TAD I LQUOT
JMP I TRANSF
N22,2200
0000
N5442,0054
4200
N5416,0054
1600
N17,0017
0
N5338,0123
3200
N5371,0123
7300
PAUSE
```

```
*2000
DEC12,0            /DECLINATION POINTING SUBROUTINE
TAD I 11           /GET PRESENT DECLINATION POSITION OF THE DISH
DCA TEMP1          /DEPOSIT IN TEMP1,2,3
TAD I 11
DCA TEMP2
TAD I 11
DCA TEMP3
JMS I NEGAT        /NEGATE DISH DECLINATION POSITION
CLL
TAD PROSO3         /OBTAIN DIFF.=(SOURCE DECLINATION)-(ANT. DECLINATION)
TAD TEMP3
DCA MEGA+3         /DEPOSIT DIFF. INTO DIVIDEND REGISTERS
RAL
TAD PROSO2
TAD TEMP2
DCA MEGA+2
RAL
TAD PROSO1
TAD TEMP1
DCA MEGA+1
DCA MEGA+4
TAD MEGA
JMS I DDIVP        /DIVIDE DIFFERENCE BY 1.8 DEGREES
N22
DCA TEMP1          /DEPOSIT QUOTIENT IN TEMP1,2
TAD I LQUOT
DCA TEMP2
DCA TEMP3
TAD TEMP1          /GET TEMP1
SPA CLA            /IS IT POSITIVE?
JMP.+4             /NO, JUMP 4 POSITIONS AHEAD
6434               /YES, SET DIRECTION CONTROLS TO CW
JMS I NEGAT        /NEGATE TEMP1,2
JMP.+3             /JUMP 3 POSITIONS AHEAD
CLA                /CLEAR AC
6454               /SET DIRECTION TO CCW
JMP I DEC12        /JUMP OUT OF THE SUBROUTINE
HR12,0             /HOUR ANGLE POINTING SUBROUTINE
TAD I 11           /GET PRESENT HOUR ANGLE
DCA TEMP1          /DEPOSIT IT IN TEMP1, TEMP2, &TEMP3
TAD I 11
DCA TEMP2
TAD I 11
DCA TEMP3
JMS I NEGAT        /NEGATE TEMP1, TEMP2, &TEMP3
CLL
TAD TEMP3          /OBTAIN DIFF.=(SOURCE HOUR)-(ANT. HOUR ANGLE)
TAD PROSO3
DCA TEMP3
RAL
TAD TEMP2
TAD PROSO2
DCA TEMP2
RAL
TAD TEMP1
TAD PRCSO1
DCA TEMP1          /REGISTERS TEMP1,2,3 CONTAIN DIFFERENCE D
TAD TEMP1          /GET THE INTEGRAL PART OF D
SMA CLA            /IS IT NEGATIVE? CLEAR AC
JMP POSD           /NO, JUMP TO POSD
JMS I NEGAT        /YES, OBTAIN ITS ABSOLUTE VALUE D
TAD M6
TAD M6
TAD TEMP1          /FORM |D|-12
SPA CLA            /IS AC POSITIVE? CLEAR AC
JMP.+10            /NO, JUMP 8 LOCATIONS AHEAD
6434               /SET DIRECTION TO CW
JMS I NEGAT        /NEGATE TEMP1,2,3
TAD M24
CIA
TAD TEMP1          /OBTAIN 24-|D|
DCA TEMP1          /DEPOSIT IT IN TEMP1
JMP STPNT          /JUMP TO STPNT
CLA
6454               /SET DIRECTION TO CCW
JMP STPNT          /JUMP TO STPNT
POSD,CLA
TAD M6
TAD M6
TAD TEMP1          /OBTAIN D-12
SMA CLA            /IS AC NEGATIVE? CLEAR AC
JMP.+3             /NO, JUMP 3 LOCATIONS AHEAD
6434               /YES, SET DIRECTION TO CCW
JMP STPNT          /JUMP TO STPNT
CLA
6454               /SET DIRECTION TO CCW
JMS I NEGAT        /NEGATE TEMP1,2,3
TAD M24
CIA
TAD TEMP1          /OBTAIN 24-D
DCA TEMP1          /DEPOSIT IT IN TEMP1
STPNT,CLA CLL
TAD TEMP1
DCA MEGA+1
TAD TEMP2
DCA MEGA+2
TAD TEMP3
DCA MEGA+3
DCA MEGA+4
TAD MEGA
JMS I DDIVP        /DIVIDE ADJUSTED DIFFERENCE BY 1.8 DEGREES
N22
DCA TEMP1
TAD I LQUOT
DCA TEMP2
JMS I DMULTP       /MULTIPLY THE QUOTIENT BY 15 DEG./HOUR
TEMP1
N17
TAD I CONTB
DCA TEMP1          /TEMP1, TEMP2 CONTAIN (ADJUSTED DIFFERENCE)*(15/1.8)
TAD I CONTC        /THIS NUMBER IS NEGATIVE
DCA TEMP2
JMP I HR12         /JUMP OUT OF THE SUBROUTINE
PAI,3110
3755
PI12,2060
2510
CONS10,0000
0363
PAUSE
```

```
*2200
PAGE9,TAD TEMP1    /GET INTEGRAL PART OF H+α-t
TAD M24            /ADD -24
SPA                /IS THE DIFFERENCE POSITIVE?
SKP                /NO, SKIP
DCA TEMP1          /YES, DEPOSIT THE DIFFERENCE IN TEMP1
CLA
JMS I ROT6L        /ROTATE CONTENTS OF TEMP1,2,3 6 POSITIONS LEFT
JMS I DMULTP       /FORM THE PRODUCT ( /12)*(H+α-t)
TEMP1
PI12
DCA TEMP1          /DEPOSIT HIGH ORDER TERM OF THE PRODUCT IN TEMP1
JMS I ROT2L        /ROTATE PRODUCT BY 2 BINARY POSITIONS LEFT
TAD I CONTB
DCA TEMP2          /ARGUMENT IS CONTAINED IN TEMP1,2
JMS I CKARG        /CHECK IF -π<ARG<π
JMS I DCOSP        /OBTAIN COS(π/12*(H+α-t))
TEMP1
TAD I HARG
DCA COSTI          /REGISTERS COSTI,+1 CONTAIN COS((π/12)*(H+α-t))
TAD I LARG
DCA COSTI+1
JMS I DSINP        /OBTAIN SIN((π/12)*(H+α-t))
TEMP1
TAD I HARG
DCA SINTI          /REGISTERS COSTI,+1 CONTAIN SIN((π/12)*(H+α-t))
TAD I LARG
DCA SINTI+1
JMS I DMULTP       /MULTIPLY (COSTI)*COS((π/12)*(T/2))
COSTI
COSMDT             /WHERE T IS INTEGRATION LENGTH
DCA TEMP1
JMS I ROT1L
DCA  COSDIF
TAD I CONTB
DCA COSDIF+1
JMS I DMULTP       /MULTIPLY (SINTI)*SIN((π/12)*(T/2))
SINTI
SINMDT
DCA TEMP1
JMS I ROT1L
DCA TEMP1
CLL
TAD I CONTB        /FORM SUM OF THE TWO PRODUCTS
TAD COSDIF+1
DCA COSDIF+1       /DEPOSIT THE SUM IN COSDIF,+1
RAL
TAD TEMP1
TAD COSDIF
DCA COSDIF         /COSDIF,+1 CONTAIN COS((π/12)*(H+α-t-T/2))
JMS I DMULTP       /MULTIPLY (SINTI)*COS((π/12)*(T/2))
SINTI
COSMDT
DCA TEMP1
JMS I ROT1L
DCA PROSO1
TAD I CONTB
DCA PROSO2
JMS I DMULTP       /MULTIPLY (COSTI)*SIN((π/12)*(T/2))
COSTI
SINMDT
DCA TEMP1          /DEPOSIT THE LAST PRDUCT IN TEMP1,2,3
JMS I ROT1L
DCA TEMP1
TAD I CONTB
DCA TEMP2
DCA TEMP3
JMS I NEGAT        /NEGATE CONTAINS OF TEMP1,2,3
CLL
TAD TEMP2          /OBTAIN (SINTI)*COS((π/12)*(H+α-t-T/2))-(COSTI)*
TAD PROSO2         /SIN((π/12)*(T/2))
DCA SINDIF+1       /DEPOSIT DIFFERENCE IN SINDIF,+1
RAL
TAD TEMP1
TAD PROSO1
DCA SINDIF         /SINDIF,+1 CONTAIN SIN((π/12)*(H+α-t-T/2))
JMS I COMPE        /DO DELAY COMPENSATION
CLA
CMA                /INITIALIZE REGISTERS IN WHICH THE PARAMETERS
TAD M6             /SOURCE HOUR ANGLE, U&V ARE TO BE DEPOSITED
TAD TOPOS
DCA 17             /DEPOSIT INITIAL REGISTER IN 17
CLL
TAD TIME+2         /OBTAIN SUM=(PRESENT TIME)+(INTEGRATION TIME)/2
TAD MIDLTM+1
DCA TEMP3
RAL
TAD TIME+1
TAD MIDLTM
DCA TEMP2
RAL
TAD TIME
DCA TEMP1          /TEMP1,2,3 CONTAIN THE ABOVE SUM
CLL
TAD TEMP3          /OBTAIN SOURCE HOUR ANGLE AT CENTER OF
TAD I MALF+2       /INTEGRATION INTERVAL=t+T/2 - α
DCA TEMP3
RAL
TAD TEMP2
TAD I MALF+1
DCA TEMP2
RAL
TAD TEMP1
TAD I MALF
DCA TEMP1          /DEPOSIT HOUR ANGLE IN TEMP1,2,3
TAD TEMP1          /GET INTEGRAL PART OF HOUR ANGLE (TEMP1)
SMA CLA            /IS IT NEGATIVE?
JMP.+5             /NO, JUMP 5 LOCATIONS AHEAD
TAD M24            /YES, ADD 24 TO TEMP1
CIA
TAD TEMP1
DCA TEMP1          /DEPOSIT SUM BACK IN TEMP1
JMP I PAG10        /JUMP TO PAGE 10
COSDIF,0
0
SINDIF,0
0
MALF,MALPH
MALPH+1
MALPH+2
PAG10,PAGE10
PAUSE
```

```
*2400
PAGE10,JMS I ROT6L  /ROTATE CONTENTS OF TEMP1,2,3 6 BITS LEFT
TAD TEMP1           /GET THE ROTATED HOUR ANGLE AND
DCA I 17            /STORE IT BY MEANS OF THE SELF-INDEXING
TAD TEMP2           /REGISTER 17
DCA I 17
JMS I DMULTP        /MULTIPLY (d/λ)*COSD*SIN((π/12)*(H+α-t-T/2))
CONST3
SINDIF
DCA TEMP1           /THIS PRODUCT IS THE PARAMETER U
JMS I ROT1L
DCA I 17
TAD I CONTB         /STORE U
DCA I 17
JMS I DMULTP        /MULTIPLY (d/λ)*COSD*SINδ*COS((π/12)*(H+α-t-T/2))
CONST2
COSDIF
DCA TEMP1
JMS I ROT1L
DCA TEMP1           /DEPOSIT IT IN TEMP1,2,3
TAD I CONTB
DCA TEMP2
DCA TEMP3
JMS I NEGAT         /NEGATE CONTENTS
CLL
TAD TEMP2           /ADD (d/λ)*COSδ*SIND TO TEMP1,2,3
TAD CONST1+1
DCA TEMP2
RAL
TAD TEMP1
TAD CONST1
DCA TEMP1           /THE SUM IS THE PARAMETER V
TAD TEMP1
DCA I 17            /STORE V
TAD TEMP2
DCA I 17
2443 TAD INTEGR     /GET INTEGRATION TIME EXPRESSED IN NUMBER OF CLOCK
DCA CMINTG          /PULSES;INITIALIZE INTEGRATION INTERVAL COUNT
TAD INTEGR+1        /CONTAINED IN REGISTERS CMINTG & CMINTG+1
DCA CMINTG+1
DCA SUM1            /CLEAR REGISTERS THAT STORE Σ_i COS²γ_i
DCA SUM1+1
DCA SUM1+2
DCA SUM2            /CLEAR REGISTERS THAT STORE Σ_i SIN²γ_i
DCA SUM2+1
DCA SUM2+2
TAD M24
DCA TEMPO           /DEPOSIT -24 IN TEMPO TO KEEP COUNT
CMA                 /THE 24 REGISTERS THAT STORE Σ COS²γi & Σ SIN²γi
TAD TOPOS           /FOR THE FOUR DATA CHANNELS ARE LOCATED BETWEEN
DCA 10              /SUMPEL AND SUMPEL+27
DCA I 10            /CLEAR THESE REGISTERS SEQUENTIALLY BY
ISZ TEMPO           /INCREMENTING TEMPO
JMP.-2
DATA,IOF            /INTEGRATION CYCLE BEGINS HERE
CMA                 /INITIALIZE REGISTERS THAT WILL STORE THE
TAD STORE           /INPUTS FROM THE A-D CONVERTER
DCA 10              /DEPOSIT INITIAL REGISTER IN 10
6311
6312                /WAIT FOR THE CLOCK THAT WILL INITIATE THE DATA
JMP.-1              /TAKING CYCLE
CLA
6743                /SCAN INPUT DEVICE 74
NOP
NOP
NOP
NOP
NOP
DCA I 10            /DEPOSIT BY MEANS OF SELF-INDEXING REGISTER 10
6703                /SCAN INPUT DEVICE 70
NOP
NOP
NOP
NOP
NOP
DCA I 10            /DEPOSIT
6643                /SCAN INPUT DEVICE 64
NOP
NOP
NOP
NOP
NOP
DCA I 10            /DEPOSIT
6603                /SCAN INPUT DEVICE 60
NOP
NOP
NOP
NOP
NOP
DCA I 10            /DEPOSIT
6334                /REACTIVATE CLOCK INTERRUPT
ION                 /TURN INTERRUPT ON
JMS I TMINC         /INCREMENT TIME REGISTER BY 0.2(1+0.0027)/3600 HOURS
TAD COSTI+1         /GET COS((π/12)*(H+α-t_{i-1}))
DCA COSIM1+1        /DEPOSIT IT IN SCRAP REGISTER
TAD COSTI
DCA COSIM1
TAD SINTI+1         /GET SIN((π/12)*(H+α-t_{i-1}))
DCA SINIM1+1        /DEPOSIT IT IN SCRAP REGISTER
TAD SINTI
DCA SINIM1
JMS I DMULTP        /MULTIPLY SIN((π/12)*(H+α-t_{i-1}))*(2π/86400)*
SINIM1              /0.2(1+0.0027)
CONS10
DCA TEMP1
CLL
TAD COSIM1+1        /ADD TO THE ABOVE PRODUCT COS((π/12)*(H+α-t_{i-1}))
TAD I CONTB
DCA COSTI+1
RAL
TAD TEMP1
TAD COSIM1
DCA COSTI           /COSTI,+1 CONTAIN COS((π/12)*(H+α-t_i))
JMS I DMULTP        /MULTIPLY COS((π/12)*(H+α-t_{i-1}))*(2π/86400)*
COSIM1              /0.2(1+0.0027)
CONS10
DCA TEMP1
TAD I CONTB
DCA TEMP2
DCA TEMP3
JMS I NEGAT         /NEGATE THE ABOVE PRODUCT
CLL
JMP I PAG11         /JUMP TO PAGE 11
SAVERL,0            /THESE ARE THE FOUR REGISTERS IN
0                   /WHICH THE DATA ARE STORED
0                   /AS SOON AS THEY ARE RECEIVED
0
PAG11,PAGE11
PAUSE
```

```
*2600
PAGE11,TAD TEMP2 /FORM SIN((π/12)*(H+α-t_{i-1})-(2π/86400)*
TAD SINIM1+1        /0.2COS((π/12)*(H+α-t_{i-1}))
DCA SINTI+1         /DEPOSIT IT IN SINTI,+1
RAL
TAD TEMP1
TAD SINIM1
DCA SINTI           /SINTI,+1 NOW CONTAIN SIN((π/12)*(H+α-t_i))
JMS I DMULTP        /MULTIPLY (d/λ)*COSδ*COSD*COSTI
CONST5
COSTI
DCA TEMP1
JMS I ROT1L
DCA TEMP1
CLL
TAD CONST4+2        /ADD TO THE ABOVE PRODUCT (d/λ)*SIND*SINδ
TAD I CONTC
DCA PROSO3
RAL
TAD CONST4+1
TAD I CONTB
DCA PROSO2
RAL
TAD TEMP1
TAD CONST4
DCA PROSO1          /REGISTERS PROSO1,2,3 NOW CONTAIN (d/λ)*SINθ_i
TAD PROSO1          /GET PROSO1
SMA CLA             /IS AC NEGATIVE? CLEAR AC
JMP.+2              /NO,JUMP 2 LOCATIONS AHEAD
TAD MS7000          /YES, SET FLAG TO 7000
DCA ALFLG           /SET FLAG TO 0
TAD MS7000          /GET 7000
CMA                 /COMPLEMENT IT
AND PROSO2          /MASK THE FRACTIONAL PART OF (d/λ)*SINθ_i
SZA                 /IS THE HIGH ORDER FRACTIONAL PART 0?
JMP.+3              /NO, JUMP 3 LOCATIONS AHEAD
TAD PROSO3          /YES, GET THE LOW ORDER FRACTIONAL PART
SZA CLA             /SKIP ON ZERO AC, CLEAR AC
TAD ALFLG           /ADD FLAG AND DEPOSIT AC IN PROSO2
DCA PROSO2          /PROSO2,3 NOW CONTAIN THE SIGNED FRACTIONAL PART
JMS I DMULTP        /OF (d/λ)*SINθ_i; MULTIPLY PROSO2,3 BY 2π
PAI
PROSO2
DCA TEMP1
JMS I ROT3L         /ROTATE 3 LOCATIONS LEFT
TAD I CONTB
DCA TEMP2           /TEMP1,2 CONTAIN ARGUMENT
JMS I CKARG         /CHECK IF -π<ARGUMENT<π
JMS I  DCOSP        /OBTAIN COS((2πd/λ)SINθ_i)
TEMP1
TAD I HARG
DCA COSGAM          /COSGAM,+1 CONTAIN COS((2πd/λ)SINθ_i)
TAD I LARG
DCA COSGAM+1
JMS I DSINP         /OBTAIN SIN((2πd/λ)SINθ_i)
TEMP1
TAD I HARG
DCA SINGAM          /SINGAM,+1 CONTAIN SIN((2πd/λ)SINθ_i)
TAD I LARG
DCA SINGAM+1
JMS I DMULTP        /OBTAIN (COSGAM)²
COSGAM
COSGAM
DCA TEMP1
CLL
JMS I ROT1R         /ROTATE ONE RIGHT
CLL
TAD SUM1+2          /ADD (COSGAM)² TO THE CONTENTS OF
TAD I CONTB         /SUMMING REGISTERS SUM1,+1,+2
DCA SUM1+2
RAL
TAD SUM1+1
TAD TEMP1
DCA SUM1+1
RAL
TAD SUM1
DCA SUM1
JMS I DMULTP        /OBTAIN (SINGAM)²
SINGAM
SINGAM
DCA TEMP1
CLL
JMS I ROT1R         /ROTATE ONE RIGHT
CLL
TAD SUM2+2          /ADD (SINGAM)² TO THE CONTENTS OF
TAD I CONTB         /SUMMING REGISTERS SUM2,+1,+2
DCA SUM2+2
RAL
TAD SUM2+1
TAD TEMP1
DCA SUM2+1
RAL
TAD SUM2
DCA SUM2
TAD NDVICE          /GET INPUT DEVICE INDEX (-4)
DCA CNTDEV          /DEPOSIT -4 INTO THE COUNT REGISTER
TAD STORE           /GET THE GROUP OF REGISTERS CONTAINING THE DATA
DCA ADRES           /SAMPLES; DEPOSIT IN ADRES THE FIRST OF THEM
TAD I ADRES         /GET INPUT SAMPLE
TAD MS7000          /SUBTRACT 2
DCA I ADRES         /DEPOSIT DEFFERENCE BACK IN THE SAME REGISTER
ISZ ADRES           /INITIALIZE FOR NEXT SAMPLE
ISZ CNTDEV          /IS DEVICE INDEX ZERO?
JMP .-5             /NO, JUMP BACK 5 LOCATIONS
TAD STORE           /YES, THE SECTION FROM THIS LOCATION TO THE END OF
IAC                 /THIS PAGE OBTAINS FROM THE DATA CORRESPONDING
IAC                 /TO THE CROSS-POLARIZATION CORRELATION FUNCTIONS
DCA ADRES           /(R1*L2) & (R2*L1), THE THIRD AND FOURTH
TAD ADRES           /STOKES PARAMETERS; THIS IS DONE BY TAKING
IAC                 /FIRST THE SUM AND THEN THE DIFFERENCE OF THESE
DCA DIXE            /TWO PRODUCTS
TAD I ADRES
TAD I DIXE
DCA TEMP1
TAD I DIXE
CIA
TAD I ADRES
DCA I DIXE
TAD TEMP1
DCA I ADRES
JMP I PAG12         /JUMP TO PAGE 12
COSGAM,0
0
SINGAM,0
0
PAG12,PAGE12
PAUSE
```

```
*3000
PAGE12, TAD NDVICE /OBTAIN INPUT DEVICE INDEX (-4)
DCA CNTDEV          /DEPOSIT -4 INTO THE COUNT REGISTER
CMA                 /INITIALIZE DATA STORAGE REGISTERS
TAD STORE           /GET SAVERL-1
DCA 10              /DEPOSIT IT IN 10
TAD TOPOS           /GET SUMPEL (FIRST OF SUMMING REGISTERS)
DCA DIXE            /DEPOSIT IT IN DIXE
LSOFIT,TAD I 10     /GET DATA SAMPLE OF DEVICE #1 (y_i)
DCA PROSO1          /DEPOSIT IT IN PROSO1
DCA PROSO2
JMS I DMULTP        /MULTIPLY y_i COS γ_i
PROSO1
COSGAM
DCA TEMP1           /DEPOSIT HIGH ORDER TERM OF PRODUCT IN TEMP1
JMS I PARE          /CHECK FOR SIGN, SET LINK IF NEGATIVE
JMS I ROT1R         /ROTATE ONE RIGHT
CLL
TAD DIXE            /GET CONTENT OF DIXE (SUMPEL)
IAC
IAC
DCA ADRES           /DEPOSIT SUMPEL+2 IN ADRES
TAD I ADRES         /ADD CONTENT OF SUMPEL+2 TO CONTB WHICH
TAD I CONTB         /CONTAINS THE LOW ORDER TERM OF y_i COS γ_i
DCA I ADRES         /DEPOSIT SUM IN SUMPEL+2
TAD DIXE            /GET SUMPEL
IAC
DCA ADRES           /DEPOSIT SUMPEL+1 IN ADRES
RAL
TAD I ADRES         /GET CONTENT OF SUMPEL+1
TAD TEMP1           /ADD TEMP1
DCA I ADRES         /DEPOSIT SUM IN SUMPEL+1
RAL                 /ROTATE LINK LEFT
TAD I DIXE          /ADD SUMPEL (HIGH ORDER Σ^{i-1}_l y_l COS γ_l )
TAD TEMPO           /ADD PROPER SIGN OF y_i COS γ_i
DCA I DIXE          /DEPOSIT SUM IN SUMPEL
JMS I DMULTP        /MULTIPLY y_i SIN γ_i
PROSO1
SINGAM
DCA TEMP1           /TEMP1 CONTAINS HIGH ORDER TERM OF y_i SIN γ_i
JMS I PARE
JMS I ROT1R
CLL
TAD DIXE            /GET SUMPEL
TAD TRIA            /ADD 3
IAC
IAC
DCA ADRES           /DEPOSIT SUMPEL+5 IN ADRES
TAD I ADRES         /GET CONTENT OF SUMPEL+5
TAD I CONTB         /ADD TO IT LOW ORDER TERM OF y_i SIN γ_i
DCA I ADRES         /DEPOSIT IN SUMPEL+5
TAD DIXE
TAD TRIA
IAC
DCA ADRES           /DEPOSIT IN ADRES SUMPEL+4
RAL
TAD I ADRES         /GET CONTENT OF SUMPEL+4
TAD TEMP1           /ADD TEMP1
DCA I ADRES         /DEPOSIT IN SUMPEL+4
TAD DIXE
TAD TRIA
DCA ADRES           /DEPOSIT IN ADRES SUMPEL+3
RAL                 /ROTATE LINK LEFT
TAD I ADRES         /ADD SUMPEL+3 (HIGH ORDER TERM OF Σ^{i-1}_l y_l SIN γ_l )
TAD TEMPO           /ADD SIGN OF y_i SIN γ_i
DCA I ADRES         /DEPOSIT SUM IN SUMPEL+6
TAD DIXE            /GET SUMPEL
TAD EXI             /ADD SIX
DCA DIXE            /DEPOSIT SUMPEL+6 IN DIXE
ISZ CNTDEV          /INCREMENT DEVICE INDEX REGISTER
JMP LSOFIT          /JUMP TO LSOFIT IF INDEX 0
IS7 CM300           /CHECK FOR COMPENSATION
SKP                 /SKIP
JMS I COMPE         /COMPENSATE
CLA CLL
TAD CMINTG+1        /INCREMENT INDEX REGISTER THAT KEEPS
IAC                 /TRACK OF THE NUMBER OF CLOCK PULSES
DCA CMINTG+1        /RECEIVED IN THE PRESENT INTEGRATION CYCLE
RAL
TAD CMINTG
DCA CMINTG
TAD CMINTG+1
SZA CLA
JMP I DATAC
TAD CMINTG
SZA CLA             /IS THE INTEGRATION CYCLE OVER?
JMP I DATAC         /NO, JUMP TO DATA
6321                /YES, CLEAR CLOCK INTERRUPT FLAG
6324                /ACTIVATE CLOCK INTERRUPT
CMA
TAD TOPOS           /GET SUMPEL-1
DCA 10              /DEPOSIT IT IN 10
TAD 10              /GET SUMPEL-1
DCA 11              /DEPOSIT IT IN 11
TAD NDVICE          /GET DEVICE INDEX (-4)
DCA CNTDEV          /DEPOSIT IN CNTDEV
REDIVD,JMS I MEGI
JMS I DDIVP         /DIVIDE Σ_i y_i COS γ_i / Σ_i COS² γ_i
SUM1
DCA I 11            /DEPOSIT HIGH ORDER QUOTIENT IN SUMPEL
TAD I LQUOT
DCA I 11            /DEPOSIT LOW ORDER QUOTIENT IN SUMPEL+3
JMS I MEGI
JMS I DDIVP         /DIVIDE Σ_i y_i SIN γ_i / Σ_i SIN² γ_i
SUM2
DCA I 11            /DEPOSIT HIGH ORDER QUOTIENT IN SUMPEL+2
TAD I LQUOT
DCA I 11            /DEPOSIT LOW ORDER QUOTIENT IN SUMPEL+3
ISZ CNTDEV          /INCREMENT DEVICE INDEX
JMP REDIVD          /JUMP TO REDIVD IF INDEX 0
3155 TAD N17P       /ADD 15 (INITIALIZE REGISTERS TO RECEIVE THE CALIBRATION DATA)
TAD TOPOS           /ADD SUMPEL
DCA 17              /DEPOSIT SUMPEL+15 IN 17
IOF
6311
6312                /WAIT FOR CLOCK
JMP .-1
JMS I TMINC
JMP I PAG13         /JUMP TO PAGE 13
EXI,6
DATAC,2465
N17P,17
MEGI, MEGI10
PAG13,PAGE13
PAUSE
```

```
*3200
PAGE13,CLA
6343                /SAMPLE CALIBRATION DEVICE #1
NOP
NOP
NOP
NOP
NOP
TAD MS7000          /SUBTRACT 2
RAL CLL
DCA I 17            /DEPOSIT IT IN SUMPEL+16
DCA I 17
6443                /SAMPLE CALIBRAION DEVICE #2
NOP
NOP
NOP
NOP
NOP
TAD MS7000          /SUBTRACT 2
RAL CLL
DCA I 17            /DEPOSIT IT IN SUMPEL+18
DCA I 17
6503                /SAMPLE CALIBRATION DEVICE #3
NOP
NOP
NOP
NOP
NOP
TAD MS7000          /SUBTRACT 2
RAL CLL
DCA I 17            /DEPOSIT IN SUMPEL+20
DCA I 17
6543                /SAMPLE CALIBRATION DEVICE #4
NOP
NOP
NOP
NOP
NOP
TAD MS7000          /SUBTRACT 2
RAL CLL
DCA I 17            /DEPOSIT IT IN SUMPEL+22
DCA I 17
6321                /CLEAR CLOCK INTERRUPT FLAG
ION                 /TURN INTERRUPT ON
JMP I PAG21         /JUMP TO PAGE 21
3254 PAG21,PAGE21
DMEGA, 0            /SUBROUTINE THAT IS USED PRIOR TO
DCA MEGA+1          /THE DIVIDE SUBROUTINE TO SET UP THE
DCA MEGA+2          /DIVIDEND IN THE PROPER FORMAT
DCA MEGA+3
DCA MEGA+4
TAD MEGA
JMP I DMEGA
3264 NEGATE,0       /THIS SUBROUTINE GIVES THE 2'S
CLA CLL             /COMPLEMENT OF A TRIPPLE PRECISION NUMBER
TAD TEMP3
CIA
DCA TEMP3
RAL
DCA KRIK
TAD TEMP2
CMA
TAD KRIK
DCA TEMP2
RAL
DCA KRIK
TAD TEMP1
CMA
TAD KRIK
DCA TEMP1
JMP I NEGATE
3306 CHKARG, 0      /CHECKS THE SIGN OF THE ARGUMENT OF A SINE OR COSI
TAD TEMP1           /GET HIGH ORDER ARGUMENT
SMA CLA             /IS ACCUMULATOR NEGATIVE?
JMP POSARG          /NO, JUMP TO POSARG
DCA TEMP3           /YES,
JMS I NEGAT         /NEGATE CONTENTS OF TEMP1,2,3( |α| )
TAD TEMP1           /GET AGAIN HIGH ORDER TERM OF |α|
TAD MPIOT           /FORM |α| - π
SMA CLA             /IS IT NEGATIVE?
JMP .+3             /NO, JUMP 3 LOCATIONS AHEAD
JMS  I NEGAT        /YES, NEGATE
JMP SIFTL           /JUMP TO SIFTL
JMS I NEGAT         /NEGATE
CLL
TAD TEMP2           /OBTAIN 2π- |α|
TAD TWOPI+1
DCA TEMP2
RAL
TAD TEMP1
TAD TWOPI
DCA TEMP1
JMP SIFTL           /JUMP TO SIFTL
POSARG,CLA
TAD TEMP1           /GET HIGH ORDER TERM OF α
TAD MPIOT           /FORM α - π
SMA CLA             /IS IT NEGATIVE?
JMP.+2              /NO, JUMP 2 LOCATIONS AHEAD
JMP SIFTL           /YES, JUMP TO SIFTL
CLA CLL
TAD TEMP2           /FORM α -2π
TAD MTWOPI+1
DCA TEMP2
RAL
TAD TEMP1
TAD MTWOPI
DCA TEMP1
SIFTL,CLL
TAD TEMP2           /TEMP1 AND TEMP2 CONTAIN THE ARGUMENT
RAL                 /ADJUSTED TO BE -π < ARG < π
DCA TEMP2           /THEN TEMP1,2 ARE ROTATED ONE POSITION
TAD TEMP1           /LEFT SO THAT THE BINARY POINT IS IN THE
RAL                 /PROPER PLACE
DCA TEMP1
JMP I CHKARG        /JUMP OUT OF THE SUBROUTINE
MPIOT,6333
6012
TWOPI,3110
3755
MTWOPI,4667
4023
PAUSE
```

```
*5200
PAGE21,CLA CLL
TAD K246
JMS I TYPO          /TYPE &; THREE & IS THE CODE
TAD K246            /INDICATING THE BEGINNING OF THE
JMS I TYPO          /DATA PUNCH OUT
TAD K246
JMS I TYPO
JMS I BPUNCH        /PUNCH OUT DATA
CLA
TAD K244
JMS I TYPO          /TYPE $; THREE $ IS THE CODE INDICATING
TAD K244            /THE END OF THE PUNCH OUT
JMS I TYPO
TAD K244
JMS I TYPO
JMS I CRLFP         /TYPE LINE FEED AND CARRIAGE RETURN
JMS I CRLFP
CMA
TAD M6
TAD TOPOS           /GET THE REGISTER THAT CONTAINS THE HOUR ANGLE
DCA 10
TAD I 10            /GET AND DEPOSIT THE HIGH ORDER TERM
DCA TEMP1           /OF THE HOUR ANGLE INTO TEMP1
TAD I 10            /AND THE LOW ORDER INTO TEMP2
DCA  TEMP2
TAD TEMP1           /GET TEMP1
AND MS7700          /GET THE INTEGRAL PART OF TEMP1
RTR CLL             /ROTATE IT 6 POSITIONS RIGHT
RTR
RTR
JMS I DCPRNT        /PRINT INTEGRAL PART OF THE HOUR ANGLE
JMS I PUNCT         /PRINT A POINT (.)
TAD MS7700
CMA
AND TEMP1           /MASK THE FRACTIONAL PART OF TEMP1
DCA TEMP1           /DEPOSIT IN TEMP1
JMS I DMULTP        /MULTIPLY THE FRACTIONAL PART BY 1000
N1000
TEMP1
DCA TEMP1           /DEPOSIT THE PRODUCT IN TEMP1,2,3
TAD I CONTB
DCA TEMP2
TAD I CONTC
DCA TEMP3
JMS I ROT6L         /ARRANGE THE BINARY POINT BY ROTATING 6 LEFT
TAD TEMP1           /ADD TEMP1
JMS I DCPRNT        /PRINT IT
JMS I CRLFP         /PRINT CARRIAGE RETURN AND LINE FEED
JMS I CRLFP
CMA
TAD TOPOS           /GET SUMPEL-1
DCA 10
TAD M6              /SET UP A -12 COUNT SINCE THERE ARE TWELVE
TAD M6              /NUMBERS WITH THE SAME FORMAT TO BE PRINTED
DCA CNTDEV          /DEPOSIT -12 IN CNTDEV
CLABCD,TAD I 10     /GET FIRST NUMBER (HIGH ORDER TERM)
DCA TEMP1           /DEPOSIT IT IN TEMP1
TAD I 10            /LOW ORDER TERM
DCA TEMP2           /DEPOSIT IT IN TEMP2
TAD TEMP1           /GET TEMP1
SPA CLA             /SKIP IF POSITIVE
JMP .+11            /JUMP 11 LOCATIONS AHEAD
JMS ROTP            /JUMP TO ROTP SUBROUTINE
JMS I SPRNT         /PRINT OUT INTEGRAL PART (POSITIVE)
JMS I PUNCT         /PRINT A POINT (.)
TAD MS7000
CMA
AND TEMP1           /MASK FRACTIONAL PART OF TEMP1
DCA TEMP1           /DEPOSIT IT IN TEMP1
JMP FRCNL
JMS ROTP            /JUMP TO SUBROUTINE ROTP
TAD MS7770          /ADD THE NEGATIVE SIGN TO THE ROTATED TEMP1
DCA PROSO1          /DEPOSIT SIGNED INTEGRAL PART IN PROSO1
TAD MS7000          /IN THE NEXT 15 INSTRUCTIONS WE CHECK WHETHER
CMA                 /THE FRACTIONAL PART IS ZERO
AND TEMP1           /MASK THE FRACTIONAL PART OF TEMP1 (HIGH ORDER)
DCA TEMP1           /DEPOSIT IN TEMP1
TAD TEMP1           /GET TEMP1 AGAIN
SZA CLA             /SKIP ON ZERO AC; CLEAR AC
JMP.+4              /JUMP +4
TAD TEMP2           /ADD TEMP2
SNA CLA             /SKIP ON NON-ZERO AC; CLEAR AC
JMP.+7              /JUMP +7
TAD TEMP1           /GET TEMP1
TAD MS7000          /ADD THE NEGATIVE SIGN
DCA TEMP1           /DEPOSIT IT IN TEMP1
DCA TEMP3
JMS I NEGAT         /OBTAIN THE ABSOLUTE VALUE OF THE FRACTIONAL PART
IAC                 /ADD 1 TO INTEGRAL PART IF FRACTIONAL IS NOT ZERO
JMP TO5371          /JUMP TO TO5371 (5372)
JMS I SPRNT         /PRINT INTEGRAL PART (NEGATIVE)
JMS I PUNCT
FRCNL,JMS I DMULTP /MULTIPLY FRACTIONAL PART BY 1000
TEMP1
N1000
DCA TEMP1
JMS I ROT3L
TAD TEMP1
JMS I DCPRNT        /PRINT FRACTIONAL PART
JMS I CRLFP         /TYPE CARRIAGE RETURN AND LINE FEED
JMS I CRLFP
ISZ CNTDEV          /HAVE ALL THE NUMBERS BEING PRINTED?
JMP CLABCD          /NO, PRINT NEXT
TAD M6              /YES, PRINT 6 CRLF'S
DCA CNTM6
JMS I CRLFP
ISZ CNTM6
JMP.-2
JMP I PAG22         /JUMP TO PAGE 22
ROTP,0
TAD TEMP1
AND MS7000
RTL CLL
RTL
JMP I ROTP
K246,246
K244,244
BPUNCH,BPUN
SPRNT,SSPRNT
MS7770,7770
PAG22, PAGE22
TO5371, TAD PROSO1
SZA                 /IS AC ZERO?
JMP FRCNL-2         /NO
TAD MINUS           /YES, GET THE SIGN (-)
JMS I TYPO          /PRINT IT
JMP FRCNL-2
MINUS, 255
PAUSE
```

```
     *5400
     PAGE22,ISZ CNTN     /IS THE NUMBER OF INTEGRATIONS OVER?
     JMP I NEWCLE        /NO, START A NEW INTEGRATION CYCLE
     ISZ 16              /YES, IS THE NEXT SOURCE THE CALIBRATION SOURCE?
     JMP I CONPNT        /NO, GO AND POINT TO SOURCE
     JMP I RESETP        /YES, FIRST RESET AND THEN POINT
     NEWCLE, ARCHI
     CONPNT, POINTP
5407 RESETP, RESET
     DEC45, 0            /THIS SUBROUTINE COMPUTES THE NUMBER
     JMS I DMULTP        /OF PULSES NEEDED TO POINT ANT. #1 &
     TEMP1               /THEN POINTS ANT. #1
     N5442
     DCA TEMP1           /TEMP1,2 CONTAIN THE NUMBER OF PULSES AS
     TAD I CONTB         /A NEGATIVE NUMBER
     DCA TEMP2
     CYCL45, CLA
     6411
     6451                /SEND PULSE
     6412                /WAS PULSE RECEIVED?
     JMP.-1              /NO
     JMS I PULSE         /YES, INCREMENT TEMP1,2 AND INSERT DELAY BETWEEN
     TAD TEMP1           /PULSES; GET TEMP1
     SPA CLA             /IS TEMP1 POSITIVE?
     JMP CYCL45          /NO
     JMP I DEC45         /YES
     PULSEP,0
     TAD N6000           /ESTABLISH A DELAY OF 4.5 MSEC BETWEEN PULSES
     DCA TEMPO
     ISZ TEMPO           /HAS THE DELAY EXPIRED?
     JMP.-1              /NO
     CLA CLL             /YES
     TAD TEMP2           /INCREMENT TEMP1,2
     IAC
     DCA TEMP2
     RAL
     TAD TEMP1
     DCA TEMP1
     JMP I PULSEP        /JUMP OUT OF SUBROUTINE
     N6000,6000
5447 COMPEN, 0           /THIS IS THE DELAY COMPENSATION SUBROUTINE
     CLA CLL
     JMS I DMULTP        /MULTIPLY COSδCOSDCOS((2π/24)*(H+α-t))
     COSDDE
     COSTI
     DCA TEMP1           /DEPOSIT IN TEMP1
     JMS I ROT1L         /ROTATE CONTENTS OF TEMP1,B,C BY ONE LOCATION LEFT
     DCA TEMP1
     CLL
     TAD I CONTB
     TAD SINDDE+1        /ADD SINδSIND TO THE ABOVE PRODUCT
     DCA TEMP2
     RAL
     TAD TEMP1
     TAD SINDDE
     DCA TEMP1           /TEMP1,2 CONTAIN SINθ
     DCA TEMP3
     DCA TEMPO           /CLEAR FLAG
     TAD TEMP1
     SMA CLA             /IS SINθ<0
     JMP .+4             /NO, JUMP 4 LOCATIONS AHEAD
     JMS I NEGAT         /YES, NEGATE IT
     CMA                 /COMPLEMENT AC
     DCA TEMPO           /SET FLAG TO -1
     CLA
     TAD BASL            /GET BASELINE LENGTH
     DCA MEGA+1
     TAD BASL+1
     DCA MEGA+2
     DCA MEGA+3
     DCA MEGA+4
     TAD MEGA
     JMS I DDIVP         /DIVIDE IT BY THE VELOCITY OF LIGHT
     CNANO
     DCA PROSO1          /PROSO1,2 CONTAIN d/C
     TAD I LOUOT
     DCA PROSO2
     JMS I DMULTP        /MULTIPLY (d/C)*SINθ
     PROSO1
     TEMP1
     DCA TEMP1
     JMS I ROT1L         /ROTATE ONE LOCATION LEFT
     DCA TEMP1
     TAD I CONTB
     DCA TEMP2
     TAD TEMP1           /DEPOSIT (d/C)*SINθ IN DIVIDEND
     DCA MEGA+2
     TAD TEMP2
     DCA MEGA+3
     DCA MEGA+1
     DCA MEGA+4
     TAD MEGA
     JMS I DDIVP         /DIVIDE BY 1.25NS WHICH IS THE BASIC
     N125                /DELAY UNIT; THE OTHERS ARE 2.5,5,10,20,40,80,160
     DCA TEMP3           /DEPOSIT THE QUOTIENT (8-BIT NUMBER) IN TEMP3
     TAD TEMPO           /GET FLAG
     SZA CLA             /IS IT -1?
     JMP.+5              /YES, JUMP 5 LOCATIONS AHEAD
     6301                /NO, SET DELAY IN IF STRIP #2 TO ZERO
     TAD TEMP3           /GET TEMP3
     6351                /ADJUST DELAY #1
     JMP.+4              /JUMP 4 LOCATIONS AHEAD
     6351                /SET DELAY #1 TO ZERO
     TAD TEMP3           /GET TEMP3
     6301                /ADJUST DELAY #2
     CLA
     TAD M300            /RESET TIME COUNT FOR NEXT COMPENSATION
     DCA CM300
     JMP I COMPEN
     M300, 7324
     CNANO, 2314
     6314
     N125, 0001
     2000
     D180, 0550
     0000
     N100, 144
     0
     PAUSE
```

```
*5600
FLGCHK, JMP TO5765 /JUMP TO 5765
6361                /IS FLAG OF DEVICE 36 UP?
SKP                 /NO, SKIP
JMP SR36            /YES, GO TO SERVE DEVICE 36
6371                /IS FLAG OF DEVICE 37 UP?
SKP                 /NO, SKIP
JMP SR37            /YES, GO TO SERVE DEVICE 37
6321                /IS FLAG OF DEVICE 32 UP?
SKP                 /NO, SKIP
JMP SR32            /YES, GO TO SERVE DEVICE 32
6331                /IS FLAG OF DEVICE 33 UP?
SKP                 /NO, SKIP
JMP SR33            /YES, GO TO SERVE DEVICE 33
ION                 /TURN INTERRUPT ON
JMP TO5772          /JUMP TO 5772
JMP I 0             /JUMP TO LOCATION 0
SR36, 6411
6362                /SEND STEPPING PULSE TO ANT. #2
6412                /WAS PULSE RECEIVED?
JMP.-1              /NO
CLA CLL             /YES
TAD I STEP2P+1      /ADD THE STEP TO THE HR2 REGISTER
TAD I HR2P+2
DCA I HR2P+2
RAL
TAD I STEP2P
TAD I HR2P+1
DCA I HR2P+1
RAL
TAD I HR2P
JMP I 5764          /GO TO CHECK IF HR2<24
JMP FLGCHK+4
SR37, 6411
6372                /SEND STEPPING PULSE TO ANT. #1
6412                /WAS PULSE RECEIVED?
JMP.-1              /NO
CLA CLL             /YES
TAD I STEP1P+1      /ADD THE STEP TO THE HR1 REGISTER
TAD I HR1P+2
DCA I HR1P+2
RAL
TAD I STEP1P
TAD I HR1P+1
DCA I HR1P+1
RAL
TAD I HR1P
JMP I 5763          /GO TO CHECK IF HR1<24
LAS                 /READ SWITCH REGISTER
AND TRIA            /MASK IT WITH 3
SNA CLA             /IS AC NON-ZERO
JMP FLGCHK+7        /NO
TAD GET3            /YES
DCA 13              /GET INDEX COORDINATES OF DISHES
TAD GET4
DCA 11
JMS TRANPR          /RETURN DISHES TO INDEX POSITION
JMS I HR12P
JMS I HR37P
JMS TRANPR
JMS I HR12P
JMS I HR36P
JMS TRANPR
JMS I DEC12P
JMS I DEC45P
JMS TRANPR
JMS I DEC12P
JMS I DEC43P
HLT                 /HALT PROGRAM
SR32, JMS I TMINC /INCREMENT TIME REGISTER
JMP FLGCHK+12
SR33, ION           /THIS SERVES THE TIME CHECK INTERRUPT; TURN
CLL CLA             /INTERRUPT ON
TAD TIME+2          /OBTAIN GST=LST+LONGITUDE
TAD LONGI+2
DCA PROSO3
RAL
TAD TIME+1
TAD LONGI+1
DCA PROSO2
RAL
TAD TIME
TAD LONGI
DCA PROSO1          /PROSO1,2,3 CONTAIN GST
JMS I DAYX24        /COMPUTE (#DAYS)*24*(9.857/3600); DEPOSIT IN
JMP I PAG24         /TEMP1,2,3; JUMP TO PAGE 24
TRANPR, 0
JMS I TRANSX
TAD PROSO3
DCA PROSO3
RAL
TAD PROSO2
TAD TEMPO
DCA PROSO2
JMP I TRANPR
SAVEAC, 0
HR2P, HR2
HR2+1
HR2+2
STEP2P, STEP2
STEP2+1
HR1P, HR1
HR1+1
HR1+2
STEP1P, STEP1
STEP1+1
GET3, HR1Z-1
GET4, HR1-1
HR12P, HR12
HR37P, HR37
HR36P, HR36
DEC12P, DEC12
DEC45P, DEC45
DEC43P, DEC43
DAYX24, DAY24
PAG24, PAGE24
*5763
6557
6566
TO5765, DCA SAVEAC /SAVE AC CONTENT
RAL
DCA SAVELK          /SAVE LINK CONTENT
JMP TO5601
SAVELK, 0
TO5772, CLA CLL
TAD SAVELK          /RETRIEVE LINK CONTENT
RAR
TAD SAVEAC          /RETRIEVE AC CONTENT
JMP I 0
PAUSE

*6000
PAGE24, CLL
TAD TEMP3           /ADD TEMP1,2,3 TO UT AT JANUARY 0
TAD SIDHR0+2        /CONTAINED IN SIDHR0,+1,+2
DCA TEMP3
RAL
TAD TEMP2
TAD SIDHR0+1
DCA TEMP2
RAL
TAD TEMP1
TAD SIDHR0
DCA TEMP1           /DEPOSIT SUM IN TEMP1,2,3
JMS I NEGAT         /NEGATE THE SUM
CLL
TAD TEMP3           /OBTAIN GST-UTHR0-(# DAYS)*24*(9.857/3600)
TAD PROSO3
DCA PROSO3
RAL
TAD TEMP2
TAD PROSO2
DCA PROSO2
RAL
TAD TEMP1
TAD PROSO1          /PROSO1,2,3 CONTAIN DIFFERENCE
DCA PROSO1
TAD PROSO1          /NOW WE MULTIPLY (PROSO1,2,3)*(1-9.857/3600)=GCT
DCA MEGA+2          /DEPOSIT PROSO1,2,3 IN DIVIDEND
TAD PROSO2
DCA MEGA+3
TAD PROSO3
DCA MEGA+4
DCA MEGA+1
TAD MEGA
JMS I DDIVP         /DIVIDE BY 3600
N7020
DCA TEMP1           /DEPOSIT IN TEMP1,2
TAD I LOUOT
DCA TEMP2
JMS I DMULTP        /MULTIPLY TEMP1*9.857
TEMP1
CONVER
DCA TEMP1           /DEPOSIT PRODUCT IN TEMP1,2,3
TAD I CONTB
DCA TEMP2
TAD I CONTC
DCA TEMP3
JMS I NEGAT         /NEGATE TEMP1,2,3
CLL
TAD TEMP3           /FORM (PROSO1,2,3)-(TEMP1,2,3)=GCT
TAD PROSO3
DCA TEMP3
RAL
TAD TEMP2
TAD PROSO2
DCA TEMP2
RAL
TAD TEMP1
TAD PROSO1
DCA TEMP1           /TEMP1,2,3 CONTAIN GCT IN HOURS
JMS I DMULTP        /MULTIPLY FRACTIONAL PART OF GCT BY 60
TEMP2
N60
DCA TEMP2           /DEPOSIT INTEGRAL PART OF PRODUCT IN TEMP2 (MINUTES)
TAD I CONTB
DCA PROSO1          /DEPOSIT FRACTIONAL PART IN PROSO1,2,3
TAD I CONTC
DCA PROSO2
JMS I DMULTP        /MULTIPLY FRACTIONAL MINUTES BY 60
PROSO1
N60
DCA TEMP3           /TEMP3 CONTAINS THE SECONDS
TAD I CONTB
DCA PROSO1
TAD I CONTC
DCA PROSO2
JMS I DMULTP
PROSO1
N1000
DCA TEMPO
JMS I CRLFP         /TYPE CARRIAGE RETURN
TAD TEMP1
JMS I DCPRNT        /TYPE THE HOURS
JMS I CRLFP
TAD TEMP2
JMS I DCPRNT        /TYPE THE MINUTES
JMS CRLFP
TAD TEMP3
JMS I DCPRNT        /TYPE THE SECONDS
JMS CRLFP
TAD TEMPO
JMS I DCPRNT
JMS I CRLFP
CLA
6135 JMP I ARXI     /JUMP TO LOCATION 1660
SILLY, CLA          /THIS IS A WAITING LOOP USED WHILE WE ARE
DCA TEMPO           /GETTING SET FOR THE TIME CHECK
ISZ TEMPO
JMP.-1
JMP SILLY
6143 ROT1RT, 0      /THIS SUBROUTINE ROTATES THE CONTENTS
TAD TEMP1           /OF TEMP1, B AND C BY ONE LOCATION
RAR                 /RIGHT
DCA TEMP1
TAD I CONTB
RAR
DCA I CONTB
TAD I CONTC
RAR
DCA I CONTC
JMP I ROT1RT
MEGI10, 0           /SETS UP THE DIVIDEND BY MEANS OF
TAD I 10            /THE SELF-INDEXING REGISTER 10
DCA MEGA+1
TAD I 10
DCA MEGA+2
TAD I 10
DCA MEGA+3
DCA MEGA+4
TAD MEGA
JMP I MEGI10
ARXI, ARHI
PAUSE
```

```
*6200
ROT1LF,0            /ROTATE CONTENTS OF TEMP1,B,C
TAD I CONTC         /BY ONE LOCATION LEFT; B,C ARE THE LOW ORDER
RAL CLL             /REGISTERS IN WHICH THE PRODUCT IS STORED;
DCA I CONTC         /THE HIGH ORDER IS IN THE ACCUMULATOR
TAD I CONTB         /WHICH IN THIS CASE WAS DEPOSITED IN TEMP1
RAL
DCA I CONTB
TAD TEMP1
RAL
JMP I ROT1LF
ROT3RT,0            /ROTATES CONTENTS OF TEMP1,B,C THREE
TAD M3              /LOCATIONS RIGHT
DCA CNTM3
TAD TEMP1
RAR CLL
DCA TEMP1
TAD I CONTB
RAR
DCA I CONTB
TAD I CONTC
RAR
DCA I CONTC
ISZ CNTM3
JMP ROT3RT+3
JMP I ROT3RT
ROT3LF,0            /ROTATES THE CONTENTS OF TEMP1,B,C THREE
TAD M3              /LOCATIONS LEFT
DCA CNTM3
TAD I CONTC
RAL CLL
DCA I CONTC
TAD I CONTB
RAL
DCA I CONTB
TAD TEMP1
RAL
DCA TEMP1
ISZ CNTM3
JMP ROT3LF+3
JMP I ROT3LF
TMINCR,0            /INCREMENTS THE TIME REGISTER BY
CLL CLA             /0.2*(1+0.0027)/3600 HOURS
TAD TIME+2
TAD INCHR+1
DCA TIME+2
RAL
TAD TIME+1
TAD INCHR
DCA TIME+1
RAL
TAD TIME
DCA TIME
TAD TIME
TAD M24
SPA
SKP
DCA TIME
CLA
JMP I TMINCR
INCHR, 0000
1646
ROT6LF,0            /ROTATES CONTENTS OF TEMP1,2,3
TAD M6              /SIX LOCATIONS LEFT
DCA CNTM6
TAD TEMP3
RAL CLL
DCA TEMP3
TAD TEMP2
RAL
DCA TEMP2
TAD TEMP1
RAL
DCA TEMP1
ISZ CNTM6
JMP ROT6LF+3
JMP I ROT6LF
ROT2LF,0            /ROTATES CONTENTS OF TEMP1,B,C
TAD M2              /TWO LOCATIONS LEFT
DCA CNTM2
TAD I CONTC
RAL CLL
DCA I CONTC
TAD I CONTB
RAL
DCA I CONTB
TAD TEMP1
RAL
DCA TEMP1
ISZ CNTM2
JMP ROT2LF+3
JMP I ROT2LF
PARA,0              /CHECKS THE SIGN OF A NUMBER BEFORE
CLA CLL             /THE NUMBER IS ROTATED RIGHT
TAD TEMP1           /GET HIGH ORDER TERM OF NUMBER
SMA CLA             /IS IT NEGATIVE?
JMP.+3              /NO, JUMP 3 AHEAD
STL                 /YES, SET LINK TO  1
CMA                 /COMPLEMENT AC
DCA TEMPO           /DEPOSIT -1 IN TEMPO
JMP I PARA
CRLF,0              /GIVES A CARRIAGE RETURN AND A LINE FEED
CLA
TAD KCR
JMS I TYPO
TAD KLF
JMS I TYPO
JMP I CRLF
KCR,215
KLF,212
TYPEPT,0            /TYPES (.)
CLA
TAD PT256
JMS I TYPO
JMP I TYPEPT
PT256,256
TYPE,0              /TYPES ANY CHARACTER
TLS
TSF
JMP.-1
TCF
CLA
JMP I TYPE
PAUSE
```

```
*6403
MIDDL, 0            /THIS SUBROUTINE COMPUTES THE INTEGRATION TIME, T,
CLA                 /IN HOURS AND THEN CALCULATES COS(T/2) AND SIN(T/2).
TAD INTEGR          /THE LAST TWO FUNCTIONS ARE USED FOR THE
DCA TEMP1           /CALCULATION OF U AND V.
TAD INTEGR+1
DCA TEMP2
DCA TEMP3
JMS I NEGAT
JMS I DMULTP
TEMP1
PNT1
DCA TEMP1
TAD I CONTB
DCA TEMP2
TAD TEMP1
DCA MEGA+1
TAD TEMP2
DCA MEGA+2
DCA MEGA+3
DCA MEGA+4
TAD MEGA
JMS I DDIVP
N3600
DCA MIDLTM          /MIDLTM,+1 CONTAIN T/2 IN HOURS
TAD I LQUOT
DCA MIDLTM+1
JMP I TO6433
TO6433,7245         /JUMP TO 7245 TO COMPUTE (π/12)*(T/2)
*6437
TAD I CONTB
DCA TEMP2
JMS I DCOSP
TEMP1
TAD I HARG
DCA COSMDT          /COSMDT,+1 CONTAIN COS((2π/24)(T/2))
TAD I LARG
DCA COSMDT+1
JMS I DSINP
TEMP1
TAD I HARG
DCA SINMDT          /SINMDT,+1 CONTAIN SIN((2π/24)(T/2))
TAD I LARG
DCA SINMDT+1
JMP I MIDDL
PNT1, 1463 .
1462
COSMDT, 0
0
SINMDT, 0
0
DEC43,0             /THIS SUBROUTINE IS USED IN THE POINTING
JMS I DMULTP        /OF DECLINATION #2
TEMP1
N5416
DCA TEMP1
TAD I CONTB
DCA TEMP2
CYCL43, CLA
6411
6431
6412
JMP.-1
JMS I PULSE
TAD TEMP1
SPA CLA
JMP CYCL43
JMP I DEC43
*6510               /PROGRAM STARTS HERE
6434
IOF
6334                /DEACTIVATE CLOCK INTERRUPT
6321                /CLEAR FLAG 32
6331                /CLEAR FLAG 33
6374                /DEACTIVATE TRACKING INTERRUPT
6371                /CLEAR FLAG 37
6371
6361                /CLEAR FLAG 36
6361
JMP I PROGM
PROGM,200
CHK24,0             /CHECKS WHETHER A
TAD I OPERAT        /NUMBER IS GREATER THAN 24
TAD 0074
SPA
SKP
DCA I OPERAT
CLA
JMP I CHK24
OPERAT,0
*6540
PATCH,0             /CORRECTION PATCH
1027
3007
1026
3006
1025
3005
JMP I PATCH
*6550               /CHECKS WHETHER STIME IS
DCA I TEMPST        /GREATER THAN 24
TAD TEMPST
DCA OPERAT
JMS CHK24
JMP I TO1425
TO1425,1425
TEMPST,1515
*6557               /CHECKS WHETHER HR1>24
DCA I HR1P
TAD HR1P
DCA OPERAT
JMS CHK24
JMP I TO5657
HR1P,6721
TO5657,5657
*6566               /CHECKS WHETHER HR2>24
DCA I HR2P
TAD HR2P
DCA OPERAT
JMS CHK24
JMP I TO5637
HR2P,6724
TO5637,5637
```

```
*6630
N60, 0074
0
N1000, 1750
0
N3600, 0000
7020
N86400, 2536
0000
DAYS,0          /NUMBER OF DAYS SINCE JANUARY 0
N, 0            /NUMBER OF INTEGRATIONS ON THE CALIBRATION SOURCE
0               /NUMBER OF INTEGRATIONS ON THE SOURCE
LCT, 0
0
0
0
RACL,0
0
0
0
RAS, 0
0
0
0
HOURB, 0
0
0
0
DECL, 0
0
0
0
DECS, 0
0
0
0
DECB, 0
0
0
0
BASLD, 0
0
0
0
0
STDECL, 0       /DECLINATION OF CALIBRATION SOURCE IN DEGREES
0
0
STDECS, 0       /DECLINATION OF SOURCE IN DEGREES
0
0
0
DECAL, 0        /DECLINATION OF CALIBRATION SOURCE IN RADIANS
0
DELTS, 0        /DECLINATION OF SOURCE IN RADIANS
0
DECLB, 0        /DECLINATION OF BASELINE IN RADIANS
0
HRJAN, 6        /UNIVERSAL TIME AT 0 HR. AT JANUARY 0 OF 1969
45
67
5656
WLONG, 4
54
25
7412
HR1Z, 27        /INDEX HOUR OF ANTENNA #1
72
34
0
HR2Z, 0         /INDEX HOUR OF ANTENNA #2
1
45
0
DEC1Z, 52       /INDEX DECLINATION OF ANTENNA #1
66
52
6
DEC2Z, 52       /INDEX DECLINATION OF ANTENNA #2
52
55
6
HR1, 0          /PRESENT HOUR ANGLE OF ANTENNA #1
0
0
HR2,0           /PRESENT HOUR ANGLE OF ANTENNA #2
0
0
DEC1, 0         /PRESENT DECLINATION OF ANTENNA #1
0
0
DEC2, 0         /PRESENT DECLINATION OF ANTENNA #2
0
0
HRANGL, 0       /STORES THE HOUR ANGLE THAT IS TYPED OUT
0
YU, 0           /STORES U
0
VI, 0           /STORES V
0
SUMPEL, 0       /STORES Σ yi COS γi FOR DEVICE #1
0
0
0               /STORES Σ yi SIN γi FOR DEVICE #1
0
0
0               /STORES Σ yi COS γi FOR DEVICE #2
0
0
0               /STORES Σ yi SIN γi FOR DEVICE #2
0
0
0               /STORES Σ yi COS γi FOR DEVICE #3
0
0
0               /STORES Σ yi SIN γi FOR DEVICE #3
0
0
0               /STORES Σ yi COS γi FOR DEVICE #4
0
0
0               /STORES Σ yi SIN γi FOR DEVICE #4
0
0
PAUSE
```

```
*7215           /CORRECTION REFERRED TO LOCATION 519
TAD TEMP3
TAD I CONTC
DCA TEMP3
RAL
TAD TEMP2
TAD I CONTB
DCA TEMP2
RAL
TAD TEMP1
DCA TEMP1
CLL
TAD TEMP3
TAD SIDHR0+2
DCA TEMP3
RAL
TAD TEMP2
TAD SIDHR0+1
DCA TEMP2
RAL
TAD TEMP1
TAD SIDHR0
DCA TEMP1
JMP I TO522
TO522,522
*7245           /CORRECTION REFERRED TO LOCATION 6433
TAD MIDLTM
DCA MIDTMP
TAD MIDLTM+1
DCA MIDTMP+1
TAD M3
DCA CNTM3
ROTR,CLL
TAD MIDTMP
RAR
DCA MIDTMP
TAD MIDTMP+1
RAR
DCA MIDTMP+1
ISZ CNTM3
JMP ROTR
JMS I DMULTP
PI12
MIDTMP
DCA TEMP1
JMP I TOMPG
TOMPG,6437
MIDTMP,0
0
```

Acknowledgment

My deep appreciation and gratitude go to Professor Bernard F. Burke for his support, guidance, and encouragement during all of the phases of my thesis research. I would like to thank Professor Donald E. Troxel, Professor Robert P. Rafuse, Professor Donald H. Steinbrecher, and Dr. Alan E. E. Rogers for their suggestions in equipment design, and Professor David H. Staelin for his advice in the system trouble shooting. Special mention should be made of D. Cosmo Papa who designed the antenna mounts and took care of the mechanical problems that came up. I would also like to thank my colleagues Martin S. Ewing, Richard Lewis, and John W. Barrett.

References

1. R. J. Allen, Ph. D. Thesis, Massachusetts Institute of Technology, 1967 (unpublished).
2. L. Sartori and P. M. Morrison, Astrophys. J. 150, 385 (1967).
3. A. H. Barret and D. H. Staelin, Space Sci. Revs. 3, 109 (1964).
4. D. Morrison, Science 63, 815 (1969).
5. M. Ryle and A. C. Neville, Mon. Not. Roy. Astron. Soc. 125, 39 (1962).
6. S. Kenderdine, M. Ryle, and G. G. Pooley, Mon. Not. Roy. Astron. Soc. 134, 189 (1966).
7. S. H. Zisk, Ph.D. Thesis, Stanford Electronics Laboratories, 1965 (unpublished).
8. G. W. Swenson, Jr., and N. C. Mathur, Proc. IEEE 56, 2114 (1968).
9. G. W. Swenson, Jr., Ann. Rev. Astron. Astrophys. 7, 353 (1969).
10. A. E. E. Rogers, "The Haystack-Millstone Interferometer System," Technical Report 457, Research Laboratory of Electronics, Massachusetts Institute of Technology, Cambridge, Mass., March 15, 1967.
11. D. H. Staelin, Class Notes, Course 6.624, Massachusetts Institute of Technology, 1968.
12. W. M. Smart, Spherical Astronomy (Cambridge University Press, London, 1965).
13. A. H. Barret, Class Notes, Course 6.625, Massachusetts Institute of Technology, 1969.
14. J. D. Kraus, Radio Astronomy (McGraw-Hill Book Company, New York, 1966).
15. J. W. Waters, Private communication, 1969.
16. G. G. Haroules and W. E. Brown III, J. Geophys. Res. 74, 4453 (1969).
17. R. N. Bracewell, Proc. IRE 46, 97 (1958).
18. W. B. Davenport and W. L. Root, An Introduction to the Theory of Random Signals and Noise (McGraw-Hill Book Company, New York, 1958).

JOINT SERVICES ELECTRONICS PROGRAM
REPORTS DISTRIBUTION LIST

Department of Defense

Assistant Director (Research)
Office of Director of Defense, Research & Engineering
The Pentagon, Rm 3C128
Washington, D.C. 20301

Technical Library
DDR&E
Room 3C-122, The Pentagon
Washington, D.C. 20301

Director For Materials Sciences
Advanced Research Projects Agency
1400 Wilson Boulevard
Arlington, Virginia 22209

Chief, R&D Division (340)
Defense Communications Agency
Washington, D.C. 20305

Defense Documentation Center
Attn: DDC-TCA
Cameron Station
Alexandria, Virginia 22314

Dr. Alvin D. Schnitzler
Institute For Defense Analyses
Science and Technology Division
400 Army-Navy Drive
Arlington, Virginia 22202

LTC Norman D. Jorstad
Weapons Systems Evaluation Group
400 Army-Navy Drive
Arlington, Virginia 22202

Central Intelligence Agency
Attn: CRS/ADD/PUBLICATIONS
Washington, D.C. 20505

Department of the Air Force

Hq USAF (AF/RDPE)
Washington, D.C. 20330

Hq USAF/RDPS
Washington, D.C. 20330

Hq USAF (RDSD)
The Pentagon
Washington, D.C. 20330

Colonel E. P. Gaines, Jr.
ESD (MCD)
L. G. Hanscom Field
Bedford, Massachusetts 01730

Dr L. A. Wood, Director
Electronic and Solid State Sciences
Air Force Office of Scientific Research
1400 Wilson Boulevard
Arlington, Virginia 22209

Dr Harvey E. Savely, Director
Life Sciences
Air Force Office of Scientific Research
1400 Wilson Boulevard
Arlington, Virginia 22209

Mr I. R. Mirman
Hq AFSC (SGGP)
Andrews Air Force Base,
Washington, D.C. 20331

Rome Air Development Center
Attn: Documents Library (TDLD)
Griffiss Air Force Base, New York 13440

Mr H. E. Webb, Jr. (ISCP)
Rome Air Development Center
Griffiss Air Force Base, New York 13440

Dr L. M. Hollingsworth
AFCRL (CA)
L. G. Hanscom Field
Bedford, Massachusetts 01730

Hq ESD (TRI)
L. G. Hanscom Field
Bedford, Massachusetts 01730

Professor R. E. Fontana, Head
Dept of Electrical Engineering
Air Force Institute of Technology
Wright-Patterson Air Force Base,
Ohio 45433

Dr H. V. Noble, AFAL/TE
Chief, Electronics Technology Division
Air Force Avionics Laboratory
Wright-Patterson Air Force Base,
Ohio 45433

Director
Air Force Avionics Laboratory
Wright-Patterson Air Force Base,
Ohio 45433

AFAL/TEA (Mr R. D. Larson)
Wright-Patterson Air Force Base,
Ohio 45433

Director of Faculty Research
Department of the Air Force
U.S. Air Force Academy
Colorado 80840

Mr Jules I. Wittebort
Chief, Electronics Branch
Manufacturing Technology Division
AFAL/LTE
Wright-Patterson Air Force Base,
Ohio 45433

Academy Library (DFSLB)
USAF Academy, Colorado 80840

Director of Aerospace Mechanics Sciences
Frank J. Seiler Research
Laboratory (OAR)
USAF Academy, Colorado 80840

Major Richard J. Gowen
Tenure Associate Professor
Dept of Electrical Engineering
USAF Academy, Colorado 80840

Director, USAF PROJECT RAND
Via: Air Force Liaison Office
The RAND Corporation
Attn: Library D
1700 Main Street
Santa Monica, California 90406

AUL3T-9663
Maxwell Air Force Base, Alabama 36112

AFETR Technical Library
(MU-135)
Patrick Air Force Base, Florida 32925

ADTC (SSLT)
Eglin Air Force Base, Florida 32542

Hq AMD (RDR/Lt Col Godden)
Brooks Air Force Base, Texas 78235

USAFSAM (RAT)
Brooks Air Force Base, Texas 78235

Commanding General
Attn: STEWS-AD-L, Technical Library
White Sands Missile Range,
New Mexico 88002

European Office of Aerospace Research
Technical Information Office
Box 14, FPO New York 09510

VELA Seismological Center
312 Montgomery Street
Alexandria, Virginia 22314

Capt C. E. Baum
AFWL (SRE)
Kirtland Air Force Base,
New Mexico 87117

Biomedical Engineering Branch (SCB)
USAF School of Aerospace Medicine (AFSC)
Department of the Air Force
Brooks Air Force Base, Texas 78235

Department of the Army

Director
Physical & Engineering Sciences Division
3045 Columbia Pike
Arlington, Virginia 22204

Commanding General
U.S. Army Security Agency
Attn: IARD-T
Arlington Hall Station
Arlington, Virginia 22212

Commanding General
U.S. Army Materiel Command
Attn: AMCRD-TP (Dr Zarwyn)
Washington, D.C. 20315

Director
U.S. Army Advanced Materiel
Concepts Agency
2461 Eisenhower Avenue
Alexandria, Virginia 22314

Commanding General
USACDC Institute of Land Combat
Attn: Technical Library, Rm 636
2461 Eisenhower Avenue
Alexandria, Virginia 22314

Mr H. T. Darracott (AMXAM-FT)
U.S. Army Advanced Materiel
Concepts Agency
2461 Eisenhower Avenue
Alexandria, Virginia 22314

Commanding Officer
Harry Diamond Laboratories
Attn: Dr Berthold Altman (AMXDO-TI)
Connecticut Avenue and
Van Ness Street N. W.
Washington, D.C. 20438

Commanding Officer (AMXRD-BAD)
U.S. Army Ballistic Research Laboratory
Aberdeen Proving Ground
Aberdeen, Maryland 21005

U.S. Army Munitions Command
Attn: Science & Technology Information
Branch, Bldg 59
Picatinny Arsenal, SMUPA-RT-S
Dover, New Jersey 07801

Dr Herman Robl
Deputy Chief Scientist
U.S. Army Research Office (Durham)
Box CM, Duke Station
Durham, North Carolina 27706

Richard O. Ulsh (CRDARD-IP)
U.S. Army Research Office (Durham)
Box CM, Duke Station
Durham, North Carolina 27706

Technical Director (SMUFA-A2000-107-1)
Frankford Arsenal
Philadelphia, Pennsylvania 19137

Redstone Scientific Information Center
Attn: Chief, Document Section
U.S. Army Missile Command
Redstone Arsenal, Alabama 35809

Commanding General
U.S. Army Missile Command
Attn: AMSMI-RR
Redstone Arsenal, Alabama 35809

Commanding General
U.S. Army Strategic Communications
Command
Attn: SCC-ATS (Mr Peter B. Pichetto)
Fort Huachuca, Arizona 85613

Dr Homer F. Priest
Chief, Materials Sciences Division,
Bldg 292
Army Materials & Mechanics Research
Center
Watertown, Massachusetts 02172

Commandant
U.S. Army Air Defense School
Attn: Missile Science Division, C&S Dept
P. O. Box 9390
Fort Bliss, Texas 79916

Commandant
U.S. Army Command and General
Staff College
Attn: Acquisitions, Lib Div
Fort Leavenworth, Kansas 66027

Dr Hans K. Ziegler
Army Member TAC/JSEP (AMSEL-XL-D)
U.S. Army Electronics Command
Fort Monmouth, New Jersey 07703

Mr I. A. Balton, AMSEL-XL-D
Executive Secretary, TAC/JSEP
U.S. Army Electronics Command
Fort Monmouth, New Jersey 07703

Director (NV-D)
Night Vision Laboratory, USAECOM
Fort Belvoir, Virginia 22060

Commanding Officer
Atmospheric Sciences Laboratory
U.S. Army Electronics Command
White Sands Missile Range,
New Mexico 88002

Atmospheric Sciences Laboratory
U.S. Army Electronics Command
Attn: AMSEL-BL-DD (Mr Marvin Diamond)
White Sands Missile Range,
New Mexico 88002

Chief
Missile Electronic Warfare Tech
Area (AMSEL-WL-M)
Electronic Warfare Laboratory,
USAECOM
White Sands Missile Range,
New Mexico 88002

Project Manager NAVCON
Attn: AMCPM-NC, Bldg 439
(H. H. Bahr)
Fort Monmouth, New Jersey 07703

Mr A. D. Bedrosian, Rm 26-131
U.S. Army Scientific Liaison Office
Massachusetts Institute of Technology
77 Massachusetts Avenue
Cambridge, Massachusetts 02139

Commanding General
U.S. Army Electronics Command
Fort Monmouth, New Jersey 07703
Attn: AMSEL-RD-O (Dr W. S. McAfee)
GG-DD
XL-D
XL-DT
XL-G (Dr S. Kronenberg)
XL-H (Dr R. G. Buser)
BL-FM-P
CT-D
CT-R
CT-S
CT-L
CT-O
CT-I
CT-A
NL-D (Dr H. Bennett)
NL-A
NL-C
NL-P
NL-P-2
NL-R
NL-S
KL-D
KL-I
KL-E
KL-S
KL-SM
KL-T
VL-D
VL-F
WL-D
RD-PB (Miss F. Morris)

Department of the Navy

Director, Electronics Programs
Attn: Code 427
Office of Naval Research
800 North Quincy Street
Arlington, Virginia 22217

Mr Gordon D. Goldstein, Code 437
Information Systems Program
Office of Naval Research
800 North Quincy Street
Arlington, Virginia 22217

Commander
Naval Security Group Command
Naval Security Group Headquarters
Attn: Technical Library (G43)
3801 Nebraska Avenue, N. W.
Washington, D.C. 20390

Director
Naval Research Laboratory
Washington, D.C. 20390
Attn: Code 5200
Mr A. Brodzinsky, Supt,
Electronics Div

Director
Naval Research Laboratory
Attn: Dr H. Rabin, Code 7000
Washington, D.C. 20390

Code 8050
Maury Center Library
Naval Research Laboratory
Washington, D.C. 20390

Dr G. M. R. Winkler
Director, Time Service Division
U.S. Naval Observatory
Washington, D.C. 20390

Naval Air Systems Command
AIR 310 - Research Administrator
Room 424 JP-1
Washington, D.C. 20360

Dr A. L. Slafkosky
Scientific Advisor
Commandant of the Marine Corps (Code AX)
Washington, D.C. 20380

Naval Ship Systems Command
Ship 035
Washington, D.C. 20360

U.S. Naval Weapons Laboratory
Dahlgren, Virginia 22448

Naval Electronic Systems Command
Attn: Code 0311, Rm 7W12, NC #1
Department of the Navy
Washington, D.C. 20360

Commander
U.S. Naval Ordnance Laboratory
Attn: Librarian
White Oak, Maryland 20910

Director
Office of Naval Research
Boston Branch
495 Summer Street
Boston, Massachusetts 02210

Commander (ADL)
Naval Air Development Center
Attn: NADC Library
Johnsville, Warminster,
Pennsylvania, 18974

Commanding Officer
Naval Missile Center
Attn: 5632.2, Technical Library
Point Mugu, California 93042

W. A. Eberspacher, Associate Head
Systems Integration Division, Code 5340A
U.S. Naval Missile Center
Point Mugu, California 93041

Commander
Naval Electronics Laboratory Center
Attn: Library
San Diego, California 92152

Deputy Director and Chief Scientist
Office of Naval Research Branch Office
1031 East Green Street
Pasadena, California 91101

Library (Code 2124)
Naval Postgraduate School
Monterey, California93940

Glen A. Myers (Code 52Mv)
Assoc Professor of Electrical Engineering
Naval Postgraduate School
Monterey, California 93940

Officer in Charge, New London Lab.
Naval Underwater Systems Center
Attn: Technical Library
New London, Connecticut 06320

Commanding Officer
Naval Avionics Facility
Attn: D/035 Technical Library
Indianapolis, Indiana 46241

Director
Naval Research Laboratory
Attn: Library, Code 2039 (ONRL)
Washington, D.C. 20390

Commanding Officer
Naval Training Device Center
Attn: Technical Library
Orlando, Florida 32813

U.S. Naval Oceanographic Office
Attn: M. Rogofsky, Librarian (Code 1640)
Washington, D.C. 20390

Other Government Agencies

Dr H. Harrison
AEC/NASA Space Nuclear Systems
Office
AEC Headquarters (F-309)
Washington, D.C. 20545

NASA Lewis Research Center
Attn: Library
21000 Brookpark Road
Cleveland, Ohio 44135

Los Alamos Scientific Laboratory
Attn: Reports Library
P. O. Box 1663
Los Alamos, New Mexico 87544

Mr M. Zane Thornton
Deputy Director
Center for Computer Sciences and
Technology
National Bureau of Standards
U.S. Department of Commerce
Washington D.C. 20234

U.S. Postal Service
Library – Room 6012
12th & Pennsylvania Ave., N. W.
Washington, D.C. 20260

Non-Government Agencies

Director
Research Laboratory of Electronics
Massachusetts Institute of Technology
Cambridge, Massachusetts 02139

Mr Jerome Fox, Research Coordinator
Polytechnic Institute of Brooklyn
333 Jay Street
Brooklyn, New York 11201

Director
Columbia Radiation Laboratory
Columbia University
538 West 120th Street
New York, New York 10027

Director
Coordinate Science Laboratory
University of Illinois
Urbana, Illinois 61801

Director
Stanford Electronics Laboratory
Stanford University
Stanford, California 94305

Director
Microwave Laboratory
Stanford University
Stanford, California 94305

Director
Electronics Research Laboratory
University of California
Berkeley, California 94720

Director
Electronics Sciences Laboratory
University of Southern California
Los Angeles, California 90007

Director
Electronics Research Center
The University of Texas at Austin
Engineering-Science Bldg 110
Austin, Texas 78712

Division of Engineering and Applied Physics
210 Pierce Hall
Harvard University
Cambridge, Massachusetts 02138

Dr G. J. Murphy
The Technological Institute
Northwestern University
Evanston, Illinois 60201

Dr John C. Hancock, Head
School of Electrical Engineering
Purdue University
Lafayette, Indiana 47907

Dept of Electrical Engineering
Texas Technological University
Lubbock, Texas 79409

Aerospace Corporation
P. O. Box 95085
Attn: Library Acquisitions Group
Los Angeles, California 90045

Airborne Instruments Laboratory
Deerpark, New York 11729

The University of Arizona
Department of Electrical Engineering
Tucson, Arizona 85721

Chairman, Electrical Engineering
Arizona State University
Tempe, Arizona 85281

Engineering and Mathematical Sciences Library
University of California at Los Angeles
405 Hilgred Avenue
Los Angeles, California 90024

Sciences-Engineering Library
University of California
Santa Barbara, California 93106

Professor Nicholas George
California Institute of Technology
Pasadena, California 91109

Aeronautics Library
Graduate Aeronautical Laboratories
California Institute of Technology
1201 E. California Boulevard
Pasadena, California 91109

Hunt Library
Carnegie-Mellon University
Schenley Park
Pittsburgh, Pennsylvania 15213

Dr A. G. Jordan
Head of Dept of Electrical Engineering
Carnegie-Mellon University
Pittsburg, Pennsylvania 15213

Case Western Reserve University
Engineering Division
University Circle
Cleveland, Ohio 44106

Hollander Associates
Attn: Librarian
P. O. Box 2276
Fullerton, California 92633

Dr Sheldon J. Welles
Electronic Properties Information Center
Mail Station E-175
Hughes Aircraft Company
Culver City, California 90230

Illinois Institute of Technology
Department of Electrical Engineering
Chicago, Illinois 60616

Government Documents Department
University of Iowa Libraries
Iowa City, Iowa 52240

The Johns Hopkins University
Applied Physics Laboratory
Attn: Document Librarian
8621 Georgia Avenue
Silver Spring, Maryland 20910

Lehigh University
Department of Electrical Engineering
Bethlehem, Pennsylvania 18015

Mr E. K. Peterson
Lenkurt Electric Co. Inc.
1105 Country Road
San Carlos, California 94070

MIT Lincoln Laboratory
Attn: Library A-082
P. O. Box 73
Lexington, Massachusetts 02173

Miss R. Joyce Harman
Project MAC, Room 810
545 Main Street
Cambridge, Massachusetts 02139

Professor R. H. Rediker
Electrical Engineering, Professor
Massachusetts Institute of Technology
Building 13-3050
Cambridge, Massachusetts 02139

Professor Joseph E. Rowe
Chairman, Dept of Electrical Engineering
The University of Michigan
Ann Arbor, Michigan 48104

New York University
Engineering Library
Bronx, New York 10453

Professor James A. Cadzow
Department of Electrical Engineering
State University of New York at Buffalo
Buffalo, New York 14214

Department of Electrical Engineering
Clippinger Laboratory
Ohio University
Athens, Ohio 45701

Raytheon Company
Research Division Library
28 Seyon Street
Waltham, Massachusetts 02154

Rice University
Department of Electrical Engineering
Houston, Texas 77001

Dr Leo Young, Program Manager
Stanford Research Institute
Menlo Park, California 94025

GTE Waltham Research Lab Library
Attn: Documents Librarian
Esther McLaughlin
40 Sylvan Road
Waltham, Massachusetts 02154

Dr W. R. LePage, Chairman
Department of Electrical Engineering
Syracuse University
Syracuse, New York 13210

Dr F. R. Charvat
Union Carbide Corporation
Materials Systems Division
Crystal Products Department
8888 Balboa Avenue
P. O. Box 23017
San Diego, California 92123

Utah State University
Department of Electrical Engineering
Logan, Utah 84321

Research Laboratories for the
Engineering Sciences
School of Engineering and Applied Science
University of Virginia
Charlottesville, Virginia 22903

Yale University
Engineering and Applied Science Library
15 Prospect Street
New Haven, Connecticut 06520

UNCLASSIFIED
Security Classification

DOCUMENT CONTROL DATA - R & D

(Security classification of title, body of abstract and indexing annotation must be entered when the overall report is classified)

1. ORIGINATING ACTIVITY *(Corporate author)* Research Laboratory of Electronics Massachusetts Institute of Technology Cambridge, Massachusetts 02139	2a. REPORT SECURITY CLASSIFICATION Unclassified 2b. GROUP None
3. REPORT TITLE Ku-band Interferometry	
4. DESCRIPTIVE NOTES *(Type of report and inclusive dates)* Technical report	
5. AUTHOR(S) *(First name, middle initial, last name)* George D. Papadopoulos	
6. REPORT DATE December 31, 1970	7a. TOTAL NO. OF PAGES 122 7b. NO. OF REFS 18
8a. CONTRACT OR GRANT NO. DA 28-043-AMC-02536(E) b. PROJECT NO. 20061102B31F c. NASA Grant NGL 22-009-016 d. NSF Grant GP-14854	9a. ORIGINATOR'S REPORT NUMBER(S) Technical Report 481 9b. OTHER REPORT NO(S) *(Any other numbers that may be assigned this report)* None
10. DISTRIBUTION STATEMENT THIS DOCUMENT HAS BEEN APPROVED FOR PUBLIC RELEASE AND SALE; ITS DISTRIBUTION IS UNLIMITED.	
11. SUPPLEMENTARY NOTES	12. SPONSORING MILITARY ACTIVITY Joint Services Electronics Program Through U. S. Army Electronics Command

13. ABSTRACT

The construction of a Ku-band radio interferometer and some preliminary observations are reported. The interferometer was built for the purpose of mapping some discrete radio sources: the Crab Nebula, Cas A, and Cyg A. The system contains two 8 ft parabolic antennas and receives radiation at 17.128 GHz (1.75 cm). The maximum baseline length of 100 m corresponds to a resolution of 35 seconds of arc. A PDP-8 computer is incorporated in the system and used for pointing, tracking, delay compensation, and real-time data analysis. The phase stability of the system was found to be better than 10° over a period of 2 hours. Consistent fringe components were obtained from the Crab Nebula with the baseline set at 8 m.

DD FORM 1 NOV 65 1473 (PAGE 1)

UNCLASSIFIED
Security Classification

14. KEY WORDS	LINK A		LINK B		LINK C	
	ROLE	WT	ROLE	WT	ROLE	WT
Aperture Synthesis						
Ku-band Radiometer						
PDP-8 Computer, Application to Interferometric System						
Radio Astronomy						
Radio Interferometry						
Real-Time Data Processing						